Design of a Fibrin-Based Vascular Graft Seeded with Blood Outgrowth Endothelial Cells

A THESIS
SUBMITTED TO THE FACULTY OF THE GRADUATE SCHOOL
OF THE UNIVERSITY OF MINNESOTA
BY

Katherine A. Ahmann

IN PARTIAL FULFILLMENT OF THE REQUIREMENTS
FOR THE DEGREE OF
DOCTOR OF PHILOSOPHY

Robert T. Tranquillo, Advisor

November, 2010

Acknowledgments

Throughout my graduate career I have been blessed with a supportive network of intelligent and generous people. First, I would like to thank my advisor, Bob Tranquillo, for his guidance and encouragement. I have been continuously impressed with your intelligence and vision and I consider it a real privilege to have worked in your lab. Thank you also to my committee, Robert P. Hebbel, Gregory Vercellotti, and Wei Shen, for your valuable scientific advice and generosity in spending time evaluating my work.

I would also like to thank the Tranquillo lab members, who have been great colleagues and a wonderful set of people. I especially want to thank my most immediately peers, Jason Bjork, Krissy Morin, and Zeeshan Syedain, for your scientific input, and maybe more importantly, your friendship. To Justin Weinbaum and Sandy Johnson, your biochemistry insights, support and collaborations were invaluable. Sandy, you are a constant source of information and scientific advice; from plants and birds to cell culture work, I was lucky to have your brain to pick. I also want to thank Naomi Ferguson for keeping the lab running and the cells happy, and Lee Meier for countless hours working with me on the flow studies, maintaining an entertaining banter that made the time pass quickly.

Thank you to the Hebbel lab, especially Sethu Nair, Arif Somani, and Mark Roney, for help with the blood outgrowth endothelial cells. And to Debra Cocking-Johnson in the Blood Biocompatibility Lab for her help in coordinating the whole blood studies.

I would also like to thank my past mentors, Tayhas Palmore, Michael Lysaght, and Gabriel Silva, for beginning to shape my scientific perspective as an undergraduate and master's student.

Finally, I would like to thank my friends and family. Isabelle Heier and Sunny Choh, I couldn't have gotten through the writing process without you. And to my sisters, Becky Pitzl and Margy Ahmann, thank you for your encouragement and support and for always offering up a fun alternative to work. And last but not least, I am tremendously thankful to my parents, Joan and Rick Ahmann, whose limitless support and encouragement have given me great opportunities in life. I couldn't have done this without you.

Abstract

A clinical need for small-diameter vascular grafts exists, particularly in cases where coronary artery bypass surgery is the best treatment option, but the patient lacks a viable autologous graft due to repeat procedures or diseased vasculature. The comprehensive goal of this work was the *in vitro* fabrication and assessment of a completely biological, small-diameter vascular graft. Our approach uses tissue cells entrapped in a tubular fibrin gel with blood outgrowth endothelial cells (BOECs) seeded on the lumenal surface, in an attempt to recreate important properties of the medial and intimal layers of a native artery. Two major areas were examined to achieve this goal: 1) controlled fibrin degradation and its possible role in improving new matrix deposition, cellularity, and ultimately, mechanical properties and 2) seeding of BOECs on these small-diameter grafts to form a complete vessel and ensure thromboresistance.

We hypothesized that controlling the rate of fibrin degradation could allow for improved matrix remodeling in fibrin-based constructs. To this end, we examined collagen and elastin deposition and cellularity in fibrin-based constructs grown in varied concentrations of the fibrinolysis inhibitor ε-aminocaproic acid (ACA). Decreasing the concentration of ACA led to increased fibrin degradation and better biochemical and mechanical properties. The byproducts of fibrin degradation, fibrin degradation products (FDPs), were shown to be physiological stimulators of collagen deposition, a fact that can be exploited to increase collagen deposition in fibrin-based vascular constructs.

These fibrin-based constructs were then utilized as a substrate for seeding of BOECs, a novel endothelial cell expanded from circulating endothelial progenitor cells in peripheral blood. BOECs adhered to the bioartificial tissue and remained adherent under physiological shear stress. They also exhibited low expression of pro-inflammatory markers and reduced platelet binding compared to unseeded tissue. Exposure to shear stress decreased pro-inflammatory marker expression on TNF-α stimulated BOECs, increased endothelial nitric oxide synthase expression and nitric oxide production, and decreased platelet adhesion during whole blood flow. These outcomes indicate that BOECs are shear stress responsive and are functionally similar to mature endothelial cells in their response to shear stress and their ability to limit platelet binding to bioartificial vascular grafts.

Together, these lines of research allow for the formation of a functional, small-diameter vascular graft, while elucidating key aspects of the remodeling process and BOEC phenotype.

Table of Contents

List of Tables

List of Figures

Chapter 4: Adult Blood Outgrowth Endothelial Cells in Vascular Tissue Engineering

Chapter 5: Discussion and Future Directions

Appendix B: Implant Studies

Appendix C: Cyclic Distention

Chapter 1: Introduction

1.1 Motivation

In 2006, an estimated 448,000 coronary artery bypass surgeries on 253,000 patients were performed in the United States (1). Autologous transplant of the saphenous vein or internal mammary artery remains the standard for these surgeries. However, due to diseased vasculature or repeat bypass surgeries, many patients with coronary artery disease do not have an acceptable native vessel available. In an attempt to fill this pressing need, synthetic materials have been explored for use as bypass grafts. These materials have been used successfully as replacements for large-caliber arteries, but a new set of issues arise when attempting to replace small-caliber vessels, such as the coronary artery. Lower flow velocities and the more compliant nature of small-diameter vessels, combined with poor endothelial cell retention rates on synthetic materials, can cause acute thrombogenicity, anastomotic intimal hyperplasia and aneurysm formation (2, 3). These issues with synthetic grafts motivate the need for a more biological approach.

Through the use of cells and a polymeric scaffold, tissue-engineered grafts have the potential to more closely mimic the native vessel. Our group utilizes this paradigm, through the incorporation of natural biopolymer matrices and vascular cells, to create completely biological, living vascular grafts. While great progress has been made, both by our group and others, a number of key parameters still need to be elucidated. The following chapters will describe specific methods for improving tissue engineered vascular grafts, by addressing a number of these shortcomings. Specifically, the following chapters will examine 1) controlled fibrin gel remodeling and new matrix deposition, 2) fabrication of a complete vascular graft through formation of a functional neoendothelium on tissue-engineered vascular grafts, and 3) utilization of blood outgrowth endothelial cells as a possible autologous cell source for vascular tissue engineering. The current chapter will provide background on native arteries and current small-diameter graft technologies, as well as tissue engineered vascular grafts to date, in order to lay the framework for understanding key vascular graft requirements and current shortcomings.

1.2 Coronary Artery Disease and Current Vascular Grafts

Coronary artery disease (CAD) is associated with atherosclerosis, a process that causes narrowing of the blood vessels that supply oxygen and nutrients to the heart. This narrowing can lead to weakening of the wall of the heart and eventually to myocardial infarction. The progression of CAD causes a reduction of blood flow in the coronary artery and changes in fluid dynamics as the blood interacts with the diseased area (4). The current treatment for CAD, either after myocardial infarction or when a heart attack is

imminent, is replacement of the diseased arteries by coronary artery bypass surgery (CABG). The most common graft utilized is a patient's own internal mammary artery or saphenous vein, which can be used to circumvent the diseased vasculature. While nearly 500,000 bypass surgeries are performed each year (1), many other patients are in need of surgery, yet do not have healthy vasculature for use due to disease progression or previous harvest when repeat procedures are required. In addition to the limited supply, native grafts have limited dimensions, creating possible complications with size mismatch, and require surgery at a secondary site. Venous grafts are particularly prone to thrombotic and hyperplastic occlusion and have lower patency rates (5). This creates a pressing need for small diameter (< 6mm) vascular substitutes that do not rely on a patient's own vasculature.

1.3 Structure and Function of Native Arteries

Arteries are responsible for nutrient, waste and oxygen transport to the body. In order to accomplish this task, the walls of the vessel must be strong and capable of interfacing with the blood. The native arterial wall is composed of three distinct layers, the intima, media, and adventitia, each of which has a unique role in the overall vessel function.

1.3.1 Tunica Intima

The innermost layer of the artery is made up of a monolayer of endothelial cells adherent to an underlying basement membrane. This layer is referred to as the tunica intima, and has been shown to be responsible for much of the functionality of the vessel.

Healthy endothelium is anti-thrombogenic and responsible for maintaining blood homeostasis. Though the requirements for thromboresistance have not been fully defined, some combination of anticoagulant molecules, fibrinolytic activity, and anti-platelet factors is necessary for maintenance of hemostasis. Endothelial cells produce molecules such as prostacyclin (PGI_2), nitric oxide (NO), and ecto-adenosine diphosphatase (ecto-ADPase) which are important for suppressing platelet activation and adhesion (6). Endothelial cells also express molecules that control coagulation, such as von Willebrand factor (vWF), thrombomodulin (TM), tissue factor (TF) and tissue factor pathway inhibitor (TFPI), and fibrinolytic molecules, such as tissue-plasminogen activator (tPA) and urokinase-type plasminogen activator (uPA). A variety of stimuli, including viral infections, endotoxin, tumor necrosis factor (TNF), interleukin 1 (IL-1), and hypoxia, can lead to increased expression of pro-coagulant factors and decreased expression of anti-coagulant factors by ECs (7-9). Cytokine and microbial toxin stimulation of ECs also leads to the expression of the membrane adhesion molecules, P-Selectin, E-Selectin, intercellular adhesion molecule-1 (ICAM-1) and vascular adhesion molecule-1 (VCAM-1), which function as receptors and ligands for leukocyte interactions, including rolling, adhesion and emigration (6). The endothelium can also influence thrombogenicity through the regulation of vascular tone. Molecules such as NO, endothelin, and PGI_2 regulate vascular tone, causing vasodilation or constriction, thus altering flow rates in blood vessels and influencing thrombosis dynamics (10).

The endothelium serves as a permeability barrier between the blood and the vascular tissue. It regulates nutrient transport across the vessel wall and is involved in translation of mechanical signals from the blood into the artery. The tunica intima creates

a clear barrier between the blood and vascular cells within the adjoining layer, the tunica media. As a selectively permeable barrier, the endothelium inhibits smooth muscle cell (SMC) growth by blocking diffusion of circulating growth factors into the medial layer (11), while also producing molecules such as NO and transforming growth factor-β (TGF-β) that limit SMC proliferation and migration (12). A healthy endothelium thus suppresses SMC growth, while injury to the endothelium can be accompanied by intimal hyperplasia, the proliferation and migration of SMCs into the intima layer leading to narrowing of the artery. Imitating this layer will be vital for creating a functional vascular graft. Without the endothelium, the vessel would become a passive conduit without the ability to respond to its environment, and the exposure of the basement membrane would make the vessel thrombogenic.

The functional properties of the endothelium are strongly influenced by the mechanical environment, with evidence indicating an important role for shear stress in influencing endothelial cell structure, growth, and function (13, 14). Shear stress on the endothelium appears critical for maintenance of a thromboresistant surface, control of vessel diameter and vascular permeability, and even endothelial cell survival (6, 13, 15). Shear stress resulting from the flow of blood over the endothelium can lead to junction and cytoskeletal reorganization, altered EC gene expression (10) and altered expression and secretion of proteins associated with fibrinolysis, platelet and leukocyte adhesion, and coagulation. Some of these shear-responsive molecules are shown in Table 1.1, and have been elucidated most commonly with one of two types of studies: 1) research into atherosclerosis through the examination of shear stress effects at regions of disturbed or low shear stress or 2) *in vitro* studies examining the effects of shear stress when applied

to previously statically cultured cells. Both types of studies implicate shear stress as a vastly important parameter in pathophysiology and the maintenance of a quiescent, non-activated endothelium.

Table 1.1: Shear Stress-Responsive Endothelial Cell Surface Molecules.

	Molecule	Location	Response to inflammatory agonist	Shear Stress
Coagulation	**Thrombomodulin**	cell surface	Down (16)	Up (17, 18)
	Tissue Factor	cell surface	Up (19)	Up, but decreased activity due to TFPI (20)
	TF Pathway Inhibitor (TFPI)	cell surface, secreted	Constitutively expressed (20)	Up (20)
Blood Cell Interactions	**ICAM-1**	cell surface	Up (21)	Up (22-24) LSS Up, HSS Down (25) No change (26)
	VCAM-1	cell surface	Up (21)	Down (27) Unchanged (22)
	PECAM (CD31)	cell surface	No change (28)	Tyrosine phosphorylated (29)
	E-Selectin	cell surface	Up (21)	Down Unchanged (22, 24)
	Nitric Oxide (NO)	secreted	Down (30)	Up (31, 32)
	Nitric Oxide Synthase (NOS)	intracellular	Down (16)	Up (33, 34)
	Prostacylin (PGI2)	secreted	Up (35)	Up (36)
Complement	All are secreted or constitutively expressed: **Complement inhibitors, CD46, CD55, CD59, C3, C1s, factor B**			
Fibrinolysis	Secreted: **Tissue plasminogen activator (tPA-1)** and **Plasminogen activator inhibitor-1 (PAI-1)**			

*LSS: low shear stress; HSS: high shear stress

1.3.2 Tunica Media

The middle layer, or tunica media, of arteries is composed of circumferentially aligned collagen fibers, SMCs and thick elastic lamellae. This layer, with its circumferential arrangement of fibers and cells, accounts for the integrity of the vessel under physiological loading. The mechanical properties of native arteries have been described by the individual contributions of collagen, elastin, and smooth muscle in the medial layer (37, 38). Elastin has a large role in defining the mechanical properties at low strains, while collagen is the predominant influence at high strains (39). Elastin, which is arranged concentrically in the media layer, provides recoil after each cycle of vessel inflation, preventing dilation. The circumferentially aligned SMCs within the arterial wall are powerful contractile elements, responsible for vasoconstriction and dilation depending on a number of chemical and mechanical cues. Elastin, in conjunction with contractile SMCs, regulates arterial compliance. Collagen, with its high tensile strength, maintains the structure of the vessel and gives it good surgical handling properties and prevents rupture under physiological, and supra-physiological, pressures.

1.3.3 Tunica Adventitia

The medial layer and outermost layer, the tunica adventitia, are separated by the outer elastic lamina, which forms a distinct boundary between the two layers. The adventitia is made up of a loose fibrous matrix, which anchors the vessel to the surrounding connective tissue. It is composed primarily of collagen, fibroblasts, and some elastin, with nerves and small blood vessels running through this layer to supply the vessel wall with nutrients and oxygen.

1.4 Synthetic Materials

The earliest attempts at fabricating vascular grafts involved the use of endothelial cell-seeded synthetic materials (40). While synthetic materials have been successfully utilized as replacements for large-diameter blood vessels, these materials encounter a host of new issues when intended as small-diameter grafts (4). A major issue involves the likelihood of clot formation on the thrombogenic lumenal surface. This has made the endothelialization of synthetic material an important area of research, particularly since synthetic materials have displayed issues with EC attachment, survival and adhesion under flow (3). Though surface modification techniques have been promising for improving EC attachment and survival (41), long-term survival and proliferation of ECs on synthetic materials still needs to be addressed. Furthermore, *in vivo* remodeling of a non-biodegradable, synthetic graft, such as ePTFE or Dacron is limited, making long-term adaptation of the vessel impossible. The graft will not be able to grow with young patients, nor will it have all the physiological responses, such as vasoactivity, of living vessels.

1.5 Vascular Tissue Engineering

Tissue engineering relies on the use of tissue cells, a scaffold and various culture conditions to fabricate new tissues, and ultimately, new organs. The most common tissue engineering paradigm includes the use of all three of these components; however some therapies focus solely on the scaffold or the cells. As compared to synthetic materials,

tissue-engineered therapies have the potential to more closely mimic the native tissue, as well as integrate with the patient's own tissue.

The design criteria for small-diameter, tissue-engineered vascular grafts are motivated by the functions of each of the arterial wall layers. The ideal artificial artery would be non-thrombogenic and non-immunogenic, most likely through the incorporation of a confluent, quiescent endothelial cell monolayer. It would possess the mechanical properties similar to the medial layer of native arteries, including physiological compliance, viscoelasticity, elastic recoil, and high burst pressure. As the vessel is exposed to continuous distention, it must not be susceptible to permanent creep or aneurysm formation. The healing response upon implantation will be another critical consideration for a tissue-engineered vascular graft, since the grafts cannot be a significant source of inflammation, hyperplasia, or fibrous capsule formation after implant. Other issues must be addressed for practical application of a tissue engineered vessel include the ease of suturing and handling, integration with native tissue upon implantation, durability, scale-up, availability, and cost. All of these issues will need to be considered for a tissue-engineered vessel to transition from the lab to clinical use.

These properties will motivate the choice of biomaterial while the incorporation of cells into the matrix could allow for important physiological properties, such active remodeling of the extracellular matrix *in vitro* prior to implantation and *in vivo*. In addition, the artery must withstand a number of dynamic forces, including the transmural pressure acting normal to the vessel wall and the tangential shear stress. Thus, a successful vascular graft will likely have mechanical properties similar to those of a native vessel, so that it can withstand the pressures associated with blood flow and avoid

compliance mismatch issues at the anastomoses. The incorporation of an EC layer will require assessment of adhesion under flow, to ensure a confluent monolayer can be established and maintained under physiological shear stress.

A variety of tissue-engineering approaches have been explored to meet these criteria, including utilization of cell sheet methods, decellularized vascular grafts, biodegradable polymer scaffolds, and biopolymer scaffolds (42). The cell sheet method relies on "self-assembly" by cells grown on tissue culture plastic (43-45). By inducing high ECM synthesis in these cells, sheets of cells and ECM can be created and rolled into tubular form to create multi-layered vessels. This translates to a vascular graft that is made only from human proteins, as the entire ECM is synthesized by human dermal fibroblast (HDFs) or SMCs. This method has allowed for the fabrication of vascular grafts with burst pressures equivalent to native vessels, but requires long culture times to produce these results (45, 46).

While the cell-sheet method starts with cells only, a second category of tissue engineering relies on an acellular scaffold that, upon implantation, can recruit cells from the host tissue. Acellular approaches avoid the necessity of isolating and expanding autologous cells, thus significantly shortening the fabrication time and allowing for quick implantation. The use of native tissue has advantages for mechanical properties and biocompatibility (47). The small intestinal submucosa (SIS) is a cell-free, collagen layer that has been rolled for use as a vascular graft with appropriate mechanical properties (48-51). Wilson et al. examined detergent and enzymatic extraction to removed cells from allograft vessels and showed no inflammation in a canine model, but limited cell recruitment (52). Gui et al. showed similar mechanical properties for decellularized

umbilical arteries compared to non-decellularized vessels; however, some of the decellularized umbilical artery grafts occluded within 24 hours of implantation as aortic replacements in nude rats, leading to higher mortality rates in those rats. The decellularized umbilical artery grafts also developed various levels of thrombosis at the proximal anastomosis sites during an 8-week implantation period. Vascular cell migration *in vivo* is not well understood and the means to recruit the appropriate cells still requires extensive research (4). Furthermore, this method will require a quick recruitment of ECs to the lumenal surface to prevent thrombus formation and long-term intimal hyperplasia. Seeding of decellularized tissue with ECs prior to implantation may prevent some of these issues.

Use of cell-seeded, polymeric scaffolds represents another promising method for vascular graft formation (53-58). Methods reliant on biodegradable polymer scaffolds require the formation of tubular constructs first followed by cell seeding, as the cells would not survive the conditions required for polymer synthesis. Even distributions of cells, and thus homogenous remodeling, are potential issues that will need to be overcome. Good results have been attained with these methods; however an inflammatory response to residual, degrading polymer will need to be ruled out.

A fourth approach utilizes biopolymers formed with entrapped cells. Biopolymers are an ideal substrate for cell attachment and signaling; however, the initial gel is inherently weak (59). The entrapment of vascular cells is required for cell-mediated restructuring to improve biopolymer organization, remodeling, and mechanical properties. The most prevalent examples of this approach involve reconstituted type I collagen gels that are populated and compacted by SMCs (60-63). As first shown by

L'Heureux et al. (60) and more thoroughly examined by our group (62), constrained compaction around a non-adhesive mandrel generates circumferential alignment of the collagen fibrils and SMCs. Cell and fiber circumferential alignment are important for improving mechanical properties, but also for vasoactivity and structural integrity. The use of biopolymers to mimic the aligned structure of the medial layer makes them promising matrix materials for artificial artery design.

1.6 Fibrin-based Vascular Constructs

Our group has also investigated the use of fibrin as an alternative biopolymer to type I collagen for the fabrication of a tissue-engineered vessel (64, 65). Fibrin gels have the same advantages as collagen-based constructs, namely direct cell entrapment during construct synthesis and the ability to produce circumferential alignment of cells and fibrils with mechanically constrained gels (Figure 1.1). Fibrin-based constructs have the added advantage of enhanced matrix remodeling compared to collagen constructs. Neonatal SMCs secrete more collagen in fibrin gels compared to collagen gels and have superior mechanical properties (65). Significant elastogenesis occurs within SMC-entrapped fibrin constructs (66), a result that has not been seen in the collagen counterpart. Our lab has also assessed gene expression over five weeks of culture for fibrin-based constructs (67). Increased expression of tropoelastin, collagen, and lysyl oxidase correlated with measured quantities of elastin and collagen deposition. Over weeks three to five of this study, organized, cross-linked collagen and elastin were detected, which was associated with an increase in mechanical properties.

Further, these media-equivalents can be endothelialized, with surface coverage greater than 98.8% and high endothelial cell retention rates (96.5%) under physiological shear stress (68). Swartz et al. implanted fibrin-based, endothelialized constructs into the jugular veins of lambs, which remained patent for up to 15 weeks. This result is promising as examination of the explants showed extensive matrix remodeling, with production of collagen and elastin fibers, as well as improved mechanical properties (69). However, these constructs would be composed primarily of fibrin at the time of implantation as they were cultured *in vitro* for only 2-3 weeks prior to implantation. The constructs were strong enough to withstand implantation into the venous circulation, but will require extensive strengthening if they are to be used for artery replacement.

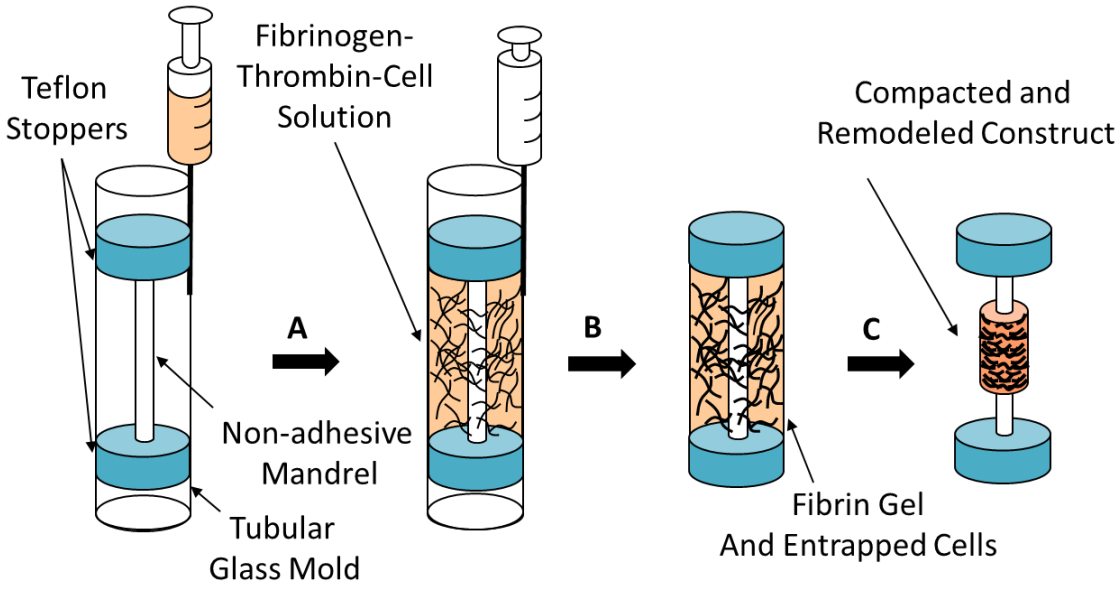

Figure 1.1: Medial layer fabrication. A) A solution containing fibrinogen, thrombin and cells is injected into a glass mold containing an inner nonadhesive mandrel with stoppers at each end. B) The solution is allowed to gel for 30 minutes at 37C and then the fibrin gel construct is removed from the outer glass mold and transferred to cell culture media. C) Over time, cell-induced compaction around the nonadhesive mandrel leads to circumferential alignment of the cells and fibrils (modified from figure by B. Isenberg).

1.7 Methods to Improve Mechanical Properties

While the results with fibrin-based scaffolds have been promising, the mechanical properties of biopolymer approaches remain inferior to native arteries. A number of conditions have been explored in order to improve the mechanical properties of biopolymer constructs, including alteration of medium conditions, addition of growth factors, gel cross-linking and mechanical conditioning. Inherent in these studies is the acknowledgement that substrate signaling from the ECM and chemical and mechanical signaling from the surrounding media are important for regulating processes such as cell growth, matrix synthesis and differentiation.

1.7.1 Chemical Signaling

In order to optimize the fabrication of fibrin-based vascular grafts, the culture conditions and addition of supplements are important parameters for producing large improvements in collagen and elastin production and tissue strength and stiffness. Previous work by our group, with disc-shaped gels or 8 mm diameter tubular gels, has shown improved collagen deposition and mechanical properties when vSMC fibrin constructs were cultured with insulin and TGF-β (65). The quantity of crosslinked elastic fibers was also enhanced by supplementation with TGF- β and insulin in neonatal vSMC fibrin constructs, and these additives overcame ascorbate's inhibition of elastogenesis in fibrin (66). These optimizations in construct culture will be utilized in the fabrication of small-diameter, fibrin-based vascular grafts.

1.7.2 Mechanical Conditioning

During natural growth and function, another set of signals is imposed by the mechanical environment. As discussed earlier in this chapter, in the vessel wall, this signaling is due to the hemodynamics of the vascular system and includes shear stress, tangential forces acting on ECs and to a lesser extent SMCs due to transverse (interstitial) flow, and mechanical stretch, a cyclic circumferential stress caused by blood pressure. Application of these mechanical signals during *in vitro* culture of tissue-engineered vessels could provide a method to influence tissue development, by enhancing ECM synthesis or altering cell proliferation or phenotype.

Cyclic stress caused by blood pressure plays a significant role in regulation of blood vessel remodeling and thus, intuitively, may be useful in regulating the development of tissue-engineered blood vessels. Studies have shown that cyclic strain can be used to regulate the phenotype of vascular SMCs in two-dimensional (70, 71) and three-dimensional culture (55, 72, 73). Groups studying cyclic strain of SMCs in three-dimensional collagen and synthetic material scaffolds have reported increased collagen (55, 56, 73-75) and elastin (74) deposition, cell proliferation (55, 73, 74) and improvements in construct mechanical properties (55, 56, 63, 74). Niklason et al. seeded bovine aortic SMCs on porous tubes of polyglycolic acid and then perfused the constructs with medium at 2.75 Hz with 5% radial distention. After 8 weeks, the mean burst pressure of strained constructs was 2000 mmHg compared to 300 mmHg in the static vessels. The collagen content and SMC densities were also significantly higher in the strained constructs and the histological appearance was similar to that of native vessels (55, 56). Nerem et al. looked at short-term cyclic distention of SMC-seeded collagen

tubular constructs at 1 Hz and 10% strain for 4 and 8 days. Distention yielded increases in construct mechanical properties and improved circumferential alignment of SMCs throughout the construct wall (63, 76).

To date, most three-dimensional construct studies have focused on a single loading condition, based on a typical resting physiological condition or the capabilities of the bioreactor system used. Optimal cyclic loading for the largest improvements in tissue structure and mechanical properties may involve pulse shapes or strain values that differ from the single loading values chosen in these experiments. Our lab has examined the effect of cyclic distention parameters on collagen-based tubular constructs with adult rat aortic SMCs (77). Strain, stretch time, and relaxation time were all shown to be important variables in controlling contruct mechanical properties. Altering the stain imposed over the course of construct culture has also been examined. By conditioning with incrementally increasing cyclic stain, human dermal fibroblasts (HDFs) and porcine interstitial valve cells (PIVCs) in fibrin-based tubular constructs have been cultured to reach mechanical properties (78), including burst pressures (79), near those of native vessels.

1.7.3 Controlled Fibrin Degradation

While fibrin has become a common biopolymer for use in cardiovascular (80-83) and vascular tissue engineering (64-67, 69, 84-87), the effects of fibrin degradation rates on new matrix synthesis is poorly defined. Fibrin can be degraded by plasmin *in vivo* and *in vitro*, and the degradation rate varies with concentration of plasmin, the local environment and the fibrinolytic nature of the surrounding cells. Fibrin degradation can

be modulated by the addition of plasmin inhibitors, such as aprotinin or ε-aminocaproic acid (ACA), which have been widely used in tissue engineering (88-92) to maintain the fibrin scaffold while new matrix is synthesized. A closer examination of the effect of fibrin degradation rate on new matrix deposition may allow for better control of this parameter, leading to improvements in construct composition and mechanics.

1.8 Endothelium Formation

1.8.1 Endothelial Cell Source

A variety of endothelial cell (EC) sources have been examined for vascular tissue engineering, including artery- and vein-derived ECs and adipose-derived microvascular ECs. All of these sources would require secondary surgical procedures prior to use and expansion times dependent on their proliferation rates. Adipose-derived ECs are more abundant than vessel wall cells and can be isolated in quantities such that *in vitro* expansion is not necessary; however, clinical trials with these cells have had inferior results compared to the use of vein-derived ECs. Progressive intimal thickening was found when adipose-derived ECs were used, likely due to the presence of contaminating myofibroblasts in the isolated cells. Thus, use of these cells would require *in vitro* purification to remove contaminating cells that promote intimal hyperplasia (93).

Blood outgrowth endothelial cells (BOECs) are a promising source of EC for *in vitro* neoendothelium formation. These cells are isolated by outgrowth of circulating progenitor cells from a 50-100 ml blood sample (94-97). In studies with human BOECS, these cells were shown to have a robust proliferative capacity, expanding from 20 cells to 10^{19} cells in 9 weeks (95). BOECs uniformly express endothelial cells markers VE-

cadherin, CD31, P1H12, thrombomodulin, von Willebrand factor, flk-1, and CD36 but do not express the hematopoietic cell markers CD45 or CD14. They have the typical endothelial cell cobblestone morphology, take up acetylated low density lipoprotein (acLDL) and contain Weibel-Palade bodies (95, 96). As identified by the presence of CD36, a marker of microvascular ECs, and the absence vascular cell adhesion molecule-1 (VCAM-1) and tissue factor (TF) as well as weak expression of intercellular adhesion molecule-1 (ICAM-1), BOECs have the phenotype of non-activated, microvascular endothelial cells (95). BOECs provides a source of autologous cells that could be derived from the patient's own blood, which would limit the need for long term anti-coagulation therapy and reduce graft rejection.

1.8.2 Neoendothelium Assessment

Rigorous assessment of endothelial cells seeded on vascular grafts *in vitro* will yield important insight into the functionality of the formed endothelium. Adhesion, morphology, and junction formation will give an idea as to the maturity of the neoendothelium. This endothelium needs to remain intact under physiological shear stress, reorient in the flow direction, and be responsive to shear stress. The thrombogenicity of the seeded tissue can then be assessed by examination of key molecules involved in clotting, platelet and leukocyte adhesion, and fibrinolysis. *In vitro* functional tests will be important benchmarks for examination of potential graft issues and outcomes (10).

Assessment of endothelium formation on vascular grafts will require implantation to determine full functionality. However, this leads to a number of complications with

choice of an appropriate animal model. Species-dependent differences in endothelial and blood cells make autologous implantation with non-human cells an incomplete picture (98). However, use of human cells will require immunosuppressant drugs or use of immunodeficient animals. This makes *in vitro* assessment methods using human cells and blood important supplementary studies.

1.9 Conclusions

A successful tissue engineered vascular graft will likely require a careful prescription of a number of the mechanical and chemical cues described above. The following chapters will examine methods to exploit these signaling mechanisms to improve the matrix properties and cell phenotype of fibrin-based bioartificial arteries. Chapter 2 will examine the role that the fibrin scaffold has in the overall structure, by altering fibrin degradation through the use of a fibrinolytic inhibitor and examining changes in cellularity and new matrix deposition. Chapter 3 utilized the outcomes from Chapter 2 to develop a functional, small diameter bioartificial artery seeded with rat BOECs. Chapter 4 will then examine the use of shear stress conditioning to alter the phenotype of human BOECs and examine adhesion and thrombogenicity on bioartificial vascular grafts.

1.10 References

1. Lloyd-Jones, D., Adams, R.J., Brown, T.M., Carnethon, M., Dai, S., De Simone, G., Ferguson, T.B., Ford, E., Furie, K., Gillespie, C., Go, A., Greenlund, K., Haase, N., Hailpern, S., Ho, P.M., Howard, V., Kissela, B., Kittner, S., Lackland, D., Lisabeth, L., Marelli, A., McDermott, M.M., Meigs, J., Mozaffarian, D., Mussolino, M., Nichol, G., Roger, V.L., Rosamond, W., Sacco, R., Sorlie, P., Roger, V.L., Thom, T., Wasserthiel-Smoller, S., Wong, N.D., and Wylie-Rosett, J. Heart disease and stroke statistics--2010 update: a report from the American Heart Association. Circulation 121, e46.

2. Bos, G.W., Poot, A.A., Beugeling, T., van Aken, W.G., and Feijen, J. Small-diameter vascular graft prostheses: current status. Arch Physiol Biochem 106, 100, 1998.

3. Thomas, A.C., Campbell, G.R., and Campbell, J.H. Advances in vascular tissue engineering. Cardiovasc Pathol 12, 271, 2003.

4. Nerem, R.M., and Seliktar, D. Vascular tissue engineering. Annu Rev Biomed Eng 3, 225, 2001.

5. Spencer, F.C. The internal mammary artery: the ideal coronary bypass graft? The New England journal of medicine 314, 50, 1986.

6. Wu, K.K., and Thiagarajan, P. Role of endothelium in thrombosis and hemostasis. Annual review of medicine 47, 315, 1996.

7. Stern, D.M., Kaiser, E., and Nawroth, P.P. Regulation of the coagulation system by vascular endothelial cells. Haemostasis 18, 202, 1988.

8. Ogawa, S., Clauss, M., Kuwabara, K., Shreeniwas, R., Butura, C., Koga, S., and Stern, D. Hypoxia induces endothelial cell synthesis of membrane-associated proteins. Proceedings of the National Academy of Sciences of the United States of America 88, 9897, 1991.

9. Key, N.S., Vercellotti, G.M., Winkelmann, J.C., Moldow, C.F., Goodman, J.L., Esmon, N.L., Esmon, C.T., and Jacob, H.S. Infection of vascular endothelial cells with herpes simplex virus enhances tissue factor activity and reduces thrombomodulin expression. Proceedings of the National Academy of Sciences of the United States of America 87, 7095, 1990.

10. McGuigan, A.P., and Sefton, M.V. The influence of biomaterials on endothelial cell thrombogenicity. Biomaterials 28, 2547, 2007.

11. Costa, M.A., and Simon, D.I. Molecular basis of restenosis and drug-eluting stents. Circulation 111, 2257, 2005.

12. Patel, S.D., Waltham, M., Wadoodi, A., Burnand, K.G., and Smith, A. The role of endothelial cells and their progenitors in intimal hyperplasia. Therapeutic advances in cardiovascular disease 4, 129.

13. Davies, P.F. Flow-mediated endothelial mechanotransduction. Physiological reviews 75, 519, 1995.

14. Gimbrone, M.A., Jr., Topper, J.N., Nagel, T., Anderson, K.R., and Garcia-Cardena, G. Endothelial dysfunction, hemodynamic forces, and atherogenesis. Annals of the New York Academy of Sciences 902, 230, 2000.

15. Traub, O., and Berk, B.C. Laminar shear stress: mechanisms by which endothelial cells transduce an atheroprotective force. Arteriosclerosis, thrombosis, and vascular biology 18, 677, 1998.

16. Bergh, N., Ulfhammer, E., Glise, K., Jern, S., and Karlsson, L. Influence of TNF-alpha and biomechanical stress on endothelial anti- and prothrombotic genes. Biochemical and biophysical research communications 385, 314, 2009.

17. Malek, A.M., Jackman, R., Rosenberg, R.D., and Izumo, S. Endothelial expression of thrombomodulin is reversibly regulated by fluid shear stress. Circulation research 74, 852, 1994.

18. Takada, Y., Shinkai, F., Kondo, S., Yamamoto, S., Tsuboi, H., Korenaga, R., and Ando, J. Fluid shear stress increases the expression of thrombomodulin by cultured human endothelial cells. Biochemical and biophysical research communications 205, 1345, 1994.

19. Matsumoto, Y., Kawai, Y., Watanabe, K., Sakai, K., Murata, M., Handa, M., Nakamura, S., and Ikeda, Y. Fluid shear stress attenuates tumor necrosis factor-alpha-induced tissue factor expression in cultured human endothelial cells. Blood 91, 4164, 1998.

20. Grabowski, E.F., Reininger, A.J., Petteruti, P.G., Tsukurov, O., and Orkin, R.W. Shear stress decreases endothelial cell tissue factor activity by augmenting secretion of tissue factor pathway inhibitor. Arteriosclerosis, thrombosis, and vascular biology 21, 157, 2001.

21. Chiu, J.J., Lee, P.L., Chen, C.N., Lee, C.I., Chang, S.F., Chen, L.J., Lien, S.C., Ko, Y.C., Usami, S., and Chien, S. Shear stress increases ICAM-1 and decreases VCAM-1 and E-selectin expressions induced by tumor necrosis factor-[alpha] in endothelial cells. Arteriosclerosis, thrombosis, and vascular biology 24, 73, 2004.

22. Nagel, T., Resnick, N., Atkinson, W.J., Dewey, C.F., Jr., and Gimbrone, M.A., Jr. Shear stress selectively upregulates intercellular adhesion molecule-1 expression in cultured human vascular endothelial cells. The Journal of clinical investigation 94, 885, 1994.

23. Chiu, J.J., Wung, B.S., Shyy, J.Y., Hsieh, H.J., and Wang, D.L. Reactive oxygen species are involved in shear stress-induced intercellular adhesion molecule-1 expression in endothelial cells. Arteriosclerosis, thrombosis, and vascular biology 17, 3570, 1997.

24. Morigi, M., Zoja, C., Figliuzzi, M., Foppolo, M., Micheletti, G., Bontempelli, M., Saronni, M., Remuzzi, G., and Remuzzi, A. Fluid shear stress modulates surface expression of adhesion molecules by endothelial cells. Blood 85, 1696, 1995.

25. Khan, O.F., and Sefton, M.V. Endothelial cell behaviour within a microfluidic mimic of the flow channels of a modular tissue engineered construct. Biomedical microdevices.

26. Sheikh, S., Rainger, G.E., Gale, Z., Rahman, M., and Nash, G.B. Exposure to fluid shear stress modulates the ability of endothelial cells to recruit neutrophils in response to tumor necrosis factor-alpha: a basis for local variations in vascular sensitivity to inflammation. Blood 102, 2828, 2003.

27. Ando, J., Tsuboi, H., Korenaga, R., Takada, Y., Toyama-Sorimachi, N., Miyasaka, M., and Kamiya, A. Down-regulation of vascular adhesion molecule-1 by fluid shear stress in cultured mouse endothelial cells. Annals of the New York Academy of Sciences 748, 148, 1995.

28. Henninger, D.D., Panes, J., Eppihimer, M., Russell, J., Gerritsen, M., Anderson, D.C., and Granger, D.N. Cytokine-induced VCAM-1 and ICAM-1 expression in different organs of the mouse. J Immunol 158, 1825, 1997.

29. Osawa, M., Masuda, M., Kusano, K., and Fujiwara, K. Evidence for a role of platelet endothelial cell adhesion molecule-1 in endothelial cell mechanosignal transduction: is it a mechanoresponsive molecule? The Journal of cell biology 158, 773, 2002.

30. Myers, P.R., Wright, T.F., Tanner, M.A., and Adams, H.R. EDRF and nitric oxide production in cultured endothelial cells: direct inhibition by E. coli endotoxin. The American journal of physiology 262, H710, 1992.

31. Kuchan, M.J., Jo, H., and Frangos, J.A. Role of G proteins in shear stress-mediated nitric oxide production by endothelial cells. The American journal of physiology 267, C753, 1994.

32. Yee, A., Bosworth, K.A., Conway, D.E., Eskin, S.G., and McIntire, L.V. Gene expression of endothelial cells under pulsatile non-reversing vs. steady shear stress; comparison of nitric oxide production. Annals of biomedical engineering 36, 571, 2008.

33. Nishida, K., Harrison, D.G., Navas, J.P., Fisher, A.A., Dockery, S.P., Uematsu, M., Nerem, R.M., Alexander, R.W., and Murphy, T.J. Molecular cloning and characterization of the constitutive bovine aortic endothelial cell nitric oxide synthase. The Journal of clinical investigation 90, 2092, 1992.

34. Davis, M.E., Grumbach, I.M., Fukai, T., Cutchins, A., and Harrison, D.G. Shear stress regulates endothelial nitric-oxide synthase promoter activity through nuclear factor kappaB binding. The Journal of biological chemistry 279, 163, 2004.

35. Zavoico, G.B., Ewenstein, B.M., Schafer, A.I., and Pober, J.S. IL-1 and related cytokines enhance thrombin-stimulated PGI2 production in cultured endothelial cells without affecting thrombin-stimulated von Willebrand factor secretion or platelet-activating factor biosynthesis. J Immunol 142, 3993, 1989.

36. Frangos, J.A., Eskin, S.G., McIntire, L.V., and Ives, C.L. Flow effects on prostacyclin production by cultured human endothelial cells. Science (New York, N.Y 227, 1477, 1985.

37. Roach, M.R., and Burton, A.C. The reason for the shape of the distensibility curves of arteries. Canadian journal of biochemistry and physiology 35, 681, 1957.

38. Bank, A.J., Wang, H., Holte, J.E., Mullen, K., Shammas, R., and Kubo, S.H. Contribution of collagen, elastin, and smooth muscle to in vivo human brachial artery wall stress and elastic modulus. Circulation 94, 3263, 1996.

39. Fung, Y.C. Biomechanics : mechanical properties of living tissues. New York: Springer-Verlag, 1993.

40. Herring, M.B. Endothelial cell seeding. J Vasc Surg 13, 731, 1991.

41. Ravi, S., Qu, Z., and Chaikof, E.L. Polymeric materials for tissue engineering of arterial substitutes. Vascular 17 Suppl 1, S45, 2009.

42. Isenberg, B.C., Williams, C., and Tranquillo, R.T. Small-diameter artificial arteries engineered in vitro. Circulation research 98, 25, 2006.

43. L'Heureux, N., Paquet, S., Labbe, R., Germain, L., and Auger, F.A. A completely biological tissue-engineered human blood vessel. Faseb J 12, 47, 1998.

44. L'Heureux, N., Stoclet, J.C., Auger, F.A., Lagaud, G.J., Germain, L., and Andriantsitohaina, R. A human tissue-engineered vascular media: a new model for pharmacological studies of contractile responses. Faseb J 15, 515, 2001.

45. L'Heureux, N., Dusserre, N., Konig, G., Victor, B., Keire, P., Wight, T.N., Chronos, N.A., Kyles, A.E., Gregory, C.R., Hoyt, G., Robbins, R.C., and McAllister, T.N. Human tissue-engineered blood vessels for adult arterial revascularization. Nature medicine 12, 361, 2006.

46. McAllister, T.N., Maruszewski, M., Garrido, S.A., Wystrychowski, W., Dusserre, N., Marini, A., Zagalski, K., Fiorillo, A., Avila, H., Manglano, X., Antonelli, J., Kocher, A., Zembala, M., Cierpka, L., de la Fuente, L.M., and L'Heureux, N. Effectiveness of haemodialysis access with an autologous tissue-engineered vascular graft: a multicentre cohort study. Lancet 373, 1440, 2009.

47. Schmidt, C.E., and Baier, J.M. Acellular vascular tissues: natural biomaterials for tissue repair and tissue engineering. Biomaterials 21, 2215, 2000.

48. Lantz, G.C., Badylak, S.F., Coffey, A.C., Geddes, L.A., and Blevins, W.E. Small intestinal submucosa as a small-diameter arterial graft in the dog. J Invest Surg 3, 217, 1990.

49. Lantz, G.C., Badylak, S.F., Hiles, M.C., Coffey, A.C., Geddes, L.A., Kokini, K., Sandusky, G.E., and Morff, R.J. Small intestinal submucosa as a vascular graft: a review. J Invest Surg 6, 297, 1993.

50. Hiles, M.C., Badylak, S.F., Lantz, G.C., Kokini, K., Geddes, L.A., and Morff, R.J. Mechanical properties of xenogeneic small-intestinal submucosa when used as an aortic graft in the dog. Journal of biomedical materials research 29, 883, 1995.

51. Huynh, T., Abraham, G., Murray, J., Brockbank, K., Hagen, P.O., and Sullivan, S. Remodeling of an acellular collagen graft into a physiologically responsive neovessel. Nat Biotechnol 17, 1083, 1999.

52. Wilson, G.J., Courtman, D.W., Klement, P., Lee, J.M., and Yeger, H. Acellular matrix: a biomaterials approach for coronary artery bypass and heart valve replacement. The Annals of thoracic surgery 60, S353, 1995.

53. Wake, M.C., Gupta, P.K., and Mikos, A.G. Fabrication of pliable biodegradable polymer foams to engineer soft tissues. Cell Transplant 5, 465, 1996.

54. Shinoka, T., Shum-Tim, D., Ma, P.X., Tanel, R.E., Isogai, N., Langer, R., Vacanti, J.P., and Mayer, J.E., Jr. Creation of viable pulmonary artery autografts through tissue engineering. The Journal of thoracic and cardiovascular surgery 115, 536, 1998.

55. Niklason, L.E., Gao, J., Abbott, W.M., Hirschi, K.K., Houser, S., Marini, R., and Langer, R. Functional arteries grown in vitro. Science (New York, N.Y 284, 489, 1999.

56. Niklason, L.E., Abbott, W., Gao, J., Klagges, B., Hirschi, K.K., Ulubayram, K., Conroy, N., Jones, R., Vasanawala, A., Sanzgiri, S., and Langer, R. Morphologic and mechanical characteristics of engineered bovine arteries. J Vasc Surg 33, 628, 2001.

57. Hoerstrup, S.P., Zund, G., Sodian, R., Schnell, A.M., Grunenfelder, J., and Turina, M.I. Tissue engineering of small caliber vascular grafts. Eur J Cardiothorac Surg 20, 164, 2001.

58. Shin'oka, T., Imai, Y., and Ikada, Y. Transplantation of a tissue-engineered pulmonary artery. The New England journal of medicine 344, 532, 2001.

59. Weinberg, C.B., and Bell, E. A blood vessel model constructed from collagen and cultured vascular cells. Science (New York, N.Y 231, 397, 1986.

60. L'Heureux, N., Germain, L., Labbe, R., and Auger, F.A. In vitro construction of a human blood vessel from cultured vascular cells: a morphologic study. J Vasc Surg 17, 499, 1993.

61. Hirai, J., and Matsuda, T. Self-organized, tubular hybrid vascular tissue composed of vascular cells and collagen for low-pressure-loaded venous system. Cell Transplant 4, 597, 1995.

62. Barocas, V.H., Girton, T.S., and Tranquillo, R.T. Engineered alignment in media equivalents: magnetic prealignment and mandrel compaction. Journal of biomechanical engineering 120, 660, 1998.

63. Seliktar, D., Black, R.A., Vito, R.P., and Nerem, R.M. Dynamic mechanical conditioning of collagen-gel blood vessel constructs induces remodeling in vitro. Annals of biomedical engineering 28, 351, 2000.

64. Grassl, E.D., Oegema, T.R., and Tranquillo, R.T. Fibrin as an alternative biopolymer to type-I collagen for the fabrication of a media equivalent. Journal of biomedical materials research 60, 607, 2002.

65. Grassl, E.D., Oegema, T.R., and Tranquillo, R.T. A fibrin-based arterial media equivalent. Journal of biomedical materials research 66, 550, 2003.

66. Long, J.L., and Tranquillo, R.T. Elastic fiber production in cardiovascular tissue-equivalents. Matrix Biol 22, 339, 2003.

67. Ross, J.J., and Tranquillo, R.T. ECM gene expression correlates with in vitro tissue growth and development in fibrin gel remodeled by neonatal smooth muscle cells. Matrix Biol 22, 477, 2003.

68. Isenberg, B.C., Williams, C., and Tranquillo, R.T. Endothelialization and flow conditioning of fibrin-based media-equivalents. Annals of biomedical engineering 34, 971, 2006.

69. Swartz, D.D., Russell, J.A., and Andreadis, S.T. Engineering of fibrin-based functional and implantable small-diameter blood vessels. American journal of physiology 288, H1451, 2005.

70. Sumpio, B.E., Banes, A.J., Link, W.G., and Johnson, G., Jr. Enhanced collagen production by smooth muscle cells during repetitive mechanical stretching. Arch Surg 123, 1233, 1988.

71. Birukov, K.G., Shirinsky, V.P., Stepanova, O.V., Tkachuk, V.A., Hahn, A.W., Resink, T.J., and Smirnov, V.N. Stretch affects phenotype and proliferation of vascular smooth muscle cells. Molecular and cellular biochemistry 144, 131, 1995.

72. Kim, B.S., Nikolovski, J., Bonadio, J., Smiley, E., and Mooney, D.J. Engineered smooth muscle tissues: regulating cell phenotype with the scaffold. Experimental cell research 251, 318, 1999.

73. Jeong, S.I., Kwon, J.H., Lim, J.I., Cho, S.W., Jung, Y., Sung, W.J., Kim, S.H., Kim, Y.H., Lee, Y.M., Kim, B.S., Choi, C.Y., and Kim, S.J. Mechano-active tissue engineering of vascular smooth muscle using pulsatile perfusion bioreactors and elastic PLCL scaffolds. Biomaterials 26, 1405, 2005.

74. Kim, B.S., Nikolovski, J., Bonadio, J., and Mooney, D.J. Cyclic mechanical strain regulates the development of engineered smooth muscle tissue. Nat Biotechnol 17, 979, 1999.

75. Solan, A., Mitchell, S., Moses, M., and Niklason, L. Effect of pulse rate on collagen deposition in the tissue-engineered blood vessel. Tissue engineering 9, 579, 2003.

76. Seliktar, D., Nerem, R.M., and Galis, Z.S. The role of matrix metalloproteinase-2 in the remodeling of cell-seeded vascular constructs subjected to cyclic strain. Annals of biomedical engineering 29, 923, 2001.

77. Isenberg, B.C., and Tranquillo, R.T. Long-term cyclic distention enhances the mechanical properties of collagen-based media-equivalents. Annals of biomedical engineering 31, 937, 2003.

78. Syedain, Z.H., Weinberg, J.S., and Tranquillo, R.T. Cyclic distension of fibrin-based tissue constructs: evidence of adaptation during growth of engineered connective tissue. Proceedings of the National Academy of Sciences of the United States of America 105, 6537, 2008.

79. Syedain, Z.H., Meier, L.A., Bjork, J.W., Lee, A., and Tranquillo, R.T. Implantable arterial grafts from human fibroblasts and fibrin using a multi-graft pulsed flow-stretch bioreactor with noninvasive strength monitoring. Biomaterials, 2010.

80. Ye, Q., Zund, G., Benedikt, P., Jockenhoevel, S., Hoerstrup, S.P., Sakyama, S., Hubbell, J.A., and Turina, M. Fibrin gel as a three dimensional matrix in cardiovascular tissue engineering. Eur J Cardiothorac Surg 17, 587, 2000.

81. Jockenhoevel, S., Zund, G., Hoerstrup, S.P., Chalabi, K., Sachweh, J.S., Demircan, L., Messmer, B.J., and Turina, M. Fibrin gel -- advantages of a new scaffold in cardiovascular tissue engineering. Eur J Cardiothorac Surg 19, 424, 2001.

82. Williams, C., Johnson, S.L., Robinson, P.S., and Tranquillo, R.T. Cell sourcing and culture conditions for fibrin-based valve constructs. Tissue engineering 12, 1489, 2006.

83. Robinson, P.S., Johnson, S.L., Evans, M.C., Barocas, V.H., and Tranquillo, R.T. Functional tissue-engineered valves from cell-remodeled fibrin with commissural alignment of cell-produced collagen. Tissue engineering 14, 83, 2008.

84. Yee, K.O., Rooney, M.M., Giachelli, C.M., Lord, S.T., and Schwartz, S.M. Role of beta1 and beta3 integrins in human smooth muscle cell adhesion to and contraction of fibrin clots in vitro. Circulation research 83, 241, 1998.

85. Cummings, C.L., Gawlitta, D., Nerem, R.M., and Stegemann, J.P. Properties of engineered vascular constructs made from collagen, fibrin, and collagen-fibrin mixtures. Biomaterials 25, 3699, 2004.

86. Yao, L., Swartz, D.D., Gugino, S.F., Russell, J.A., and Andreadis, S.T. Fibrin-based tissue-engineered blood vessels: differential effects of biomaterial and culture parameters on mechanical strength and vascular reactivity. Tissue engineering 11, 991, 2005.

87. Hong, H., and Stegemann, J.P. 2D and 3D collagen and fibrin biopolymers promote specific ECM and integrin gene expression by vascular smooth muscle cells. Journal of biomaterials science 19, 1279, 2008.

88. Hunter, C.J., and Levenston, M.E. Maturation and integration of tissue-engineered cartilages within an in vitro defect repair model. Tissue engineering 10, 736, 2004.

89. Mol, A., van Lieshout, M.I., Dam-de Veen, C.G., Neuenschwander, S., Hoerstrup, S.P., Baaijens, F.P., and Bouten, C.V. Fibrin as a cell carrier in cardiovascular tissue engineering applications. Biomaterials 26, 3113, 2005.

90. Rowe, S.L., and Stegemann, J.P. Interpenetrating collagen-fibrin composite matrices with varying protein contents and ratios. Biomacromolecules 7, 2942, 2006.

91. Bian, W., and Bursac, N. Engineered skeletal muscle tissue networks with controllable architecture. Biomaterials 30, 1401, 2009.

92. Kupcsik, L., Alini, M., and Stoddart, M.J. Epsilon-aminocaproic acid is a useful fibrin degradation inhibitor for cartilage tissue engineering. Tissue engineering 15, 2309, 2009.

93. Arts, C.H., Blankensteijn, J.D., Heijnen-Snyder, G.J., Verhagen, H.J., Hedeman Joosten, P.P., Sixma, J.J., Eikelboom, B.C., and de Groot, P.G. Reduction of non-endothelial cell contamination of microvascular endothelial cell seeded grafts decreases thrombogenicity and intimal hyperplasia. Eur J Vasc Endovasc Surg 23, 404, 2002.

94. Solovey, A., Lin, Y., Browne, P., Choong, S., Wayner, E., and Hebbel, R.P. Circulating activated endothelial cells in sickle cell anemia. The New England journal of medicine 337, 1584, 1997.

95. Lin, Y., Weisdorf, D.J., Solovey, A., and Hebbel, R.P. Origins of circulating endothelial cells and endothelial outgrowth from blood. The Journal of clinical investigation 105, 71, 2000.

96. Ingram, D.A., Caplice, N.M., and Yoder, M.C. Unresolved questions, changing definitions, and novel paradigms for defining endothelial progenitor cells. Blood 106, 1525, 2005.

97. Ingram, D.A., Mead, L.E., Tanaka, H., Meade, V., Fenoglio, A., Mortell, K., Pollok, K., Ferkowicz, M.J., Gilley, D., and Yoder, M.C. Identification of a novel hierarchy of endothelial progenitor cells using human peripheral and umbilical cord blood. Blood 104, 2752, 2004.

98. Byrom, M.J., Bannon, P.G., White, G.H., and Ng, M.K. Animal models for the assessment of novel vascular conduits. J Vasc Surg 52, 176, 2010.

Chapter 2: Fibrin-Based Tissue Construct Degradation and Remodeling

2.1 Introduction

This chapter examines the importance of fibrin degradation in new matrix deposition in fibrin-based constructs. Methods to optimize fibrin degradation will require an understanding of the effects of fibrin degradation and the generation of fibrin degradation products in matrix deposition and cell proliferation. This chapter has been published in a modified form in Tissue Engineering Part A (1). Fibrin zymography was performed by Justin Weinbaum and the development of the ELISA for fibrin degradation products (FDPs) is the work of Sandra Johnson.

The plasma protein fibrinogen has been widely utilized in the field of tissue engineering. Scaffolds fabricated from fibrin gel have been successfully employed for growth of bone marrow stromal cells (2), chondrocytes (3), osteoblasts (4), and nerve axons (5). They have been used as scaffolds in cardiovascular tissue engineering (6-9) and seeded with smooth muscle cells (SMCs) for vascular tissue engineering (10-18).

Fibrin gel has also been explored as a method for *in vitro* and *in vivo* cell delivery (19-21) and drug delivery (22). Furthermore, fibrin glues are already FDP approved and have a proven track in surgery and clinical practice as a hemostatic agent (23).

As a biopolymer, fibrin has a number of advantages, including the option for direct cell entrapment during construct fabrication, the availability of sites for cellular adhesion and binding of matrix molecules and growth factors, and the ability to produce alignment of cells and fibrils in gels that are mechanically constrained during gel compaction (24, 25). Fibrin-based constructs undergo extensive matrix remodeling as the cells degrade fibrin and deposit extracellular matrix (ECM) (12-14). vSMC secrete more collagen and elastin in fibrin gel compared to collagen gel, producing constructs with superior mechanical properties (11, 13).

Fibrin gel is formed by the thrombin-catalyzed self-assembly of fibrin monomers, derived from fibrinogen, into native protein filaments. This process forms a fibrin gel entrapping the cells suspended in the fibrinogen solution, analogous to the entrapment of platelets in a fibrin clot during wound healing (26, 27). The serine protease plasmin acts *in vivo* to resorb the thrombus, after activation of the zymogen plasminogen by urokinase (uPA) or tissue plasminogen activator (tPA) (28). Fibrin degradation can be modulated by the addition of plasmin inhibitors, such as aprotinin or ε-aminocaproic acid (ACA). ACA inhibits uPA (29), tPA (30), and plasmin (31, 32), and is widely used in tissue engineering to slow fibrin degradation (20, 33-36).

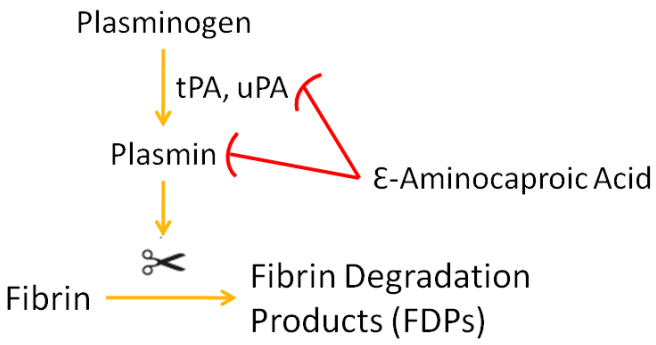

Figure 2.1: Fibrinolysis and inhibition by Aminocaproic Acid (ACA).

Controlling the rate of fibrinolysis is of great importance when using fibrin gel as a tissue scaffold. Extensive degradation of the gel before the cells secrete sufficient ECM results in construct failure; however, excessive fibrinolytic inhibition could limit fibrin remodeling into tissue and also result in failure. This is one practical reason why the rate of fibrin degradation needs to be carefully controlled. Fibrin gels are more than inert scaffolds for cell seeding, though. As a biopolymer, fibrin has protein and cellular binding sites that create a bioactive surface for cell growth. Its presence in the system may improve initial seeding as well as construct growth over time (20). It is also possible that the degradation of fibrin into fibrin degradation products (FDP) may provide direct stimulus for the cells. FDP have been shown to have biological activity in simplified systems and may aid in the remodeling of the fibrin constructs. For example, plasmin-generated FDP fragment E and atherosclerotic plaque extracts have been shown to have mitogenic effects on SMCs (37), and plasmin-derived FDP stimulated collagen synthesis in the chick chorioallantoic membrane model (38).

The goal for this study was to examine how fibrin degradation affects proliferation of and matrix deposition by vSMC in fibrin-based tissue constructs. An ELISA was developed to monitor levels of bovine FDP in the medium of fibrin-based tissue constructs. The fibrinolytic inhibitor ACA was utilized to alter fibrin degradation by plasmin and examine the effects on collagen and elastin deposition and cell proliferation in fibrin constructs over long-term culture. FDP concentrations in the interstitial fluid of the constructs were measured in order to estimate the FDP concentrations in proximity to the vSMC during construct degradation. To determine if these concentrations of FDP were bioactive, cell cultures were supplemented with exogenous FDP over a range of concentrations and changes in cellularity and collagen content were measured. Finally, to demonstrate that FDP were bioactive in the tissue constructs, exogenous FDP were added under conditions of fibrin degradation inhibition.

2.2 Materials and Methods

2.2.1 Cell Culture

vSMC were isolated from 1-3 day old Fischer rat aortae, as previously described (12). Cell type was verified by staining with α-smooth muscle actin and smooth muscle myosin heavy chain antibodies (Abcam Inc., Cambridge, MA; Figure 2.2). The cells were maintained in DMEM/F12 supplemented with 100 U/ml penicillin, 100 U/ml streptomycin (Invitrogen, Carlsbad, CA), and 15% fetal bovine serum (FBS; Thermo Fisher Scientific, Waltham, MA). All culture flasks were seeded with 20,000 cells/cm^2, split near confluence, and used at passage six for construct fabrication.

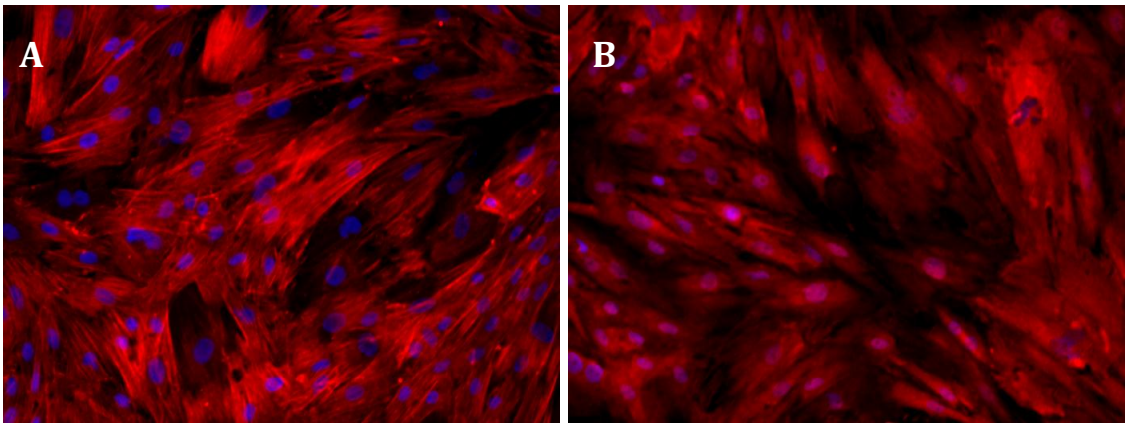

Figure 2.2: Neonatal rat SMCs display a normal SMC phenotype. At passage 6, vSMCs express A) α-smooth muscle actin and B) smooth muscle myosin heavy chain.

2.2.2 Fabrication of Fibrin-based Adherent Disc Constructs

Adherent disc constructs were prepared as previously described (12). For these studies, the initial concentrations were $5x10^5$ vSMC/ml and 3.3 mg/ml fibrinogen solid (F4753, Sigma Aldrich, St. Louis, MO); 200 µl of fibrin gel was used for each 1 cm diameter disc construct. After fibrin gelation, construct medium consisting of DMEM/F12, antibiotic/antimycotic (Invitrogen), 10% FBS, 50 µg/ml ascorbate (Sigma Aldrich), 1 ng/ml TGF-β (R&D Systems, Minneapolis, MN), and 2 µg/ml insulin (Sigma Aldrich), plus 3, 6, or 12 mM ACA (Thermo Fisher Scientific) was added at an initial volume of 2 ml per construct and replaced with 1 ml of this supplemented medium every 2-3 days. A medium sample was collected prior to each medium change. Constructs were harvested weekly for 5 weeks.

In a separate set of experiments, constructs grown in 3 and 12 mM ACA received 0, 100, 250 or 500 µg/ml bovine plasmin-derived FDP 24 hours after casting and again

with each medium change. FDP were formed as described in the ELISA section. Constructs were harvested at 1 week.

2.2.3 Fabrication of Fibrin-based Tubular Constructs

The fabrication of tubular constructs has been previously described (39). The tubular constructs were prepared using the same fibrin gel solutions as the disc constructs, however the solution of fibrinogen, thrombin, and cells was injected into a tubular glass mold 7.5 cm long with a 9 mm outer diameter and a 2 mm inner glass mandrel. The mandrel was pre-coated in 5% Pluronics F127 (Sigma) for 3 hours to limit adhesion between the fibrin gel and the mandrel. The fibrinogen solution was allowed to gel for 30 minutes and then the mandrel and fibrin gel was ejected from the glass mold and cultured in the same medium as the adherent disc constructs. Constructs were incubated statically on the mandrel and medium was changed three times per week until harvest at 5 weeks.

2.2.4 ELISA for Bovine Fibrin Degradation Products

FDP present in media were quantified with a competitive ELISA using anti-bovine fibrinogen (American Diagnostica Inc., Stamford, CT) as the primary antibody and purified bovine fibrinogen (Aniara, Mason, OH) as the coating antigen and concentration standard. This fibrinogen was converted to fibrin using the same conditions as construct preparation, digested overnight at 37°C with human plasmin (Sigma Aldrich) at 0.04 U/mg protein in 50 mM Tris, 100 mM NaCl, 10 mM $CaCl_2$, pH 7.6. Plasmin was quenched with aprotinin (Sigma Aldrich) at 100 KIU/ml and the digest (BV-FDP) was adjusted to 1 µg/ml in PBS.

EIA/RIA plates (Corning Inc., Lowell, MA) were coated overnight at 4°C with BV-FDP. All other incubations were 1 hour at room temperature in PBST. The plate was then blocked with 1% BSA (IgG and protease free, Jackson ImmunoResearch Laboratories, Inc., West Grove, PA). Solutions of primary antibody (3.33 µg/ml) plus either known amounts of BV-FDP or diluted sample media were incubated, added to the plate and incubated again to allow free antibody to bind to the FDP coated on the plate. Since the ELISA also detected fibrinogen products in FBS, both media and standards were at kept at the same FBS concentration. Attached primary antibody was bound to an HRP-conjugated secondary antibody (Jackson ImmunoResearch) used at 1:50,000. The bound HRP was incubated with TMB substrate solution (Thermo Fisher Scientific) to yield color inversely proportional to FDP concentration. After quenching with 2.5 M H_2SO_4, the plates were read at 450 nm with background subtraction (BioTek Instruments, Inc., Winooski, VT). Completely digested vSMC constructs contained 330 µg FDP.

In one set of experiments, constructs were harvested daily and pooled to allow for quantification of interstitial FDP. In these studies, 100 KIU/ml aprotinin and 10 µM Galardin (Millipore, Billerica, MA) were added to the medium one hour prior to harvest and samples of medium were collected for quantification. Then, all medium was aspirated from the construct surface and the constructs were collected into chilled vials and centrifuged at 10,000 x g at 4°C for 15 minutes. The supernatant was collected and used to quantify FDP within the construct via ELISA.

2.2.5 Fibrinogen Zymography

Polyacrylamide gels were prepared with the addition of 375 μg/ml fibrinogen to the resolving phase. Medium, human activated plasmin, or α_2-antiplasmin (Abcam Inc.) were loaded as indicated then separated by electrophoresis. The gel was rinsed, extracted in 2.5% Triton X-100 (Sigma Aldrich), rinsed again, then incubated in reaction buffer (50 mM Tris pH 7.4, 1 mM $CaCl_2$, 1 mM $MgCl_2$) at 37°C overnight. ACA was added to the buffer as indicated. Digested gels were stained (Blue BANDit, Amresco Inc., Solon, OH) then scanned for qualitative analysis.

2.2.6 Stimulation of Cell Monolayers

vSMC were plated in 6 well plates at an initial density of 20,000 cells/cm^2 and were maintained in construct medium. At 24 hours and again with every feeding, either BV-FDP (0, 100, 250, 500 μg/ml) or ACA (0, 3, 6, 12 mM) was added to the medium. The medium was changed on day 3 and 6 and harvested at 1 week.

2.2.7 Biochemical and Histochemical Analysis

DNA was quantified with a modified Hoechst assay (40). Cellularity was determined assuming 7.6 pg of DNA per cell (41). Collagen content was measured with the hydroxyproline assay of Stegemann and Stadler (42), with collagen per sample calculated using a conversion factor of 7.46 μg of collagen per μg of 4-hydroxyproline (43). Elastin content was measured using the modified ninhydrin assay (13, 44).

Constructs for histology were fixed in 4% paraformaldehyde for 3 hours, followed by infiltration with a solution of 30% sucrose and 5% DMSO. Samples were frozen in

OCT (Tissue-Tek, Torrance, CA), sectioned into 9 μm thick cross-sections and then stained with Lillie's trichrome and Picrosirius red (45). Images were taken with an Zeiss Axiovert or Olympus IX70 inverted microscope equipped with color CCD camera. For Picrosirius red imaging, samples were placed between crossed plane polarizers.

2.2.8 Mechanical Testing

Tubular constructs were sectioned into 2-3 mm long rings and mechanically tested using a Microbionix mechanical testing system (MTS Systems). Before testing, tissue thickness was measured using a 50-g force probe attached to a displacement transducer. Rings were mounted and tested as previously described (46). True strain was calculated based on the change in length of the tissue over time. The stress was calculated as force divided by the initial cross-sectional area. The elastic modulus was determined by linear regression of the linear region of the stress-strain curve.

2.2.9 Statistical Analysis

Statistical analysis was performed using one-way ANOVA for cell culture studies conducted with one time point and two-way ANOVA for 5-week construct studies and construct studies with combined ACA and FDP treatments in GraphPad Prism software for Windows (GraphPad Software, Inc., San Diego, CA). Tukey post hoc analysis was conducted to evaluate significant differences. A significance level of $\alpha=0.05$ was used for all tests. Pearson's correlation coefficient was calculated to examine the correlation between fibrin degradation and ECM deposition or cellularity. Linear regression was performed to examine the relationship between FDP concentration in the culture medium

and collagen deposition. The best fit line and 95% confidence intervals are shown in Figure 2.3D.

2.3 Results

2.3.1 ACA leads to both a delay and decrease in FDP release.

Fibrin-based tissue constructs cultured in the absence of plasmin inhibition are completely degraded within 24 hours of casting, which is prevented by addition of ACA to the medium. The ACA acts to inhibit plasmin activity, limiting the rate of fibrin degradation and maintaining the fibrin scaffold while SMCs produce new ECM. To examine the effect of plasmin inhibition on scaffold digestion, an ELISA was developed to quantify FDP in the culture medium. This allowed for the non-destructive monitoring of fibrin degradation. Of particular interest were the times of peak fibrin degradation, the time course of fibrin degradation, and the cumulative FDP generated.

Addition of varying concentrations of ACA to the tissue constructs produced large differences in the rate of fibrin degradation, the peak FDP concentrations, and the time of maximal FDP release. Tissue constructs cultured with high ACA released few FDP, never exceeding a medium concentration of approximately 20 μg/ml (Figure 2.3A). For intermediate and low ACA concentrations, the maximal FDP concentration increased to approximately 50 and 120 μg/ml, respectively. Higher ACA concentrations also shifted the time of maximal FDP generation. Peaks in FDP generation occurred earliest for the low ACA samples and latest for the high ACA samples, at days 8 and 18,

respectively. After 5 weeks in culture, nearly 90% of the initial fibrin had been digested in the low ACA constructs, while in high ACA constructs only 40% of the initial fibrin was digested (Figure 2.3B).

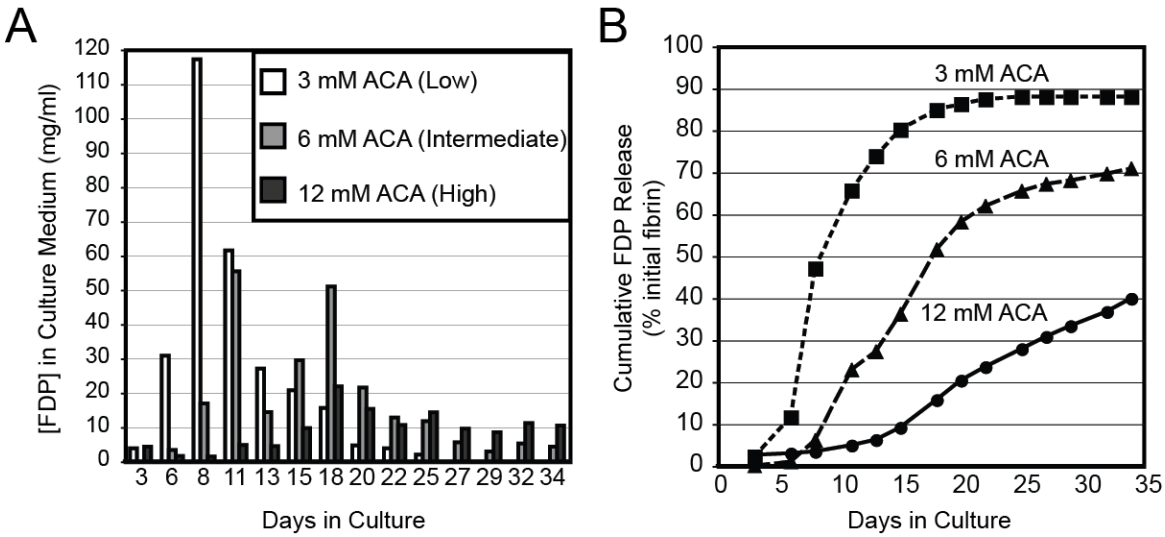

Figure 2.3: Plasmin inhibition reduces and delays FDP release from tissue constructs. A) FDP concentrations in the culture medium were measured for 5 weeks. Each data point represents analysis of pooled medium from five constructs at each ACA concentration (low, intermediate, and high, corresponding to 3, 6, and 12 mM ACA, respectively). B) Cumulative FDP release over 5 weeks is shown, expressed as a percentage of the initial fibrin that has been degraded.

2.3.2 Fibrinolytic activity in the culture medium is primarily due to plasmin.

To identify the enzyme(s) relevant to fibrinolysis in the constructs, fibrinogen zymography was used by preparing polyacrylamide gels supplemented with the same fibrinogen used in construct fabrication. Medium from constructs cultured overnight without ACA, representing peak plasmin activity, served as a positive control for this assay. The primary fibrinolytic bands appeared as a doublet near 72/74 kD and a poorly resolved doublet near 140 kD (Figure 2.4A). Addition of ACA at the levels used in

construct culture inhibited digestion by all species, pointing to their identity as complexes of the serine protease plasmin. This study, in agreement with previous work (47), demonstrates that vSMC use endogenous plasminogen activators, such as uPA, to activate plasminogen present in serum (48), producing plasmin that can be used for fibrinolysis.

Purified plasmin migrates as a doublet near 72/74 kD that, in the presence of serum-containing culture medium, shifts largely to the doublet at 140 kD, consistent with the migration of plasmin and the plasmin/α_2-antiplasmin complex, respectively (49, 50). To confirm this, a mixture of plasmin with purified α_2-antiplasmin was analyzed by zymography, and this migrated as the same 140 kD doublet (Figure 2.4B). Since plasminogen binds to α_2-antiplasmin 1000-fold more weakly than plasmin (K_D = 3 nM and 3 μM for plasmin and plasminogen, respectively) (32), and assuming a constant α_2-antiplasmin serum concentration, this complex should be relatively insensitive to plasminogen and correlate with plasmin activity. In addition, the 72/74 kD band could easily be confused with a fibrinolytic activity present in serum. Therefore, the 140 kD species was chosen for following plasmin activity generated by the constructs.

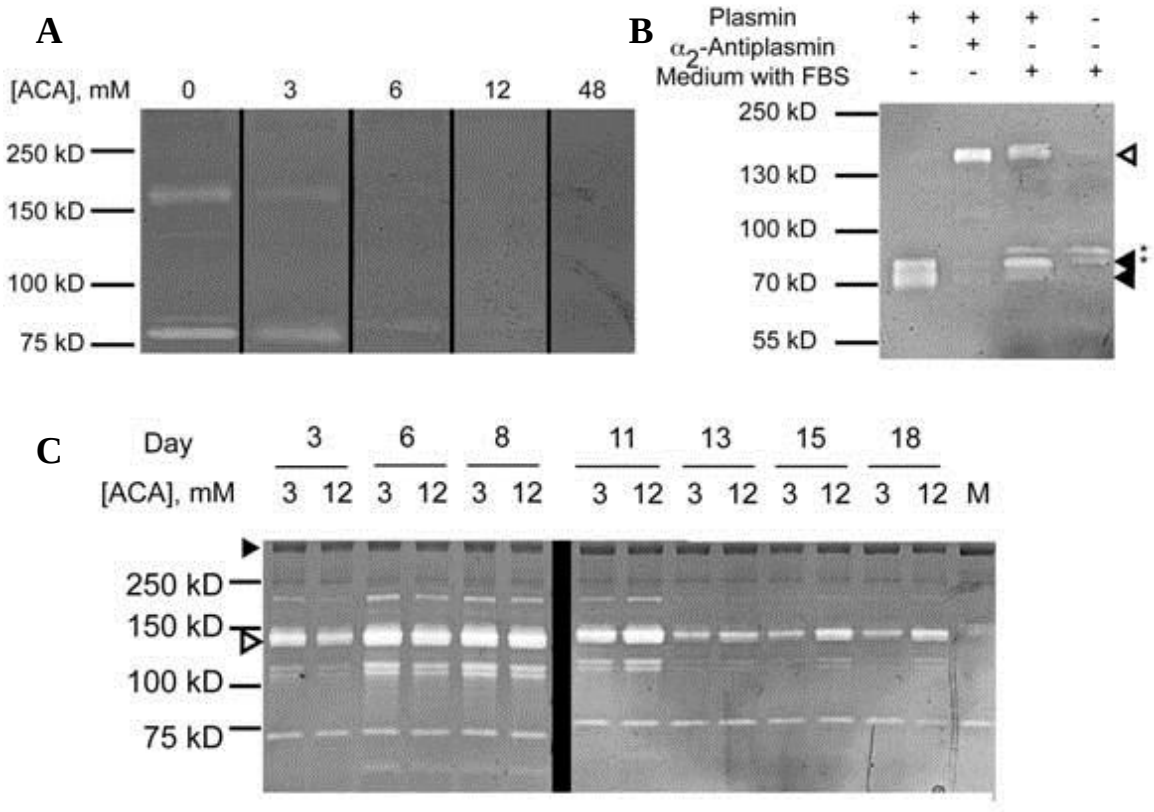

Figure 2.4: Plasmin/□2-antiplasmin complexes are detectable in the conditioned medium of tissue constructs. A, ACA added to the zymogram reaction buffer decreases fibrinolytic activity in a concentration dependent manner. B, Plasmin binds to α_2-antiplasmin in FBS-containing culture medium to form a SDS-resistant 140 kD complex. Plasmin migrated as a doublet (black arrowheads) that shifted completely or partially to a high molecular weight complex (white arrowhead) in the presence of α_2-antiplasmin or serum-containing medium, respectively. * denotes fibrinolytic activity found in FBS. C, Plasmin in tissue construct medium decreased over time and in response to plasmin inhibition. "M" denotes fresh construct medium. The white arrowhead indicates the plasmin/α_2-antiplasmin complex identified in Figure B. The black arrowhead indicates a high molecular weight protein found in the culture medium that served as a loading control.

2.3.3 Plasmin activity precedes FDP release into the medium.

Medium samples from constructs incubated in varying ACA concentrations were analyzed for plasmin activity. As expected, the 140 kD bands associated with plasmin complexes were identified in the culture medium, and this plasmin activity appeared as early as day three, prior to the peak FDP levels identified by ELISA (Figure 2.4C). Constructs grown in low levels of ACA showed the greatest initial fibrinolytic activity in the culture medium, which declined after several medium changes and was at background levels within two weeks. In contrast, the culture medium of constructs grown in high levels of ACA showed a more sustained fibrinolytic profile with lower levels of initial activity, consistent with sustained FDP production (Figure 2.3A). After two weeks, the band intensity in high ACA constructs also decreased, but remained above background levels. Similar patterns of fibrinolytic activity to that seen for the 140 kD complex were seen with bands at 110/120 and 230 kD, which are presumably also plasmin complexes.

2.3.4 Reduced ACA leads to higher collagen and elastin deposition and increased cellularity.

Constructs were harvested weekly to examine the effects of ACA on collagen and elastin deposition and construct cellularity. Collagen and elastin levels increased over the 5-week culture period in all groups (Figure 2.5A,B). Collagen content was consistently higher for constructs grown in low ACA, while high ACA samples had the lowest collagen content. Elastin levels showed a similar trend. There was a positive correlation between the percentage of FDP that had been degraded and both the collagen (r^2=0.81, $p<0.001$) and elastin (r^2=0.69, $p<0.001$) content. The weekly amounts of collagen and elastin deposited so that times of peak elastin and collagen deposition could be compared

with the concentration of FDP in the medium during the preceding week. For the low ACA group, collagen deposition was highest during the first week and decreased weekly, except for a spike at week 4 (Figure 2.5C). Constructs grown in higher concentrations of ACA, which had delayed peaks in fibrin degradation (Figure 2.3A), had delayed peaks in collagen deposition as well: the intermediate and high ACA groups had maximal collagen deposition in the second week. A positive correlation was found between the concentration of FDP in the medium and the collagen produced each week during the first two weeks of remodeling (r^2=0.84, $p<0.01$) (Figure 2.5D). In contrast to the collagen results, weekly elastin deposition did not correlate with FDP concentrations in the medium (Figure 2.5E). (r^2=0.34), p=0.22). Over the first four weeks, elastin deposition/week increased for the low ACA group and was consistently elevated compared to the high ACA group.

Increased collagen and elastin content of the low ACA tissue constructs could be due in part to higher cellularity. By week 1, the vSMC in all constructs had proliferated, with highest construct cellularity occurring in the constructs grown in the lowest ACA concentration (Figure 2.5F). The cellularity increased in all three groups over the course of the five weeks, with the highest number of population doublings occurring in the first week for all ACA concentrations.

However, the increased cellularity does not entirely explain the higher collagen in the low ACA group: in the first week, vSMC deposited more collagen per cell in the low ACA constructs than in the intermediate and high ACA constructs (Figure 2.6). Since the higher collagen deposition in the low ACA group cannot be fully explained by the

increased cellularity of these constructs, other possible factors influencing collagen deposition will be examined.

Trichrome and Picrosirius red staining of constructs harvested at 5 weeks revealed the differences in fibrin remodeling that occurred depending on ACA concentration (Figure 2.7). The low ACA constructs showed extensive remodeling with visible collagen deposition, while the high ACA constructs had more limited remodeling and minimal collagen staining. A thickness difference is also apparent in these constructs, with the less remodeled, high ACA constructs consistently appearing thicker than the low ACA constructs. Nuclear staining with Hoechst 33342 confirmed higher cellularity in the low ACA constructs compared to the high ACA constructs at 1 week (Figure 2.8A,B), as well as at the 5 week experimental end point (Figure 2.8C,D).

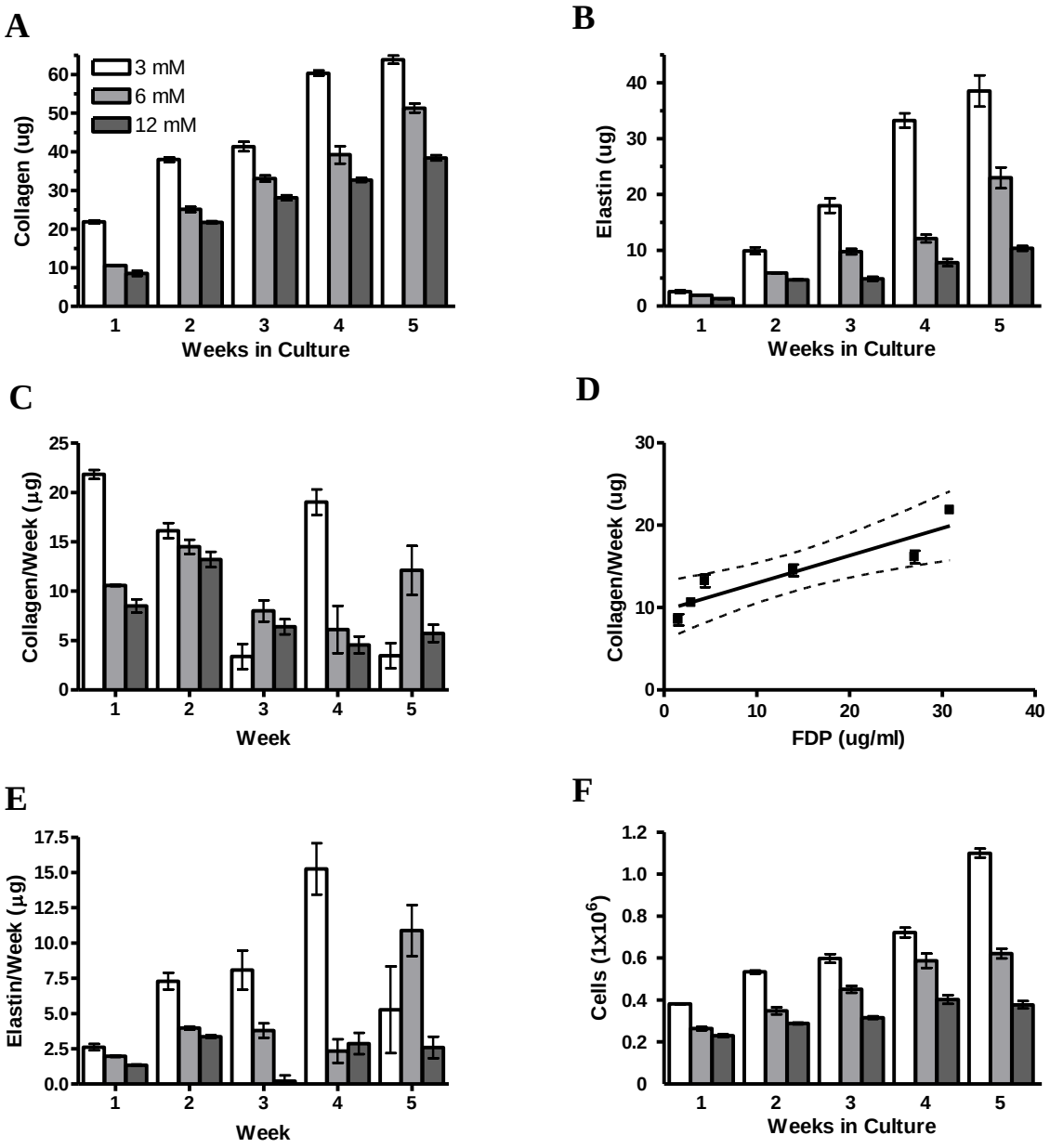

Figure 2.5: Plasmin inhibition decreases collagen and elastin content and cellular proliferation in tissue constructs. A) Collagen and B) elastin contents increased with time and were lower with higher ACA treatment. C) Net collagen deposited per week, and E) net elastin deposited per week are shown to depict times of peak ECM deposition. D) A correlation exists between the FDP concentration 24 hours prior to harvest in the medium and the collagen deposited for that week during the first two weeks of remodeling (r^2=0.84, $p<0.01$). Dashed lines represent the 95% confidence band for the regression line. F) Cellularity of constructs decreased with increasing ACA concentrations. Values are mean ± SEM for 5 constructs in all panels.

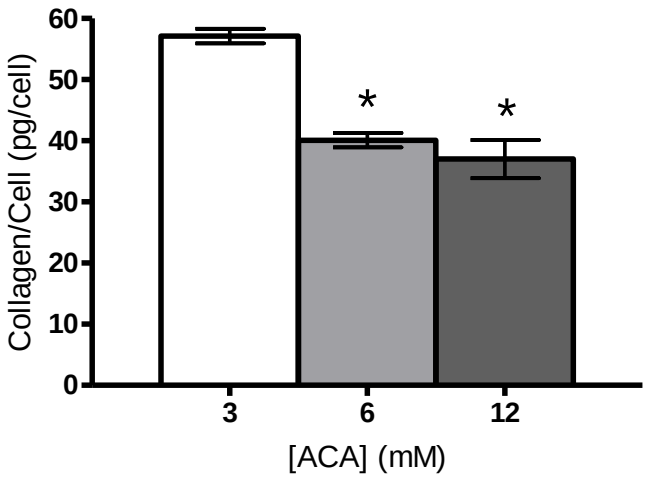

Figure 2.6: Collagen deposited per cell was higher in the low ACA constructs during the first week. * indicates a significant difference ($p<0.05$) from low ACA samples.

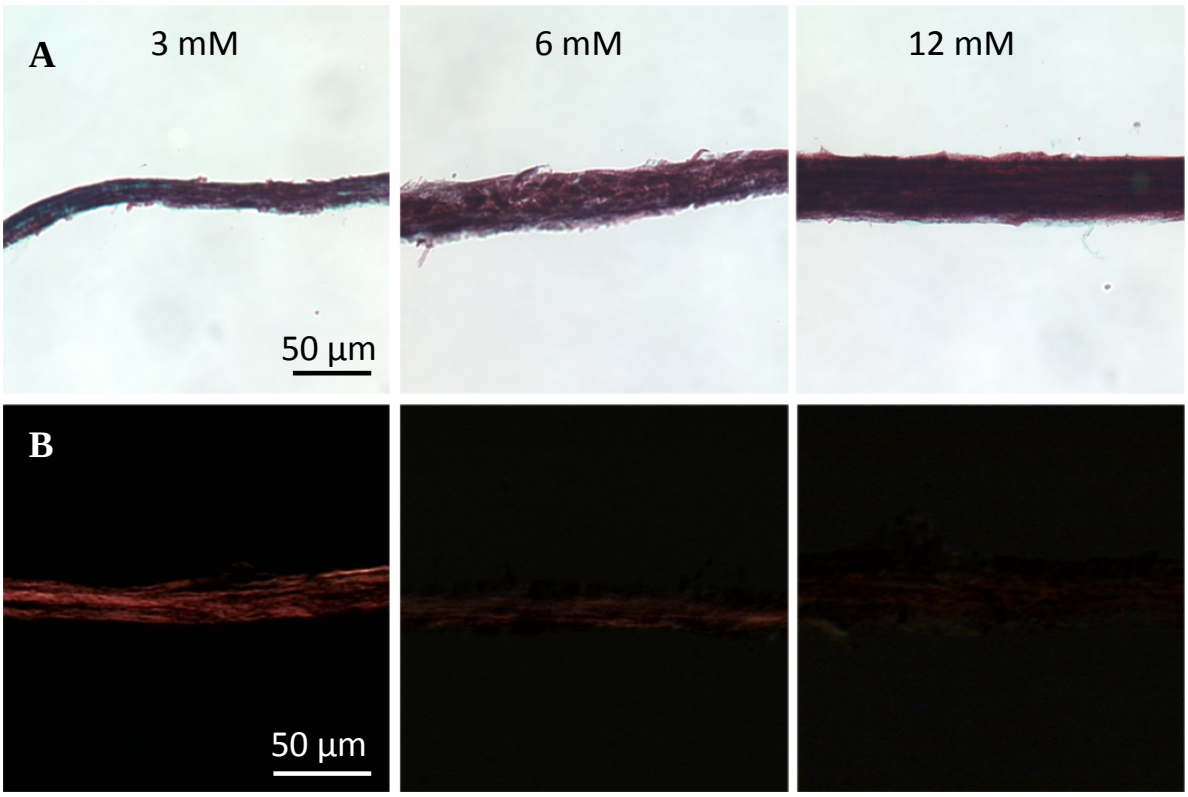

Figure 2.7: Histological sections show enhanced remodeling of low ACA constructs. A) Lillie's trichrome staining of five-week constructs shows enhanced fibrin remodeling in the low ACA constructs. Collagen-rich regions stained green, residual fibrin and other non-collagenous protein are red, and nuclei stained black. The 3 mM ACA construct has visible collagen staining and more extensive remodeling than the higher (6, 12 mM) ACA constructs. B) Picrosirius red staining indicates increased and/or more mature collagen content in low ACA constructs. Images were exposed identically to visualize staining in the 3 mM construct. Scale bar=50 µm.

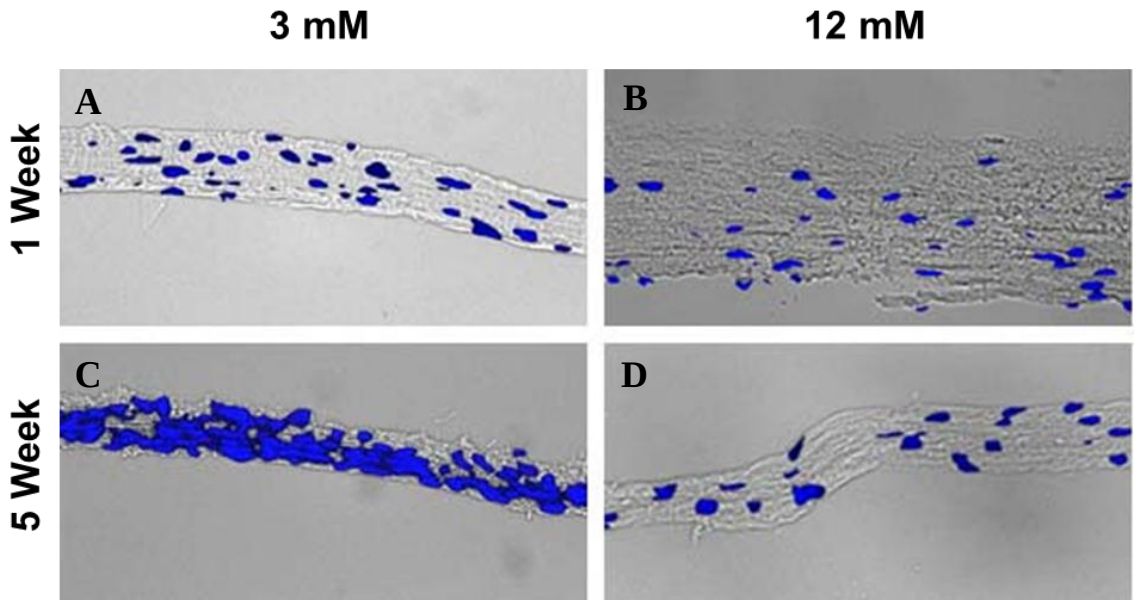

Figure 2.8: Increased cellularity is apparent in low ACA constructs. Hoechst 33342 staining of SMC nuclei shows increased staining in A,C) 3 mM ACA constructs compared to B,D) 12 mM ACA constructs. Staining was performed at A-B) 1 week of culture and C-D) 5 weeks of culture.

To address the functional consequence of reduced collagen content in fibrin-based constructs, tubular constructs were cultured in varying ACA concentrations and harvested after 5 weeks for mechanical testing. Use of 3 mM ACA produced tubular constructs that were too difficult to handle, and could not be measured accurately for thickness or mechanical properties using our current methods. This also made the 3 mM ACA constructs unpractical as vascular grafts, thus only higher ACA concentrations (6, 9 and 12 mM ACA) were examined. Tubular constructs cultured in 6 mM ACA had higher collagen and cell densities compared to 12 mM ACA constructs (Figure 2.9A,B). The 6 mM constructs were also stiffer than the 12 mM constructs (Figure 2.9C). As was apparent in the histology for the disc constructs, the tubular constructs were thicker when high ACA was used (Figure 2.9D), however this did not affect the final length of the tubular constructs (Figure 2.9E). Lillie's trichrome stains of the tubular constructs show higher staining for collagen, both on the luminal and abluminal surface, for constructs grown in low ACA (Figure 2.10). These results compare well to the results with fibrin discs and illustrate that the increased collagen deposition correlates with increased construct stiffness.

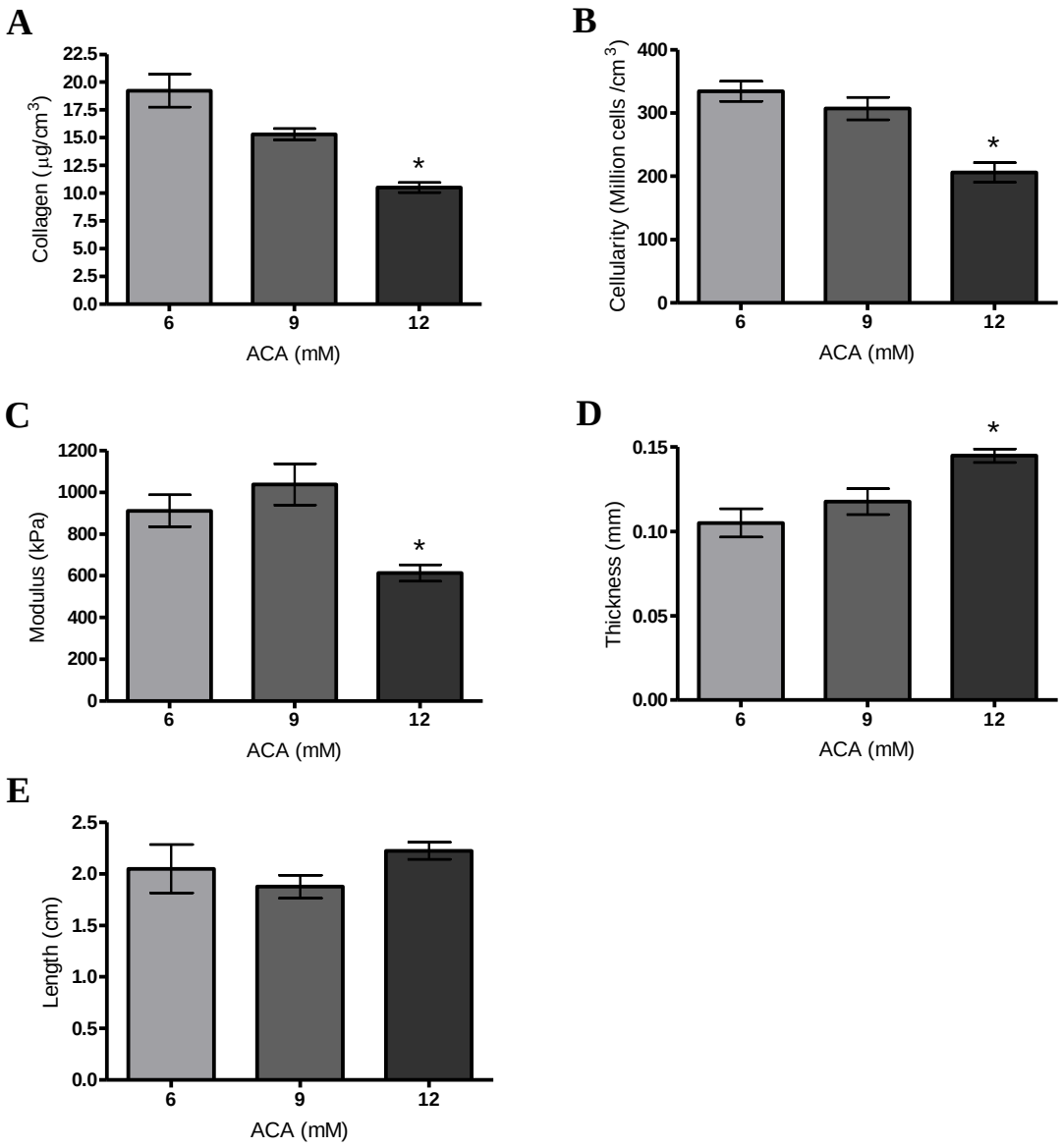

Figure 2.9: ACA decreases collagen and cell density, as well as the stiffness, of tubular fibrin-based tissue constructs after 5 weeks in culture. A) collagen density and B) cell density of constructs were decreased with high ACA treatment. C) High ACA decreased Young's modulus of tubular tissue constructs. D) Constructs grown with high ACA were thicker than low ACA constructs. E) There was no significant difference in final length of the constructs at 5 weeks. Values are mean ± standard deviation for 6 samples.

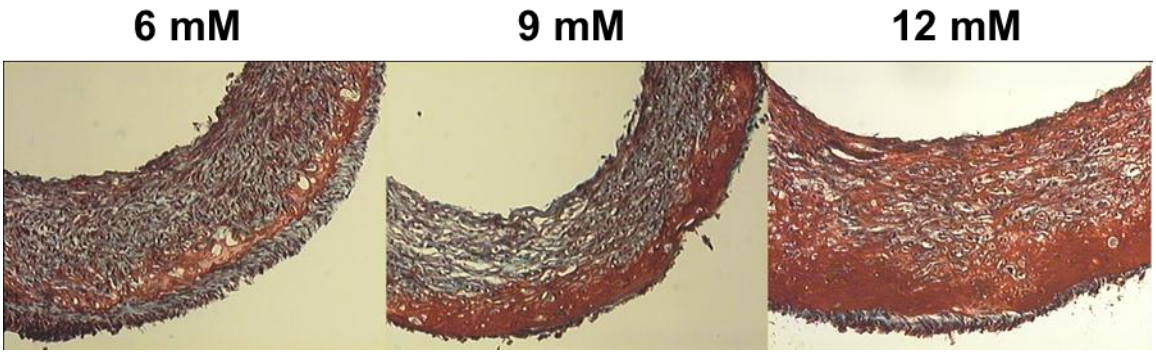

Figure 2.10: Lillie's trichrome staining of tubular constructs shows decreased fibrin remodeling with high ACA treatment. The lumenal surface of the tube is oriented towards the upper left. Collagen is stained green, residual fibrin and other non-collagenous proteins are red, and nuclei are black. The low ACA construct has visible collagen staining and more extensive remodeling than the high ACA constructs. Scale bar=20 μm.

2.3.5 ACA and FDP affect collagen deposition in vSMC culture.

ACA may influence cellularity and collagen deposition in the fibrin-based constructs through a number of mechanisms. To determine if ACA had a direct biological effect on the cells, 0, 3, 6, and 12 mM ACA were used to supplement the medium of vSMC grown on tissue culture plastic, and the cell and collagen contents were quantified after 1 week. As was seen in the constructs (Figure 2.6), significant decreases in collagen deposition per cell occurred at the higher ACA concentrations (Figure 2.11A). There was no difference in cellularity between groups (Figure 2.11B).

To examine potential stimulatory effects of FDP, plasmin-derived FDP were used to supplement the medium of vSMC cultures. There was a 50% increase in collagen deposited per cell when 250 or 500 μg/ml FDP was added (Figure 2.12A), but no difference in cellularity (Figure 2.12B).

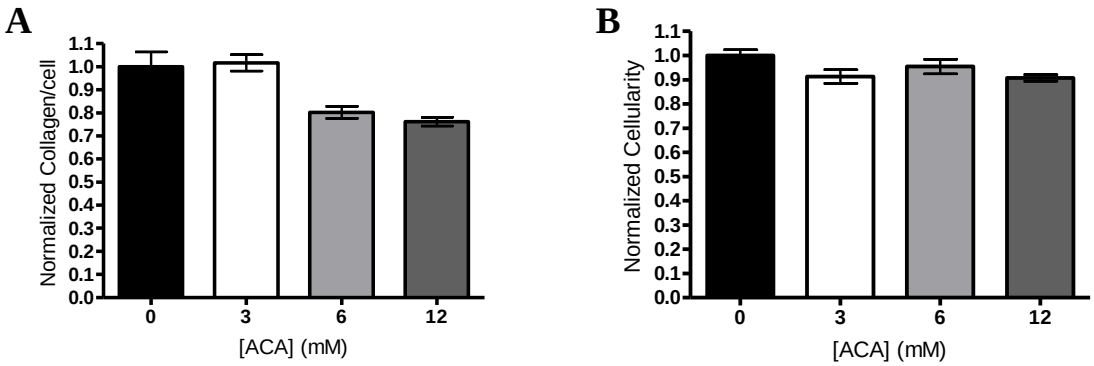

Figure 2.11: Addition of ACA to vSMC on tissue-culture plastic decreased collagen deposition. A) vSMC deposited less collagen per cell when 6 or 12 mM ACA was added. B) Cellularity was not altered by addition of ACA to the medium medium. Values for cellularity and collagen deposition per cell were normalized to the untreated control. Values are mean ± SEM for 6 wells for all panels. * indicates a significant difference compared to control ($p<0.05$).

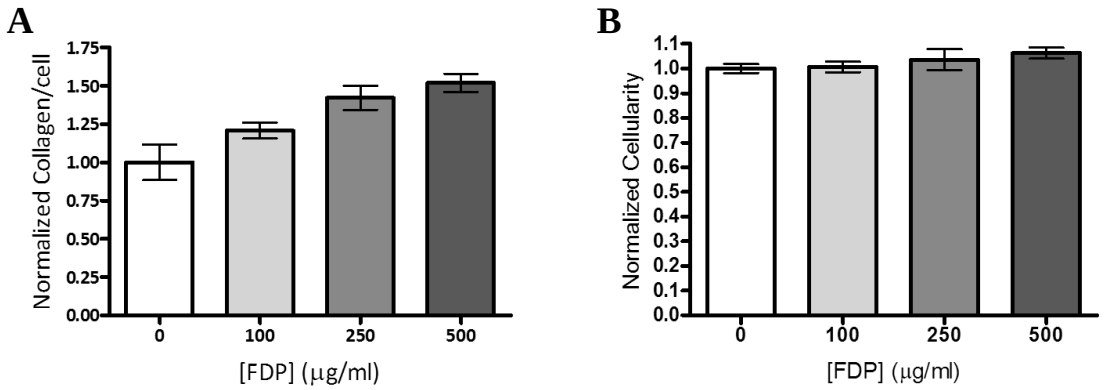

Figure 2.12: Addition of plasmin-generated FDP to vSMC on tissue-culture plastic increased collagen deposition. A) Addition of 250 or 500 μg/ml FDP increased collagen deposition per cell. B) Cellularity was not altered by addition of FDP to the medium. Values for cellularity and collagen deposition per cell were normalized to the untreated control. Values are mean ± SEM for 6 wells for all panels. * indicate a significant difference compared to control ($p<0.05$).

2.3.6 Higher concentrations of FDP are measured within the construct interstitial fluid than in the overlying medium.

The maximal FDP concentration measured in the construct medium was roughly 120 μg/ml (in the low ACA constructs), which is not in the range shown to provide biological activity in vSMC culture (Figure 2.12A). However, the concentration of FDP within the interstitial fluid of the constructs may have been higher due to a high rate of FDP production versus slow diffusion of FDP into the medium and/or binding interactions of FDP with ECM that retarded FDP diffusion into the medium. To examine this possibility, low ACA constructs were harvested for interstitial FDP measurement daily and compared to the medium FDP measurement. There were large differences in these values (Figure 2.13). The largest differences occurred on the days after a medium change, when 6-9 fold increases in FDP concentration were measured within the interstitial fluid. The average difference over the 8 days was approximately a 5-fold increase in FDP measured in the interstitial fluid compared to the medium. After 8 days, sufficient volumes of interstitial fluid were not available for harvest from the constructs. This study was done with a different isolation of vSMC, which most likely accounts for the decreased fibrinolysis in these results as compared to the earlier study (Figure 2.4A). However, it proves that substantially higher concentrations of FDP may be present within the construct than are measured within the overlying medium.

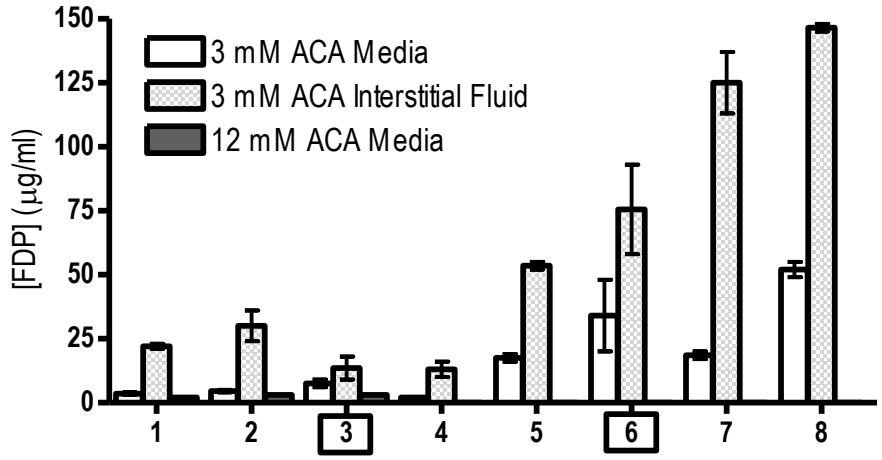

Figure 2.13: The FDP concentration measured in the interstitial fluid of the construct is higher than the FDP concentration measured in the overlying medium. FDP were measured in the medium or interstitial fluid daily for one week. Higher concentrations of FDP were present in the interstitial fluid than in the medium for constructs in 3 mM ACA based on one-way ANOVA ($p<0.05$). Values are mean ± range/2 for n=2. Medium changes occurred on days 3 and 6 and are depicted in the figures with a square around the day; the medium was sampled for the FDP measurement immediately prior to the medium change, thus the medium values are always lower on the following day.

2.3.7 Addition of FDP to construct culture increases collagen deposition.

Supplementation of construct medium with plasmin-derived FDP for one week led to increased collagen deposition (Figure 2.14A) without affecting cellularity (Figure 2.14B). Supplementing with 250 and 500 µg/ml FDP led to increased collagen deposition per cell in low ACA constructs, while an increase in collagen deposition in the high ACA constructs only occurred when 500 µg/ml FDP was added. The FDP concentration profiles shown in Figure 2.13 are from the same second set of experiments and thus represent the low and high ACA constructs that received no added FDP. There was no difference in collagen deposited per cell for these controls (Figure 2.14A) as there was in previous experiments with a different isolation of vSMC (Figure 2.6). This may be due to

the lower fibrinolysis in these constructs during week one for both low and high ACA as compared to the earlier experiments (Figure 2.3A).

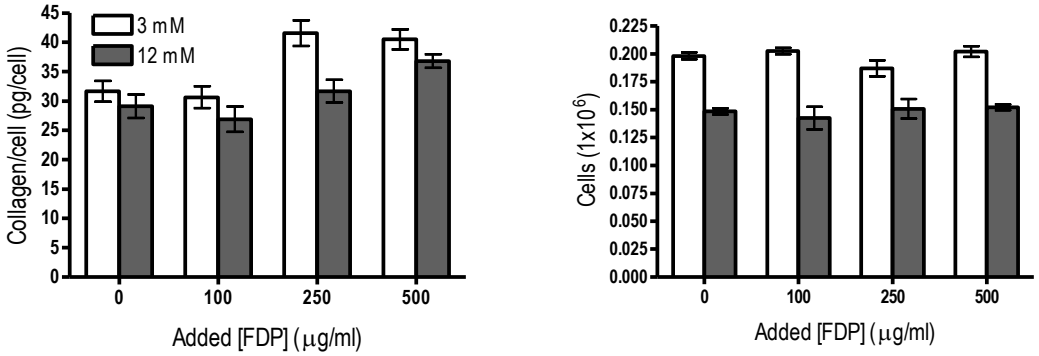

Figure 2.14: Constructs supplemented with high FDP concentrations had increased collagen deposition per cell. A) Collagen deposited per cell was enhanced when constructs were supplemented with FDP. B) Cellularity of constructs was not affected by addition of FDP. Values are mean ± SEM for 5 constructs for both panels. * indicates significant differences ($p<0.05$) compared to low ACA control (3 mM ACA). # indicates significant difference ($p<0.05$) compared to high ACA control (12 mM ACA).

2.4 Discussion

ACA has documented potency against plasmin, uPA, and tPA over the range of 3-12 mM used in this study (29-31). This potency was confirmed by the effective inhibition of zymography using these concentrations. Plasmin inhibition by ACA, either directly or through plasminogen activators, has broad effects on fibrin remodeling driven by vSMC in fibrin-based tissue constructs. Most directly, inhibition prevents the degradation of the network of fibrin fibrils that entraps the vSMC. Without ACA, active plasmin in the system leads to rapid digestion of the fibrin and resulted in the destruction of the tissue construct in less than 24 hours. The use of ACA delayed fibrin degradation, with increasing concentrations of ACA leading to delayed and diminished FDP production.

While a fibrinolytic inhibitor such as ACA is necessary in the system in order to control fibrin degradation, this study shows that ACA can also have negative side effects. Increasing the ACA concentration led to less remodeled constructs, with lower cellularity and lower collagen and elastin content.

The reasons for these negative outcomes with high ACA usage were explored in this chapter. During the first two weeks of construct incubation, the FDP concentration in the medium was highly correlated with collagen deposition. This indicates two likely possibilities for how ACA effects fibrin remodeling: 1) degradation of fibrin is required for new matrix deposition or cell proliferation and/or 2) FDP have a direct biological effect on vSMC that leads to increased matrix deposition or cell proliferation. In support of the latter, vSMC cultures and fibrin constructs supplemented with 250 or 500 μg/ml FDP deposited more collagen per cell than the untreated controls, indicating FDP generation during remodeling of fibrin constructs has the potential for direct biological activity. Cellularity in vSMC culture and constructs was not altered by FDP addition. FDP levels within the construct, and hence the effective local concentration of FDP seen by the cells, were found to be, on average, 5-fold higher than the concentration measured in the medium. Constructs cultured in 3 mM and 6 mM ACA had peak FDP of 120 and 50 μg/ml in the medium and thus could be expected to reach a biologically active FDP concentration within the interstitial fluid of the construct. Since FDP generation is severely reduced when high concentrations of ACA are utilized, FDP-mediated collagen deposition is more likely to occur at lower ACA concentrations.

In addition to inhibition of FDP generation, inhibition of plasminogen activation could have other negative effects on vSMC proliferation and matrix production. In vSMC culture, ACA negatively affected matrix deposition, as treatment with the higher concentrations of ACA (6 and 12 mM) led to decreased collagen deposition per cell. This indicates that ACA has broader effects than just limiting fibrin degradation. Many growth factors are sequestered in the ECM in a latent form; plasmin activity has been shown to release TGF-β, IGF, and FGF2 from these latent complexes, leading to increased mitogenic activity (51-53). TGF-β in particular has been shown to increase transcription and deposition of collagen vSMC in fibrin-based tissue constructs (13, 54). Thus, the use of ACA may not only inhibit fibrinolysis; it may also inhibit other positive effects of plasmin in our system.

Though increased fibrin degradation was shown to influence cellularity, especially during the first week, our results did not implicate FDP signaling or adverse effects of the ACA in cell proliferation. Cell density and contact, composition and density of the matrix, and thickness of the tissue may influence this parameter. Furthermore, the cellularity of these constructs is defined by vSMC survival as well as proliferation, confounding the analysis of vSMC DNA measurements alone. This makes a complete understanding of the effects of a three-dimensional matrix on cell survival and proliferation, and more specifically the effects of fibrin degradation on these parameters, complex and unattainable from the current data sets. Unlike collagen density, the cellularity of the constructs does not directly affect construct mechanics; increased cellularity does not necessarily equate with higher collagen deposition or mechanical

properties. Understanding the reasons for increased vSMC cellularity in lower ACA constructs could be an interesting line of questioning, but may not lead to the overall goal of a stronger construct.

This study demonstrates that plasmin can have multiple effects with regard to fibrin remodeling by vSMC in fibrin-based tissue constructs. Plasmin acts to degrade fibrin, which correlates positively with deposition of new ECM molecules collagen and elastin. One key byproduct of plasmin activity is the generation of FDP, which we have shown to increase collagen deposition by vSMC in monolayer culture and in the constructs. Therefore, in order to ultimately fabricate a fibrin-based tissue construct for implantation, the time course of plasmin activity and the associated rate of FDP generation must be carefully prescribed. This will be of particular importance as new cells types are considered or for the eventual use of autologous cells for implant. Different cell isolations can be expected to have varied fibrinolytic activity; thus, careful monitoring of fibrinolysis will be necessary to allow for appropriate remodeling of fibrin-based tissue constructs.

2.5 References

1. Ahmann, K.A., Weinbaum, J.S., Johnson, S.L., and Tranquillo, R.T. Fibrin Degradation Enhances Vascular Smooth Muscle Cell Proliferation and Matrix Deposition in Fibrin-Based Tissue Constructs Fabricated In Vitro. Tissue engineering, 2010.

2. Itosaka, H., Kuroda, S., Shichinohe, H., Yasuda, H., Yano, S., Kamei, S., Kawamura, R., Hida, K., and Iwasaki, Y. Fibrin matrix provides a suitable scaffold for bone marrow stromal cells transplanted into injured spinal cord: A novel material for CNS tissue engineering. Neuropathology, 2008.

3. Pelaez, D., Huang, C.Y., and Cheung, H.S. Cyclic Compression Maintains Viability and Induces Chondrogenesis of Human Mesenchymal Stem Cells in Fibrin Gel Scaffolds. Stem cells and development, 2008.

4. Osathanon, T., Linnes, M.L., Rajachar, R.M., Ratner, B.D., Somerman, M.J., and Giachelli, C.M. Microporous nanofibrous fibrin-based scaffolds for bone tissue engineering. Biomaterials 29, 4091, 2008.

5. Taylor, S.J., and Sakiyama-Elbert, S.E. Effect of controlled delivery of neurotrophin-3 from fibrin on spinal cord injury in a long term model. J Control Release 116, 204, 2006.

6. Ye, Q., Zund, G., Benedikt, P., Jockenhoevel, S., Hoerstrup, S.P., Sakyama, S., Hubbell, J.A., and Turina, M. Fibrin gel as a three dimensional matrix in cardiovascular tissue engineering. Eur J Cardiothorac Surg 17, 587, 2000.

7. Jockenhoevel, S., Zund, G., Hoerstrup, S.P., Chalabi, K., Sachweh, J.S., Demircan, L., Messmer, B.J., and Turina, M. Fibrin gel -- advantages of a new scaffold in cardiovascular tissue engineering. Eur J Cardiothorac Surg 19, 424, 2001.

8. Williams, C., Johnson, S.L., Robinson, P.S., and Tranquillo, R.T. Cell sourcing and culture conditions for fibrin-based valve constructs. Tissue engineering 12, 1489, 2006.

9. Robinson, P.S., Johnson, S.L., Evans, M.C., Barocas, V.H., and Tranquillo, R.T. Functional tissue-engineered valves from cell-remodeled fibrin with commissural alignment of cell-produced collagen. Tissue engineering 14, 83, 2008.

10. Yee, K.O., Rooney, M.M., Giachelli, C.M., Lord, S.T., and Schwartz, S.M. Role of beta1 and beta3 integrins in human smooth muscle cell adhesion to and contraction of fibrin clots in vitro. Circulation research 83, 241, 1998.

11. Grassl, E.D., Oegema, T.R., and Tranquillo, R.T. Fibrin as an alternative biopolymer to type-I collagen for the fabrication of a media equivalent. Journal of biomedical materials research 60, 607, 2002.

12. Grassl, E.D., Oegema, T.R., and Tranquillo, R.T. A fibrin-based arterial media equivalent. Journal of biomedical materials research 66, 550, 2003.

13. Long, J.L., and Tranquillo, R.T. Elastic fiber production in cardiovascular tissue-equivalents. Matrix Biol 22, 339, 2003.

14. Ross, J.J., and Tranquillo, R.T. ECM gene expression correlates with in vitro tissue growth and development in fibrin gel remodeled by neonatal smooth muscle cells. Matrix Biol 22, 477, 2003.

15. Cummings, C.L., Gawlitta, D., Nerem, R.M., and Stegemann, J.P. Properties of engineered vascular constructs made from collagen, fibrin, and collagen-fibrin mixtures. Biomaterials 25, 3699, 2004.

16. Swartz, D.D., Russell, J.A., and Andreadis, S.T. Engineering of fibrin-based functional and implantable small-diameter blood vessels. American journal of physiology 288, H1451, 2005.

17. Yao, L., Swartz, D.D., Gugino, S.F., Russell, J.A., and Andreadis, S.T. Fibrin-based tissue-engineered blood vessels: differential effects of biomaterial and culture parameters on mechanical strength and vascular reactivity. Tissue engineering 11, 991, 2005.

18. Hong, H., and Stegemann, J.P. 2D and 3D collagen and fibrin biopolymers promote specific ECM and integrin gene expression by vascular smooth muscle cells. Journal of biomaterials science 19, 1279, 2008.

19. Bensaid, W., Triffitt, J.T., Blanchat, C., Oudina, K., Sedel, L., and Petite, H. A biodegradable fibrin scaffold for mesenchymal stem cell transplantation. Biomaterials 24, 2497, 2003.

20. Mol, A., van Lieshout, M.I., Dam-de Veen, C.G., Neuenschwander, S., Hoerstrup, S.P., Baaijens, F.P., and Bouten, C.V. Fibrin as a cell carrier in cardiovascular tissue engineering applications. Biomaterials 26, 3113, 2005.

21. Zhang, G., Hu, Q., Braunlin, E.A., Suggs, L.J., and Zhang, J. Enhancing efficacy of stem cell transplantation to the heart with a PEGylated fibrin biomatrix. Tissue engineering 14, 1025, 2008.

22. Spicer, P.P., and Mikos, A.G. Fibrin glue as a drug delivery system. J Control Release, 2010.

23. Spotnitz, W.D. Fibrin sealant: past, present, and future: a brief review. World journal of surgery 34, 632, 2010.

24. Barocas, V.H., Girton, T.S., and Tranquillo, R.T. Engineered alignment in media equivalents: magnetic prealignment and mandrel compaction. Journal of biomechanical engineering 120, 660, 1998.

25. L'Heureux, N., Germain, L., Labbe, R., and Auger, F.A. In vitro construction of a human blood vessel from cultured vascular cells: a morphologic study. J Vasc Surg 17, 499, 1993.

26. Clark, R.A. Fibrin is a many splendored thing. J Invest Dermatol 121, xxi, 2003.

27. Cox, S., Cole, M., and Tawil, B. Behavior of human dermal fibroblasts in three-dimensional fibrin clots: dependence on fibrinogen and thrombin concentration. Tissue engineering 10, 942, 2004.

28. Rijken, D.C., and Lijnen, H.R. New insights into the molecular mechanisms of the fibrinolytic system. J Thromb Haemost 7, 4, 2009.

29. Sun, Z., Chen, Y.H., Wang, P., Zhang, J., Gurewich, V., Zhang, P., and Liu, J.N. The blockage of the high-affinity lysine binding sites of plasminogen by EACA significantly inhibits prourokinase-induced plasminogen activation. Biochimica et biophysica acta 1596, 182, 2002.

30. Bakker, A.H., Weening-Verhoeff, E.J., and Verheijen, J.H. The role of the lysyl binding site of tissue-type plasminogen activator in the interaction with a forming fibrin clot. The Journal of biological chemistry 270, 12355, 1995.

31. Anonick, P.K., Vasudevan, J., and Gonias, S.L. Antifibrinolytic activities of alpha-N-acetyl-L-lysine methyl ester, epsilon-aminocaproic acid, and tranexamic acid. Importance of kringle interactions and active site inhibition. Arterioscler Thromb 12, 708, 1992.

32. Christensen, U. Allosteric effects of some antifibrinolytic amino acids on the catalytic activity of human plasmin. Biochimica et biophysica acta 526, 194, 1978.

33. Hunter, C.J., and Levenston, M.E. Maturation and integration of tissue-engineered cartilages within an in vitro defect repair model. Tissue engineering 10, 736, 2004.

34. Rowe, S.L., and Stegemann, J.P. Interpenetrating collagen-fibrin composite matrices with varying protein contents and ratios. Biomacromolecules 7, 2942, 2006.

35. Bian, W., and Bursac, N. Engineered skeletal muscle tissue networks with controllable architecture. Biomaterials 30, 1401, 2009.

36. Kupcsik, L., Alini, M., and Stoddart, M.J. Epsilon-aminocaproic acid is a useful fibrin degradation inhibitor for cartilage tissue engineering. Tissue engineering 15, 2309, 2009.

37. Naito, M., Stirk, C.M., Smith, E.B., and Thompson, W.D. Smooth muscle cell outgrowth stimulated by fibrin degradation products. The potential role of fibrin fragment E in restenosis and atherogenesis. Thrombosis research 98, 165, 2000.

38. Thompson, W.D., Evans, A.T., and Campbell, R. The control of fibrogenesis: stimulation and suppression of collagen synthesis in the chick chorioallantoic membrane with fibrin degradation products, wound extracts and proteases. The Journal of pathology 148, 207, 1986.

39. Isenberg, B.C., Williams, C., and Tranquillo, R.T. Endothelialization and flow conditioning of fibrin-based media-equivalents. Annals of biomedical engineering 34, 971, 2006.

40. Kim, Y.J., Sah, R.L., Doong, J.Y., and Grodzinsky, A.J. Fluorometric assay of DNA in cartilage explants using Hoechst 33258. Analytical biochemistry 174, 168, 1988.

41. Kim, B.S., and Mooney, D.J. Engineering smooth muscle tissue with a predefined structure. Journal of biomedical materials research 41, 322, 1998.

42. Stegemann, H., and Stalder, K. Determination of hydroxyproline. Clinica chimica acta; international journal of clinical chemistry 18, 267, 1967.

43. Dombi, G.W., Haut, R.C., and Sullivan, W.G. Correlation of high-speed tensile strength with collagen content in control and lathyritic rat skin. The Journal of surgical research 54, 21, 1993.

44. Starcher, B. A ninhydrin-based assay to quantitate the total protein content of tissue samples. Analytical biochemistry 292, 125, 2001.

45. Kiernan, J.A. Histological and histochemical methods : theory and practice. Oxford [U.K.] ; Boston: Butterworth-Heinemann, 1999.

46. Isenberg, B.C., Williams, C., and Tranquillo, R.T. Small-diameter artificial arteries engineered in vitro. Circulation research 98, 25, 2006.

47. Ugwu, F., Lemmens, G., Collen, D., and Lijnen, H.R. Matrix metalloproteinase deficiencies do not impair cell-associated fibrinolytic activity. Thrombosis research 102, 61, 2001.

48. Cederholm-Williams, S.A. Concentration of plasminogen and antiplasmin in plasma and serum. Journal of clinical pathology 34, 979, 1981.

49. Green, K.A., Almholt, K., Ploug, M., Rono, B., Castellino, F.J., Johnsen, M., Bugge, T.H., Romer, J., and Lund, L.R. Profibrinolytic effects of metalloproteinases during skin wound healing in the absence of plasminogen. J Invest Dermatol 128, 2092, 2008.

50. Yan, D., Urano, T., Takada, Y., and Takada, A. Dissociation of alpha 2-plasmin-inhibitor-plasmin complex and regeneration of plasmin activity by SDS treatment. Thrombosis research 69, 491, 1993.

51. Campbell, P.G., Novak, J.F., Yanosick, T.B., and McMaster, J.H. Involvement of the plasmin system in dissociation of the insulin-like growth factor-binding protein complex. Endocrinology 130, 1401, 1992.

52. George, S.J., Johnson, J.L., Smith, M.A., Angelini, G.D., and Jackson, C.L. Transforming growth factor-beta is activated by plasmin and inhibits smooth muscle cell death in human saphenous vein. Journal of vascular research 42, 247, 2005.

53. George, S.J., Johnson, J.L., Smith, M.A., and Jackson, C.L. Plasmin-mediated fibroblast growth factor-2 mobilisation supports smooth muscle cell proliferation in human saphenous vein. Journal of vascular research 38, 492, 2001.

54. Weinbaum, J.S., Qi, J., and Tranquillo, R.T. Monitoring Collagen Transcription by Vascular Smooth Muscle Cells in Fibrin-Based Tissue Constructs. Tissue engineering, 2009.

Chapter 3: Fabrication of Fibrin-Based Arteries Seeded with Rat Blood Outgrowth Endothelial Cells

3.1 Introduction

The small-diameter media equivalents (MEs) fabricated in Chapter 2 will require endothelialization to limit the need for anti-coagulation therapy during implantation. With the goal of producing a complete artery, including medial and intimal layers, this chapter will examine the formation of an endothelium on the MEs. Use of an inbred rat strain for the vascular smooth muscle cells (vSMCs) and endothelial cells (ECs) should allow for implant studies in the infrarenal abdominal aorta of adult rats with minimal anti-coagulant and immunosuppressant therapy. This will be important for examining *in vivo* remodeling of the fibrin-based arteries, as well as ensuring appropriate burst pressures and thromboresistance can be maintained after implantation.

Fibrin has been shown to be a good matrix for cell adhesion (1) and, for this reason, has been utilized to coat synthetic vascular grafts prior to endothelialization (2). Swartz et al. seeded ovine umbilical vein ECs on vSMC entrapped MEs after two weeks of culture and allowed the ECs to proliferate for 10 days until confluence was reached.

These constructs were then implanted in the jugular vein of lambs for 15 weeks, after which time vWF staining showed EC were adherent on the lumenal surface (3). This is a promising first result with fibrin-based grafts, however the study brings up a number of questions. As the implanted ECs were not labeled, the source of the ECs on the lumenal surface post-excision could not be addressed. These cells could be the initial cells seeded on the graft or they may be ECs that have re-endothelialized from the host lamb, either by ingrowth from the anastomoses or through hematogenous seeding of ECs or their precursors. Further, as the ECs were seeded on the ME after only 2 weeks, this lumenal surface is likely largely composed of unremodeled fibrin. To be able to withstand arterial pressures, the MEs will need to be cultured *in vitro* longer and allowed to go through more extensive remodeling. This will likely affect the ECM composition at the lumenal surface, as well as EC adhesion.

Past work by our lab has utilized rat vECs on media equivalents fabricated with entrapped vSMCs that were cultured for 5 weeks. In these studies it was shown that MEs could be seeded with near confluent monolayers (98.8 ± 0.9%) by 48 hours post-seeding. vEC retention under shear stress was also high; retention was 96.5 ± 4.4% when steady, laminar shear stress for 48 hours at 10 dynes/cm^2. After 24 hours of steady, laminar flow, a subset of the samples was exposed to pulsatile flow with a mean shear stress of 10 dynes/cm^2 for 24 hours; retention of vEC in this group was 94.3 ± 4.3% (4). Though the mechanical properties of these MEs did not reach the required burst pressures necessary for implant, these results are a good first indication that endothelial cells can be seeded on the remodeled fibrin MEs and remain adherent under shear stress.

The following chapter examines the use of rat blood outgrowth endothelial cells (RBOECs) for endothelium formation on rat vSMC-entrapped fibrin-based MEs. BOECs represent an easily accessible source of endothelial cells, with a high proliferative capacity and a stable endothelial cell phenotype (5). The research in the following chapter is necessary for the development of a non-immunosuppressed animal model, as well as more generally for validation of the use of RBOECs with vascular grafts. The MEs with optimized fibrin degradation from Chapter 2 will be used for these studies. These MEs were also optimized at 1-2 mm inner diameter sizes and a final length of 3-4 cm to ensure the RBOEC-seeded ME will be an appropriate size for eventual inter-positional implant into the rat aorta.

3.2 Materials and Methods

3.2.1 Cell Source

RBOECs were isolated and expanded from 8 week old Fischer rats by Dr. Robert P. Hebbel's lab, as previously described for murine BOECs (6). The protocol for rat blood collection was approved by the University of Minnesota Institutional Animal Care and Use Committee (IACUC). RBOECs were cultured in EGM medium (EBM-2 medium with EGM Singlequot supplement kit; Clonetics) supplemented with an additional 8% fetal bovine serum (FBS; Hyclone), 1% penicillin/streptomycin (Invitrogen), and 0.22 mg/mL dibutyryl cyclic adenosine monophosphate (cAMP; Sigma-Aldrich, Inc.). RBOECs were cultured on type I rat tail collagen-coated flasks and subcultured upon reaching 90% confluence using 0.25% trypsin EDTA (Gibco Invitrogen

Co.). RBOECs were cryopreserved in 90% FBS with 10% dimethyl sulphoxide (Sigma-Aldrich, Inc) and used at from passage 8-14. Where specified, RBOECs expressing Green Fluorescent Protein (GFP-RBOEC) were utilized from passage 15-20. Fischer rat vascular SMCs were isolated as described in chapter 2 and utilized for ME fabrication at passage 6.

3.2.2 Fibrin-based ME Fabrication

Fibrin-based MEs were fabricated as described in the previous chapter. For these studies, the initial concentrations were $5x10^5$ vSMC/ml and 3.3 mg/ml fibrinogen solid (F4753, Sigma Aldrich, St. Louis, MO). MEs were fabricated with a 2 mm inner mandrel, and an outer tubular glass mold with an inner diameter of 9 mm and length of 7.5 cm. After fibrin gelation, the MEs were cultured in medium consisting of DMEM/F12, antibiotic/antimycotic (Invitrogen), 10% FBS, 50 µg/ml ascorbate (Sigma Aldrich), 1 ng/ml TGF-β (R&D Systems, Minneapolis, MN), 2 µg/ml insulin (Sigma Aldrich), and 6 mM ACA (Thermo Fisher Scientific). Medium was changed every 2-3 days until MEs were used for RBOEC seeding at 5 weeks. The mechanical properties and composition of MEs cultured with these conditions was examined in Chapter 2 (Figure 2.9, 2.10), however the use of a different isolation of vSMC and a different lot of fibrinogen made re-characterization necessary. In an attempt to improve ME mechanical properties, a subset of MEs was cultured with 5 ng/ml EGF instead of TGF-β.

3.2.3 ME Characterization

Histology, biochemical analysis of collagen, elastin, total protein and cellularity, and uniaxial tensile testing were performed as described in Chapter 2. Burst pressure and

compliance of the MEs were also assessed by applying an increasing intraluminal pressure until rupture. A syringe pump in line with a pressure transducer was utilized to inflate the ME after it has been attached to hose barbs and a barb fitting capped at one end (Figure 3.1). MEs were pressurized with HBSS at a rate of approximately 5 mmHg/s. Constructs were preconditioned to 120 mmHg repeatedly prior to inflation to failure and the outer diameter was continuously monitored using a laser micrometer (Mitutoyo, LSM-503H). Diameter and pressure were logged using Labview software and compliance of the constructs was calculated based on measurements between 80 and 120 mmHg to approximate rat blood pressure. The mean physiological compliance was described as a change in diameter (Δd/d) for a pressure rise from 80 mmHg to 120 mmHg and was expressed as a % per mmHg.

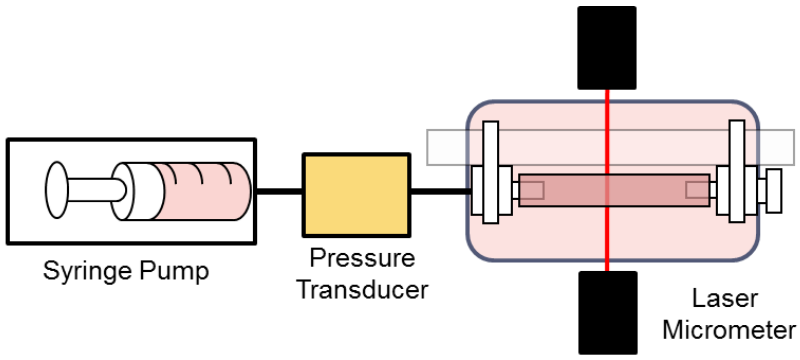

Figure 3.1: System for testing burst pressure and compliance. A syringe pump was used to pressurize the vessel, while a pressure transducer and laser micrometer collect pressure and diameter data using LabView software.

3.2.4 RBOEC Characterization

Cell type was initially characterized by Dr. Robert Hebbel's lab by positive immunostaining for endothelial cell markers VE-Cadherin, von Willebrand Factor (vWF), FLK-1, and RECA-1 and negative staining for CD14, a monocyte marker.

Further staining was performed in our lab using rabbit anti-vWF antibody (10 μg/ml; Abcam) and Cy3-conjugated donkey anti-rabbit secondary antibody (1:200 dilution; Jackson Immuno).

RBOECs were also examined for uptake of acetylated low density lipoprotein labeled with 1,1'-dioctadecyl 3,3,3',3'-tetramethyl-indocarbocyanine perchlorate (Dil-acLDL; Biomedical Technologies, Inc). RBOECs were seeded at 20,000 cell/cm^2. After 48 hours in culture, 10 μg/ml Dil-acLDL in EGM medium was added to the cells for 4 hours at 37C. RBOEC cultures were rinsed with Hanks balanced salt solution (HBSS), then fresh EGM medium added and cells were imaged by epifluorescent microscopy for ac-LDL uptake. RBOEC cultures without Dil-acLDL and vSMC cultures exposed to Dil-acLDL were used as negative controls.

3.2.5 Tubule Formation on Matrigel or Fibrin

300 μl of cold matrigel (BD Biosciences) was added to wells of a 24 well plate. Matrigel was allowed to gel for 30 minutes at 37C prior to seeding with 10,000 RBOECs/cm^2 in EGM medium. Every 24 hours for 4 days, the wells were imaged for formation of tubule-like structures and network formation.

As a second substrate, fibrin gels were also used to examine tubule formation. Acellular fibrin gels were formed in 24 well plates, using 3.3 mg/ml fibrin solid and 300 μl gel per well and the same methods described for fibrin gels in Chapter 2. RBOECs were seeded at 10,000 cells/cm^2 on the surface of these gels, and formation of tubule-like structures examined. Prior to imaging, RBOECs were stained with Dil-acLDL, as

described previously, to improve visualization. Images were taken daily for 4 days post-seeding.

3.2.6 RBOEC Monolayer Shear Stress Experiments

RBOECs were seeded on collagen-coated Permanox slides at 40,000 cells/cm^2. These cells were cultured for 48 hours, at which time confluence was reached, and then the slides were exposed to steady, laminar shear stress in a commercial parallel plate flow system (Streamer; Flexcell International Corp) (Figure 3.2). Flow was initiated at 0.5 dynes/cm^2 and increasing to 5 dynes/cm^2 at a rate of 0.5 dynes/cm^2 every 5 minutes. Shear stress was applied for 24 hours and then the RBOECs were fixed with cold, 4% PFA fixation for 10 minutes. Fixed RBOEC monolayers were stained for 1 hour with mouse anti-rat vascular cell adhesion molecule-1 (VCAM-1, 5 μg/ml; Santa Cruz Biotech), mouse anti- rat intercellular adhesion molecule-1 (ICAM-1, 2 μg/ml; Santa Cruz Biotech), or mouse IgG antibody at the same concentrations (Jackson Immuno) in phosphate buffered saline (PBS). After rinsing, Cy3-conjugated Donkey anti-mouse secondary antibody (1:200; Jackson Immuno) in PBS was applied for 45 minutes. Cell nuclei were stained with Hoechst 33342 at 1 μg/ml for 10 minutes and mounted with a glass coverslip and Vectashield fluorescent mounting medium (Vector Labs). All images were collected using an Olympus inverted microscope and analyzed using NIH Image J Software. Cell numbers per image were derived by fixed thresholding of the images, followed by counts of the independent Hoechst nuclei. These values were normalized to the known surface area of the image to yield cell density measurements.

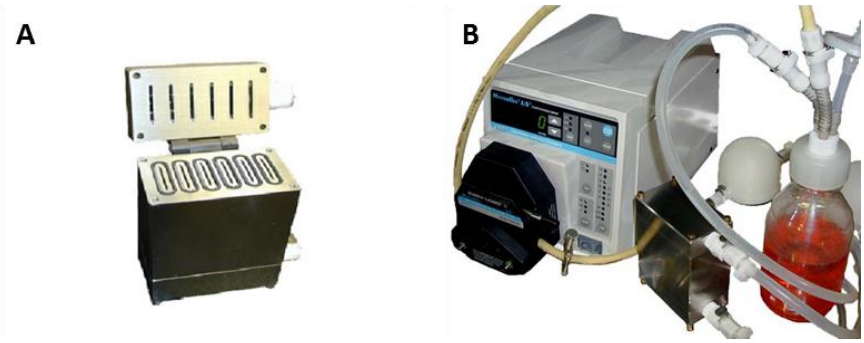

Figure 3.2: Flexcell Streamer System. This system allows application of shear stress to six slides simultaneously. A) Streamer device. B) Closed flow loop with medium reservoir, peristaltic pump, pulse dampender, and the Streamer device. (Figures from Flexcell International, www.flexcellint.com)

3.2.7 Thrombin Activation of BOECs in Monolayer Culture

BOECs were seeded on collagen-coated Permanox slides as described above. After 48 hours the cells were exposed to 2 U/ml thrombin for 24 hours in EGM medium. RBOEC activation was assessed through immunostaining for known activation markers by fixing and staining for ICAM-1 and VCAM-1, as described in the prior section.

3.2.8 Endothelialization of MEs

After 5 weeks of culture, remodeled fibrin tissue constructs were slit axially and placed lumenal surface down on a glass slide using a method adapted from Kladakis et al.(7) (Figure 3.3A-C). A rectangular Delrin ring with a 1.5 mm high wall was placed around the piece of tissue and filled with a solution of 4% low gel temperature agarose (A0701; Sigma). A glass slide was placed on top of the Delrin ring, and the agarose was allowed to gel. The sandwiched agarose and tissue was flipped and the top glass slide removed, exposing the lumenal surface of the construct. A second Delrin ring was placed on top of the first to form a well for cell culture medium. HBOECs or HUVECs in

suspension were labeled with 2.5 μM CellTracker Green (Invitrogen) for 15 minutes at 37C and then were seeded on the lumenal surface of the tissue constructs. The cells were seeded slowly, drop-wise onto the tissue at a concentration of 2 x 10^6 cells/ml, with approximately 100,000 cells added per square centimeter of tissue. One hour after seeding 5 ml of EGM medium was added to each well. 24 hours after seeding, the medium was changed to remove non-adherent cells. As controls in the shear stress experiments, RBOECs were seeded on collagen-coated Permanox slides at the same density.

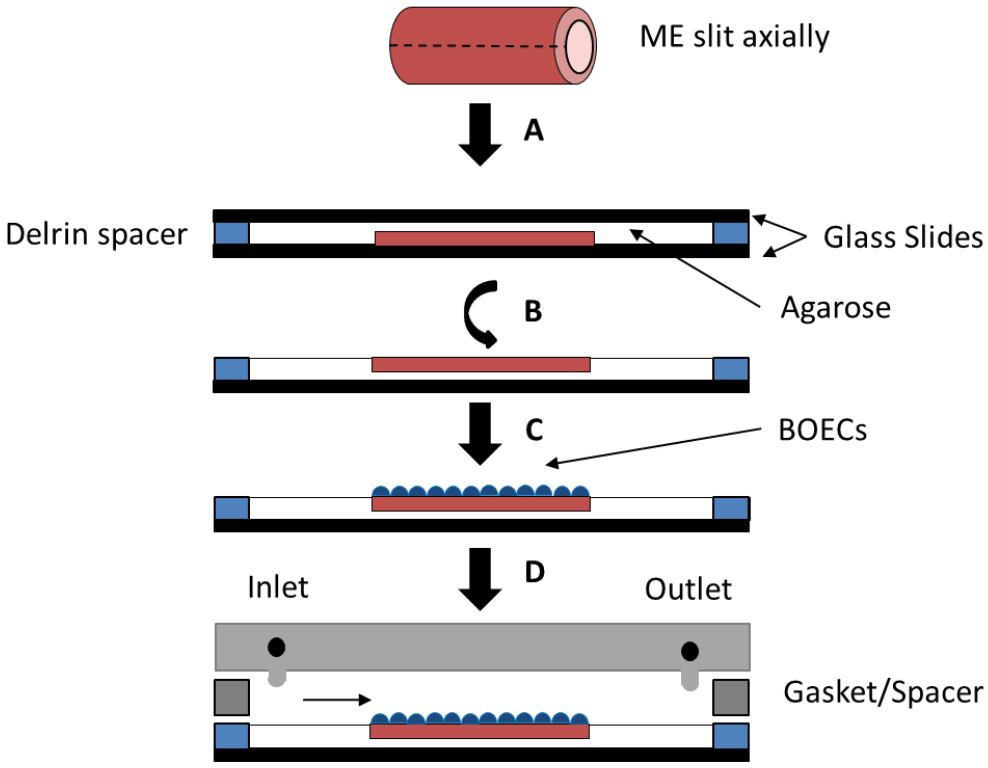

Figure 3.3: Diagram of endothelialization and parallel plate flow chamber setup. A) MEs are slit open axially and embedded lumen side down in agarose on a glass slide. A second slide is place on top. B) After the agarose gels, the system is flipped and the glass slide in contact with the ME can then be removed, exposing the lumenal surface. C) RBOECs are seeded on this surface and either cultured statically or D) placed in a PPFC where steady, laminar shear stress can be applied by the flow EGM medium across the lumenal surface.

3.2.9 Shear stress Experiments on MEs

New parallel plate flow chambers (PPFCs) were designed to allow mounting of tissue in the system. These PPFCs were fabricated based off the designs of Levesque and Nerem (8) and Nauman et al (9) and meet a number of requirements: 1) provide steady, uniform laminar flow across the surface of the construct, 2) allow mounting of an axially-sliced ME flush to the bottom surface, and 3) permit visualization by microscopy in real time (Figure 3.3; 3.4).

This system has been chosen for its well-defined flow conditions. Steady, laminar flow can be achieved through the use of parallel plate, channel flow geometry where the channel height (h) is much less than either the length (L) or width (b). To ensure two-dimensional, fully developed flow across the specimen, a small Reynolds number (Re) and estimated entrance length (L_e) are desired:

$$Re = \frac{u_{avg}\rho h}{\mu} = \frac{\tau_w \rho h^2}{6\mu^2} \tag{3.2.9-1}$$

$$L_e = 0.04hRe = 0.05\frac{\tau_w \rho h^3}{6\mu^2} \tag{3.2.9-2}$$

Here, the Reynold number and entrance length have been expressed in terms of the wall shear stress (τ_w), gap thickness (h), and the viscosity (μ) and density (ρ) of the perfusion medium. By knowing the volumetric flow rate (Q) or pressure gradient ($\frac{dp}{dx}$), the wall shear stress (τ_w) can be determined:

$$\tau_w = \frac{6\mu Q}{h^2 b} \tag{3.2.9-3}$$

$$\tau_w = \frac{-h}{2}\frac{dp}{dx} \tag{3.2.9-4}$$

The dimensions of the channel are 1.8 cm with a length of 5 cm, and a channel height that is determined by the inclusion of a silicone gasket of 250 µm. For each experiment, this height was confirmed by measuring the chamber with and without the gasket inserted using a laser micrometer.

Each PPFC was run independently in a closed loop, with a reservoir that allows gas exchange, a peristaltic pump, and a pulse dampener. A flow probe (Transonic Systems) and blood pressure transducer (Harvard Apparatus) were used to measure and confirm flow rate and pressure. EGM medium was used to prime the PPFC and flow loop prior to loading the GFP-RBOECs seeded on type I rat tail collagen-coated Permanox slides or embedded MEs on glass slides (Figure 3.4). GFP-RBOECs were cultured statically for 48 hours prior to loading in the PPFC and then were exposed to shear stress starting at 0.5 dynes/cm^2 and increasing to 5 dynes/cm^2 at a rate of 0.5 dynes/cm^2 every 5 minutes. Shear stress was held at 5 dynes/cm^2 for 24 hours prior to harvest of the GFP-RBOEC-seeded ME or collagen-coated slides.

For short duration shear stress experiments, GFP-RBOEC were seeded on the collagen-coated slides or MEs as previously described. The GFP-RBOEC were then loaded in the PPFCs and the shear stress gradually increased at 0.5 dynes/cm^2 every minute; however, prior to start of flow and then at 1, 5, 10, 25 dynes/cm^2 the shear stress was held for 20 minutes and then the surfaces imaged using an Olympus inverted microscope. These images were analyzed with ImageJ software (NIH) by fixed thresholding of the images and then quantification of the percentage of the image area covered by GFP-RBOECs.

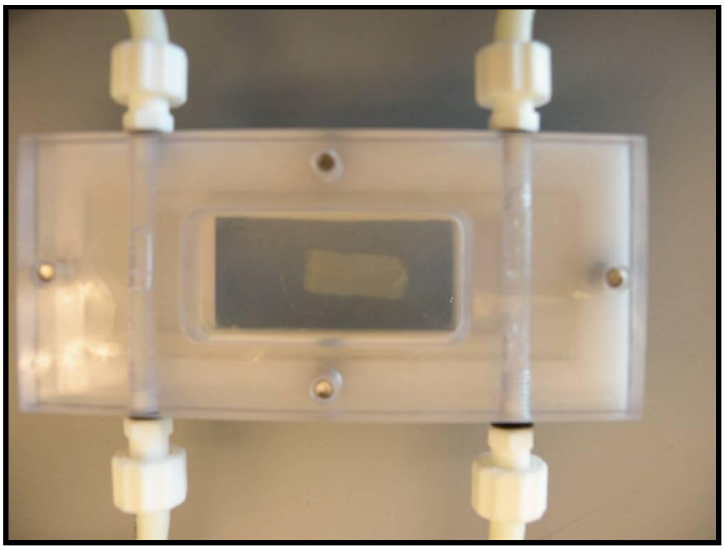

Figure 3.4: PPFC with ME. The ME embedded in agarose is loaded in the PPFC with a 0.25 mm silicone gasket on top to create the flow channel. Use of glass slides to create the chamber walls allows for real-time visualization of fluorescently-labeled RBOECs with an Olympus inverted microscope.

3.2.10 Live/Dead Staining of vSMC MEs

To ensure that the vSMC in MEs embedded in agarose were still living, non-agarose embedded MEs, MEs 2 hours post-embedding, and MEs 24 hours post-embedding were incubated in 4 μM calcein AM and 4 μM ethidium homodimer (Invitrogen) in PBS for 30 minutes at 37C. MEs were rinsed with PBS and then imaged with FITC and TRITC fluorescent filters on an Olympus IX70 inverted microscope. Live cells convert cell-permeant calcein AM to fluorescent calcein via intracellular esterase activity, producing fluorescent green cells. Dead cells take up ethidium homodimer through damaged membranes and the dye binds to nucleic acids, which enhances the fluorescences and stains the dead cells read.

3.2.11 Statistical Analysis

Statistical analysis was performed using GraphPad Prism software for Windows (GraphPad Software, Inc., San Diego, CA). Two-way ANOVA with Bonferroni *post hoc* analysis was conducted to evaluate significant differences between groups in the short duration shear stress experiments. Student t-tests were performed for comparisons of experiments with two groups. A significance level of $\alpha=0.05$ was used for all tests. All graphs indicate mean ± standard error of the mean (SE).

3.3 Results

3.3.1 ME Characterization

MEs were fabricated using the same methods as found in Chapter 2, however the use of a new isolation of vSMCs and a different lot of fibrinogen lead to different remodeling properties. Thus, the ME composition (Table 3.1) and mechanical properties (Table 3.2) are reported for the vSMC MEs utilized for these studies. A subset of MEs was supplemented with EGF instead of TGF-β. MEs cultured with EGF had higher cellularity and collagen deposition (Table 3.1), as well as a higher ultimate tensile strength (UTS), Young's modulus, and burst pressure (Table 3.2). The properties of these MEs were still inferior to the native rat aorta. Figure 3.5 illustrates the conditioning curves and pressurization to failure steps of the burst pressure testing of a representative ME that was cultured with EGF.

Table 3.1: Composition of MEs.

	Total Protein (mg/ml)	**Collagen** (mg/ml)	**Elastin** (mg/ml)	**Cellularity** (Million/ml)
ME + TGF-β	249±19	9.2±0.2	0.25±0.02	24.9±3.7
ME + EGF	163±11	22.3±3.8	0.16±0.06	186±47

Mean ± standard deviation for n=5-6 MEs.

Table 3.2: Mechanical properties of MEs and native rat aorta.

	Thickness (mm)	**UTS** (MPa)	**Modulus** (MPa)	**Burst Pressure** (mmHg)	**Compliance** (%/100 mmHg)
ME + TGF-β	0.27±0.01	0.29±0.02	0.50±0.03	127±78	N/A*
ME + EGF	0.33±0.02	0.35±0.03	1.15±0.20	497±203	4.6 ±1.3
Native rat aorta	0.12±0.01	3.52±0.62	14.07±2.05	1174±131*	

Mean ± standard deviation for n=5-6 MEs or aortic segments. *Compliance was measure from 80-120 mmHg, however many ME + TGF-β samples burst in this range. Compliance is not reported for these values. *Estimated from the measured UTS, wall thickness (t) and radius (r) using BP=UTS*t/r.

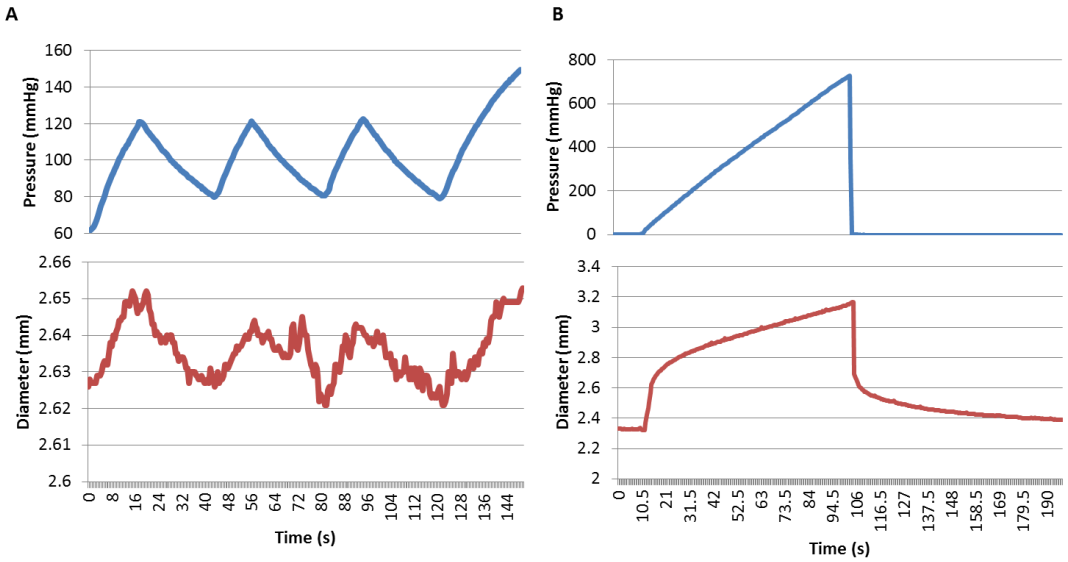

Figure 3.5: Burst pressure testing of MEs. A) The ME was pre-conditioned from 80-120 mmHG at a rate of 3 mmHg/s prior to B) inflation to failure. This data was collected from a ME supplemented with EGF.

Prominent collagen deposition was evident in the MEs cultured with TGF-β or EGF, as seen with Lillie's trichrome staining (Figure 3.6). Collagen-staining was seen throughout the ME, however it was most apparent on the lumenal surface. In Lillie's trichrome staining non-collagenous proteins, including fibrin, stain red. The lumenal surface of the MEs stained more strongly for these proteins, most likely indicating the presence of higher quantities of residual fibrin on this surface.

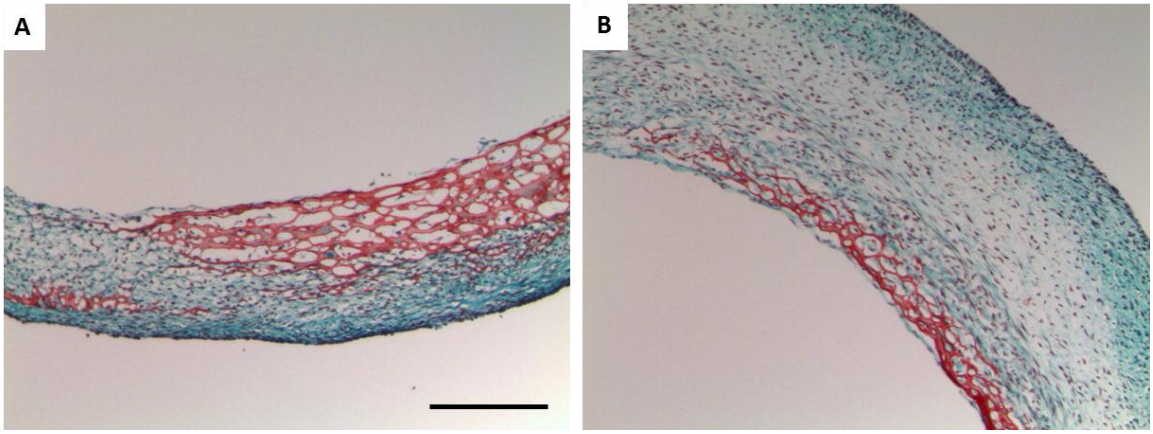

Figure 3.6: Histology of ME sections after 5 weeks in culture. Lillie's Trichrome stain of A) ME cultured with TGF-β and B) ME cultured with EGF. Collagen-rich regions stain green, residual fibrin and other non-collagenous proteins are red and nuclei stain black. Scale bar = 200 μm.

3.3.2 RBOEC Characterization

RBOECs and GFP-BOECs (Figure 3.7A) were characterized by immunostaining to ensure phenotypic similarities to mature endothelial cells. These cells stained positively for VE-Cadherin, vWF, Flk-1, and RECA-1, all markers found on mature endothelial cells (Figure 3.7B-E). RBOECs and GFP-BOECs were negative for CD14, a marker of monocytes (not shown). These cells also had functional characteristics similar to mature ECs; they took up ac-LDL (Figure 3.7F) and formed tubules on matrigel

(Figure 3.7G). Groups have reported that ECs can also form tubules on fibrin gels (10), as well as within fibrin gels (11). We examined this attribute with RBOECs seeded on acellular fibrin gels. Using our standard fibrin concentration for vascular grafts and seeding RBOECs at a low initial density, tubule-like structures formed on the surface of fibrin gels (Figure 3.8). These tubules formed predominately in areas of low cell density, while other regions of the gels had near complete monolayer formation.

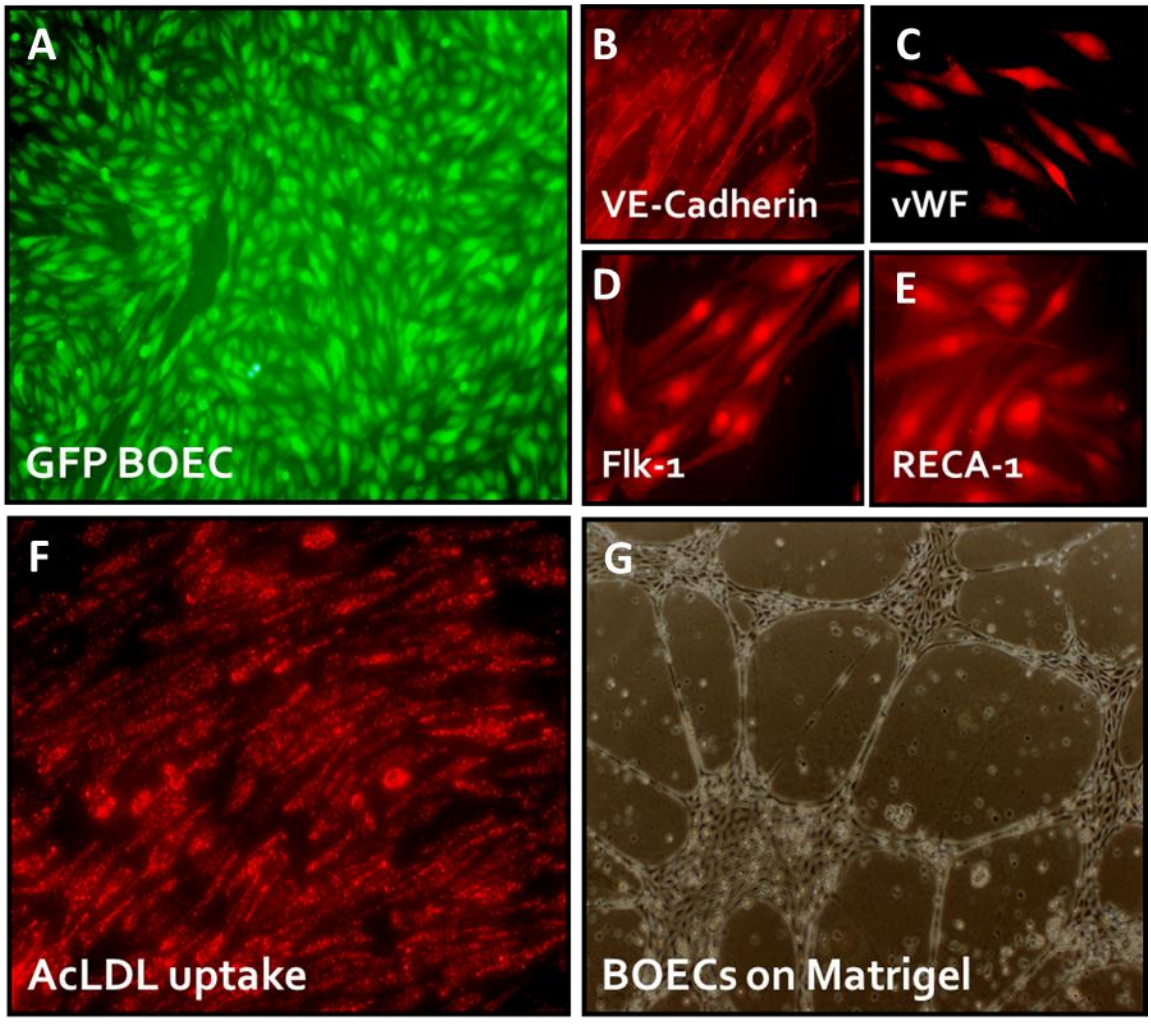

Figure 3.7: Characterization of RBOECs. A) Image showing GFP expression by RBOECs. B) VE-Cadherin. C) vWF. D) Flk-1. E) RECA-1. F) DiI acLDL uptake. G) Tubule formation on matrigel. (Images courtesy of Sethu Nair and Dr. Arif Somani).

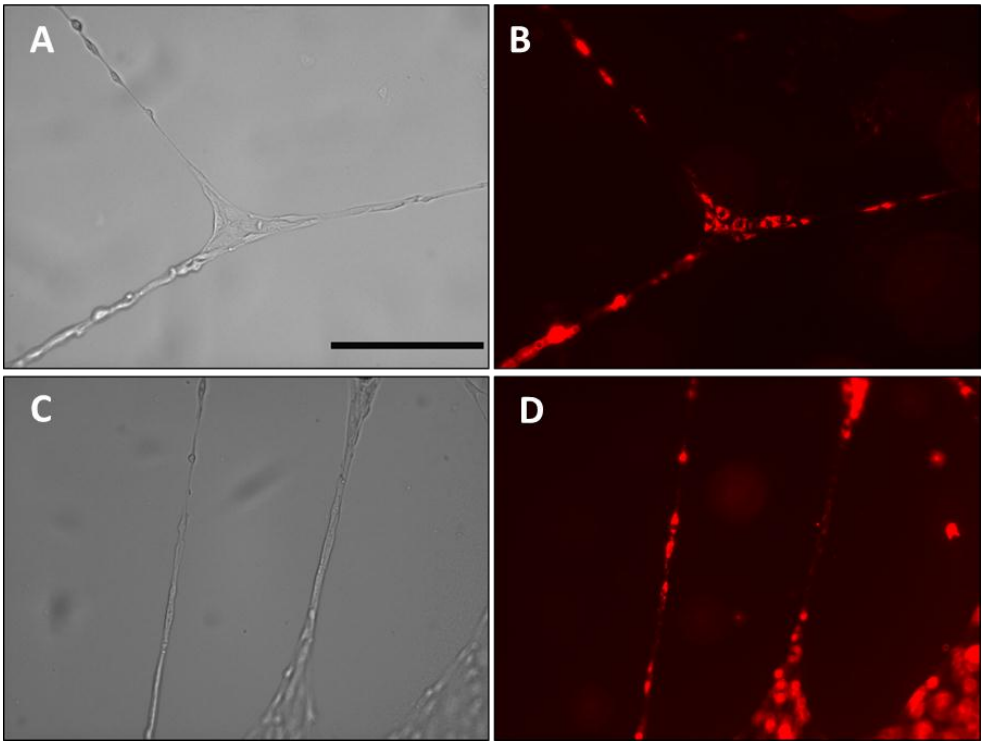

Figure 3.8: Tubule formation on 3 mg/ml fibrin gel. A,C) Transmission images. B,D) Fluorescent images of RBOECs stained with Dil-acLDL. Scale bar = 200 μm and applies to all images.

VCAM-1 and ICAM-1 expression by RBOECs was examined in response to a number of stimuli. An initial interesting point, however, is that the RBOECs expressed VCAM-1 and ICAM-1 without stimulation, a results that is not reported for human EC (12) or human BOECs (5) *in vitro*. VCAM-1 expression has been previously reported for mouse BOECs (6) as well as low, constitutive expression on the mouse aortic endothelium (13). This indicates that the basal levels of VCAM-1 and ICAM-1 may differ between species. However, this could also be due to the effects of the *in vitro* culture conditions. When RBOECs were cultured in MCDB 131 containing FBS but no additional supplements, VCAM-1 expression decreased compared to the EGM medium, which contains a variety of cytokines and growth factors (Figure 3.9A). While our

interest is not in the effects of the media on BOEC activation, this does show that the VCAM-1 and ICAM-1 expression by RBOECs *in vitro* may be a result of their specific culture conditions.

Stimulation with thrombin has been shown to increase VCAM-1 and ICAM-1 expression by human umbilical vein endothelial cells (14). In experiments with 2 U/ml thrombin added to RBOEC culture for 24 hours, VCAM-1 expression was elevated (Figure 3.9B). This shows that the RBOECs are responsive to an agonist and that the basal levels of VCAM-1 expression can be elevated by stimulation.

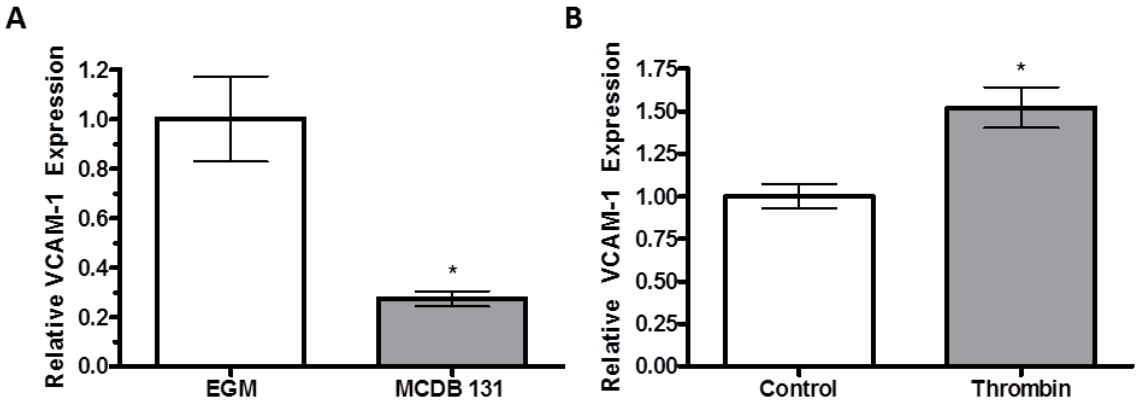

Figure 3.9: VCAM-1 expression by RBOECs. A) VCAM-1 expression is lower in MCDB 131 medium ($p<0.5$). B) VCAM-1 expression is increased by stimulation with thrombin. Plots show mean ± SE for n=3 samples.

For these studies, we were interested in finding an inflammatory marker that was also shear stress dependent. This would allow us to examine the effects of shear stress on the RBOECs and ensure they are shear stress responsive. The application of shear stress has been shown to modulate expression of ICAM-1 and VCAM-1, however this modulation is magnitude dependent; Low shear stress and disturbed flow have different effects on VCAM-1 and ICAM-1 expression than physiological shear stress (12, 15). For

these experiments, we were limited in the magnitude of shear stress we could impose by poor retention of RBOECs at higher shear stresses. Shear stresses above 5 dynes/cm^2 led to loss of RBOECs over a 24 hour period. At 5 dynes/cm^2 RBOECs were well retained on the collagen-coated surface (Figure 3.10A). Furthermore, at 5 dynes/cm^2 shear stress was able to modulate the expression of VCAM-1 (Figure 3.10B), decreasing its expression by approximately 50%. No significant difference in ICAM-1 expression was shown between static and shear stress exposure (Figure 3.10C). Higher shear stresses may be required to be able to cause or detect modulation of ICAM-1 expression.

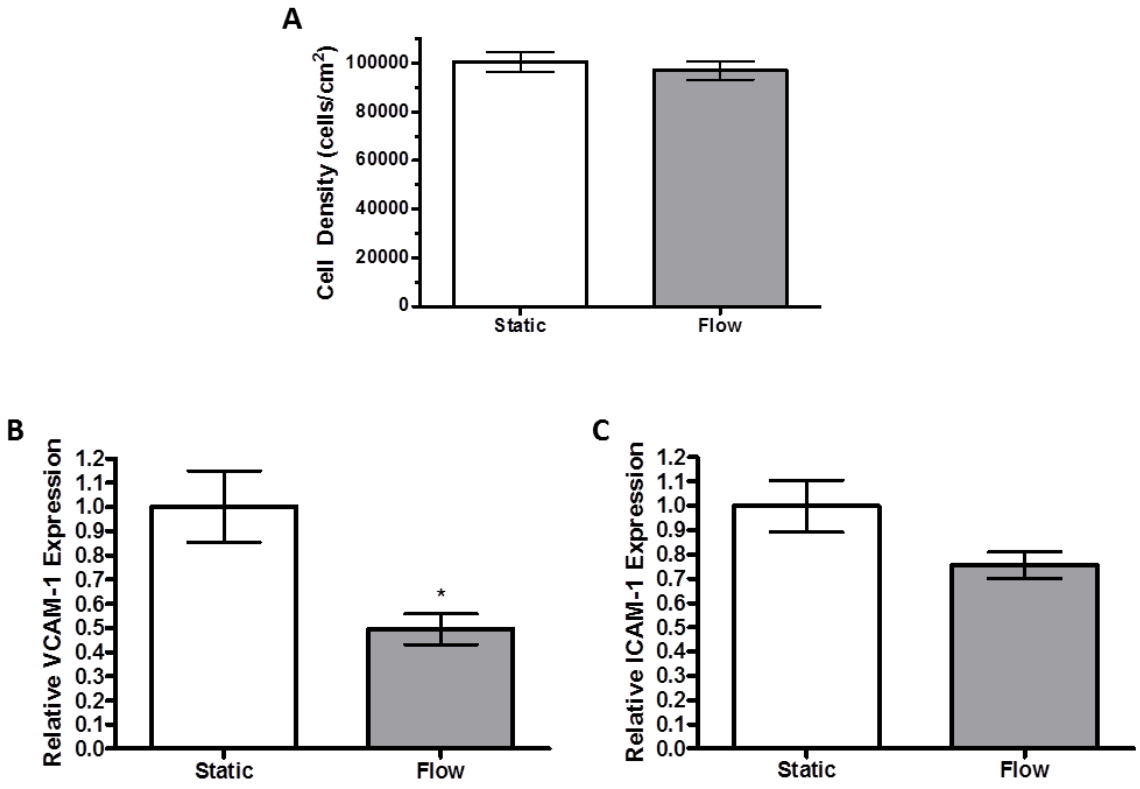

Figure 3.10: Shear stress effects the expression of VCAM-1 by RBOECs. A) Shear stress applied for 24 hours at 5 dynes/cm^2 does not alter the cell density of RBOEC monolayer cultures. B) VCAM-1 expression. *VCAM-1 expression is reduced in RBOEC exposed to shear stress ($p<0.05$). C) ICAM-1 expression. Plots show mean ± SE for n=3 samples.

3.3.3 Endothelialization of MEs

MEs were slit open and embedded lumenal surface up in agarose. To ensure that the application of 37-39 C agarose and the subsequent culture of the tissue in in this substrate did not lead to significant cell death, cells were examined for calcein AM and ethidium homodimer staining at 1 hour and 24 hours post-embedding. vSMCs stained strongly and uniformly for calcein AM, a marker of living cells at both time points and in control, non-embedded MEs. Dead cells that took up ethidium homodimer were sparse in all samples. Representative images from 24 hour samples are shown in Figure 3.11A,B.

GFP-RBOECs were seeded on non-stained MEs immediately post-embedding. After 24 hours the RBOECs were adherent and spread (Figure 3.11C,D). RBOECs adhered to the exposed surface of the bioartificial matrix but did not adhere to the agarose that surrounded this tissue (Figure 3.11D).

RBOECs were seeded on the vSMC remodeled-fibrin matrix at a subconfluent density, 50,000 cells/cm^2, or a supraconfluent density, 200,000 cell/cm^2. 24 hours after seeding the RBOECs were labeled with DiI-acLDL and examined for adhesion and confluence. The RBOECs that were seeded at less than confluence initially were able to proliferation on the matrix, reaching confluence by 96 hours (Figure 3.12A,B). RBOECs that were seeding with more cells than were required to form a confluent monolayer were confluent at 48 hours and maintained a monolayer through 2 more days of culture (Figure 3.12C,D).

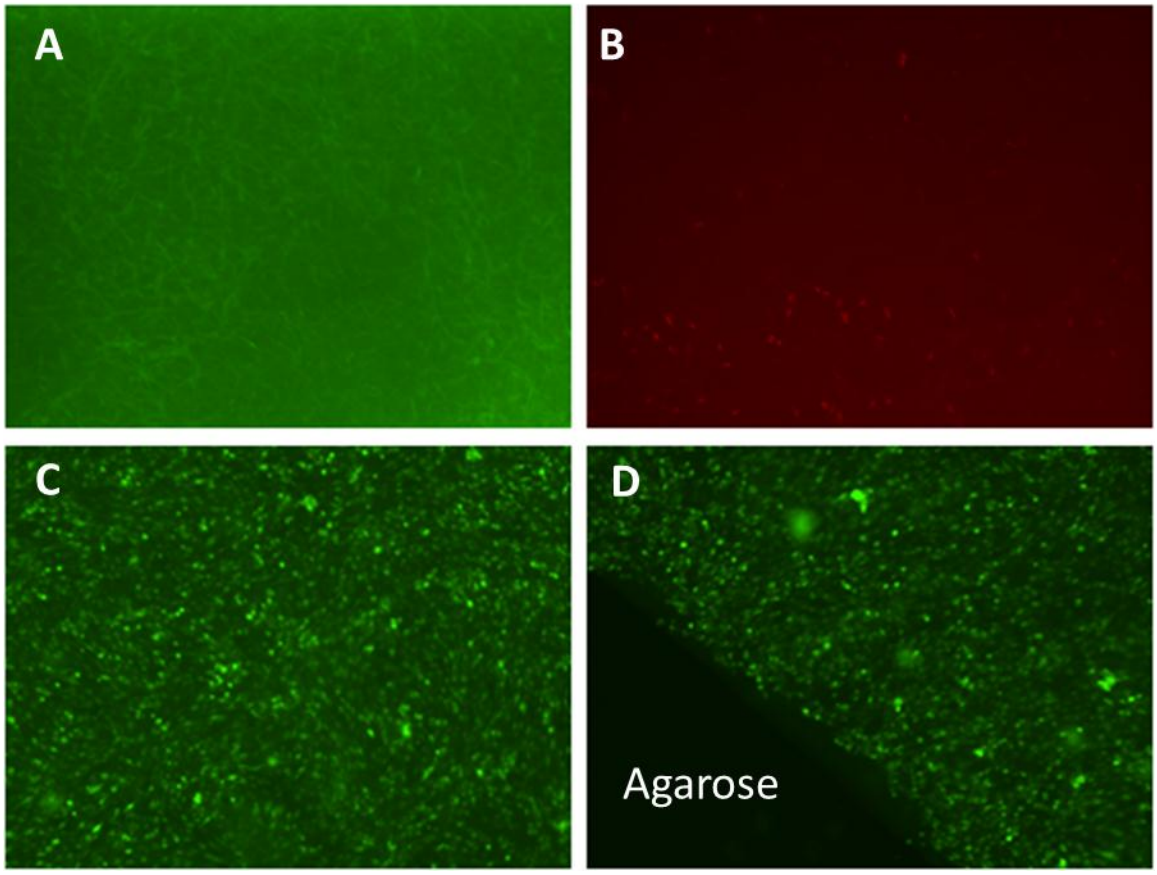

Figure 3.11: Endothelialization of MEs. MEs were embedded in agarose and seeded with GFP-RBOECs. To ensure that the method for embedding with agarose did not lead to vSMC death, 24 hours after embedding the vSMC were examined for staining with A) calcein AM for live cells and B) ethidium homodimer for dead cells. While many spread cells were visible in the tissue, few dead cells were present. C,D) GFP-BOECs were seeded on the tissue and imaged after 24 hours. C) Middle regions of the tissue showed good coverage. D) Images on the edge of the tissue show that the GFP-BOECs only adhere to the tissue and not to the agarose.

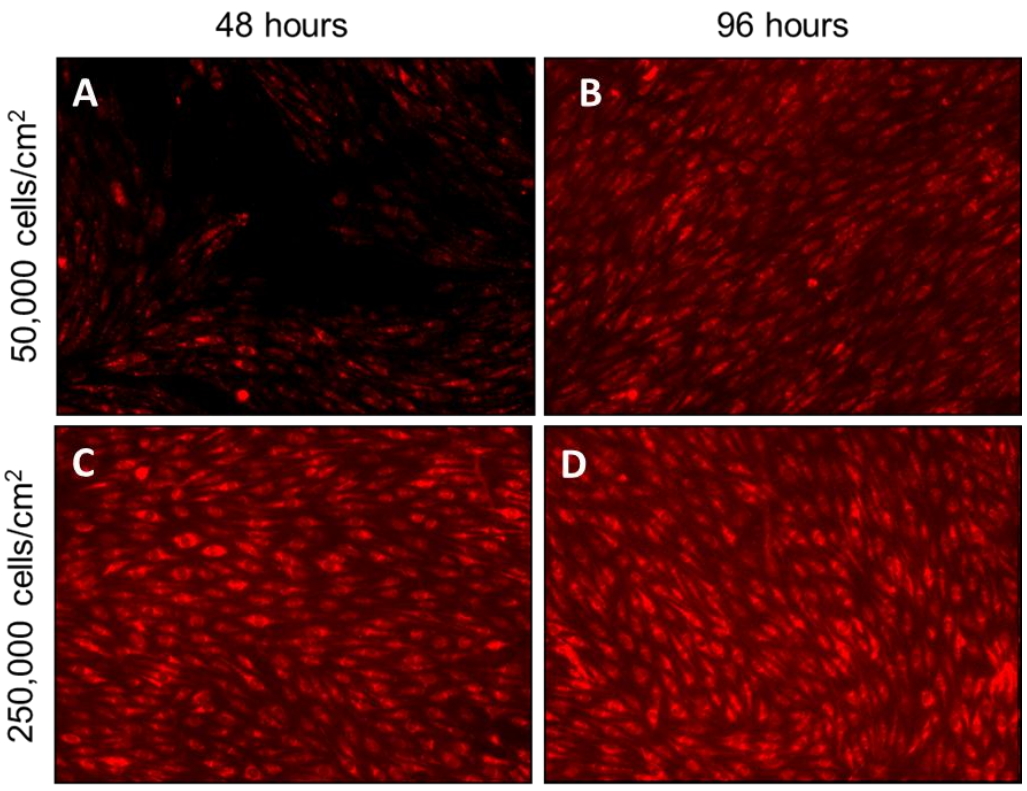

Figure 3.12: RBOECs seeded on MEs. RBOECs were seeded at A,B) subconfluent (50,000 cells/cm^2) or C,D) supraconfluent densities, then labeled with DiL-acLDL and examined at A,C) 48 hours and B,D) 96 hours.

3.3.4 RBOECs remained adherent on MEs when exposed to shear stress

RBOECs were seeded on MEs and remained adherent when exposed to steady, laminar shear stress of 5 dynes/cm^2. A confluent monolayer was present after 24 hours of flow exposure, as illustrated by images of DiI-acLDL-labeled RBOECs in cross-sections and en face (Figure 3.13).

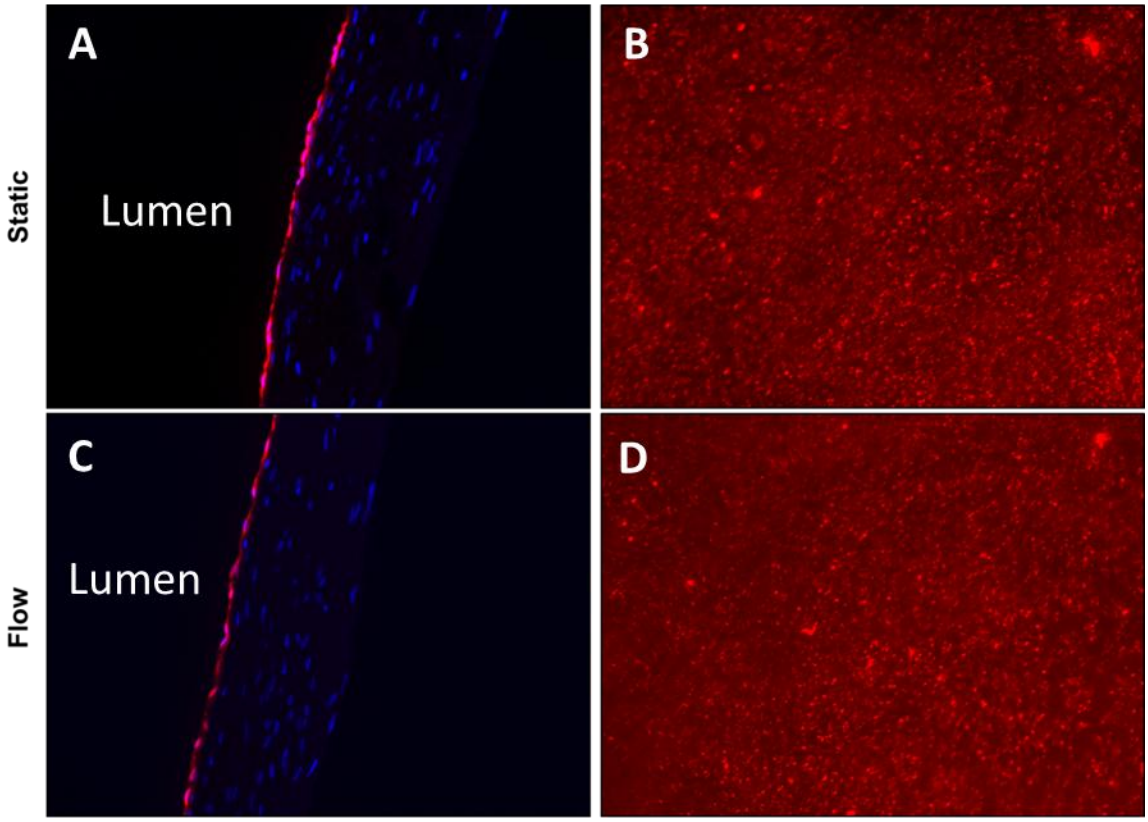

Figure 3.13: RBOECs remain adherent under 5 dynes/cm2 shear stress on MEs. RBOECs were seeded on MEs for 48 hours and then either A,B) cultured statically or C,D) exposed to shear stress for 24 hours. RBOECs were labeled for visualization with DiL-acLDL and imaged A,C) in 9 μm cross-sections or C,D) en face on fixed tissue.

Short duration shear stress experiments were performed up to a shear stress of 25 dynes/cm^2. GFP-RBOECs were seeded on collagen-coated Permanox slides or MEs. After 48 hours of culture, the RBOEC-seeded substrates were imaged and then exposed to a ramped shear stress. At 1, 5, 10, and 25 dyne/cm^2 the shear stress was held for 20 minutes and images collected. RBOEC coverage on the MEs at 1, 5, 10 or 25 dynes/cm^2 did not vary significantly from the initial, static coverage; however there was a drop in RBOEC coverage on the collagen-coated surfaces at 25 dynes/cm^2 compared to the initial coverage (Figure 3.14). A significant difference did not exist between the two surfaces at 25 dynes/cm^2. At all shear stress levels and both substrates, RBOECs remained spread and, even for the subset with the lowest coverage, 25 dynes/cm^2 shear stress with RBOECs on collagen-coated surfaces, greater than 80% coverage was maintained.

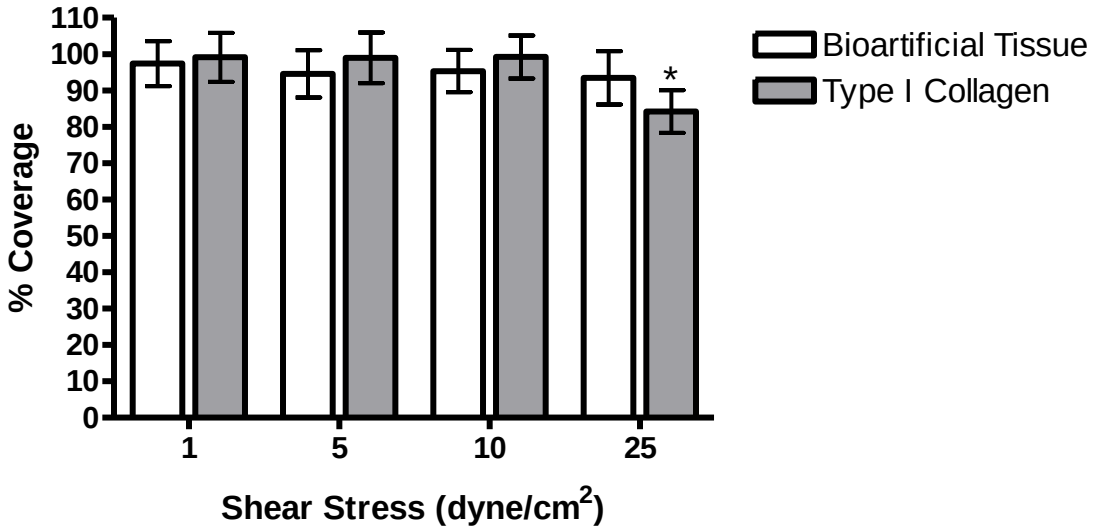

Figure 3.14: RBOEC coverage of bioartificial tissue or type I collagen-coated plastic after exposure to shear stress. RBOECs were seeded on type I collagen-coated TCP or bioartificial tissue and incrementally exposed to 1, 5, 10, or 25 dynes/cm^2 for 20 minutes and GFP-RBOEC surface coverage calculated based on the GFP staining. Plot show mean ± SE for n=3 samples. *Significant difference compared to static samples on the same substrate ($p<0.05$).

3.4 Discussion

The design of a small-diameter vascular graft has been referred to as a Holy Grail of tissue engineering (16, 17). This chapter examines methods to fabricate an entirely biological vessel, from formation of the medial, load-bearing layer, to seeding of endothelial cells to form a neoendothelium. The medial layer was formed from vSMCs embedded in a fibrin gel. Over time, the vSMC compact the gel and deposit new ECM. Optimizing the culture conditions and supplements for these MEs has been shown in to be an important method for improving collagen and elastin synthesis (18-22). Previous reports have shown that EGF improved cellularity and collagen deposition by dermal fibroblast in fibrin gels compared to control and TGF-β supplemented gels (23). We found similar results for our MEs, however the control (no EGF or TGF-β) MEs were too thin and weak for reliable testing. By supplementing with EGF we were able to reach maximal burst pressures of approximately 800 mmHg. Though resting systolic pressure in a rat is 120 mmHg, MEs for implant should be able to tolerate properties in large excess of this resting peak. Preliminary implants with MEs with burst pressures of approximately 400 mmHg were able to withstand short durations (hours) interpositionally in the rat aorta without rupture (Appendix B), which indicates that MEs fabricated with EGF may have sufficient burst pressures for implant studies in the rat abdominal aorta.

However, vSMC MEs were plagued with a number of issues that are not as prevalent with other cell types in our lab, such as human dermal fibroblasts; vSMC MEs were inconsistent in their properties, with big differences depending on the isolation, the passage number, and the fibrinogen lot, as well as between fabrications and between

dishes from the same fabrication. This made the development of reproducible MEs that could reach near-native mechanical properties a difficult endeavor. These studies, including characterization of the RBOECs and seeding of these cells on the vSMC MEs, will be useful preliminary studies for the eventual development of a fibrin-based construct for use in a rat model. However, methods to improve reproducibility with the rat vSMCs will be necessary prior to implantation.

Prior to seeding RBOECs on the lumenal surface of the MEs, these cells were characterized by immunostaining as well as basic functional assays. RBOECs displayed a phenotype typical of a mature endothelial cell, as they stained positively for VE-Cadherin and vWF. They also had functional characteristics similar to mature ECs; they took up ac-LDL and formed tubules on matrigel. These results compare well with BOEC characterizations for other species (5, 6).

RBOECs also formed tubule-like structures on fibrin, a result that has been shown for other types of ECs (10, 11). Further studies will clearly need to be performed to ensure formation of tubule lumens, as well as examination of the RBOECs within fibrin gels not simply seeded on top of fibrin. However, this was a promising initial finding; it demonstrates a functional attribute of RBOECs that compares well with what has been found with mature ECs and is of particular interest in our lab, as the angiogenic potential of RBOECs could be used in conjunction with our fibrin-based technologies to form vascularized tissues.

RBOECs responded to stimuli in an expected manner for endothelial cells. Thrombin stimulated VCAM-1 expression in RBOECs, while shear stress applied at 5

dynes/cm^2 for 24 hours was able to decrease VCAM-1 expression. As we are ultimately interested in RBOEC response to shear stress and the ability to form a quiescent, non-activated monolayer, ICAM-1 and VCAM-1 were chosen based on their shear stress-dependence (15) and their implication in leukocyte adhesion and inflammation. While these results were able to show that RBOECs are responsive to shear stress, poor retention of the RBOECs on collagen-coated plastic during 24 hours of shear stress made analysis at higher shear stress values impossible.

RBOECs were able to adhesion and proliferate on the ME lumenal surface. Using a custom-designed PPFC, steady, laminar shear stress was applied to the constructs. Good retention of the RBOEC could be maintained at 5 dynes/cm^2 for a 24 hour period, however similar results with cell loss were encountered at higher shear stress levels. Short duration shear stress studies on both MEs and collagen-coated surfaces implicate the longer flow duration as part of the problem. Greater than 80% coverage was maintained collagen-coated slides at shear stresses up to 25 dynes/cm^2. No significant loss was apparent with shear stresses up the highest tested (25 dynes/cm^2) on the MEs. This indicates that loss of the RBOECs occurs over longer durations that the 20 minute increments we were examining.

A number of methods could be examined for improving RBOEC adhesion, as well as for diagnosing the issue. Though various shear stress ramping profiles were examined for RBOECs, possibly an even slower increase, such as increasing over days instead of hours or holding at a low shear stress for longer durations prior to ramping to a set shear stress, might allow the cells to adapt and remain adherent on the surface. A variety of integrins play a pivotal role in EC adhesion to the ECM, including $\alpha_V\beta_3$ and $\alpha_5\beta_1$ for

fibrin and fibronectin binding (24). Integrin expression by RBOECs could be examined and compared to other rat EC types. This could help in diagnosing whether there is an issue with the underlying matrix or the phenotype of the RBOECs. Decreasing the trypsin concentration has been shown to improve EC adhesion to fibronectin by increasing $\alpha_5\beta_1$ integrin retention during cell lifting (25). Thus, the integrin expression profile might yield insight into the reasons for RBOEC detachment. Further studies could also examine RBOEC versus mature rat ECs on various matrix coatings under shear stress.

This chapter describes a basic characterization of the medial and endothelial layer of a bioartificial vascular graft. These results show that vSMC MEs with burst pressures up to 800 mmHg can be fabricated and seeded with a confluent layer of RBOECs. RBOECs were shown to have a typical EC phenotype, take up acLDL, form tubules on matrigel and fibrin, and respond to thrombin and shear stress stimuli. The RBOEC could adhere to fibrin-based grafts, proliferate, and form a monolayer on the surface. RBOECs would maintain a confluent monolayer on the vSMC MEs when exposed to 5 dynes/cm^2 shear stress for long durations, or 25 dynes/cm^2 for short durations. Future work aimed at improving vSMC ME reproducibility and RBOEC adhesion could transition this work into a functional, rat aortic implant.

3.5 References

1. Tawil, B. Fibrin and Its Applications. In: Guelcher, S.A., and Hollinger, J.O., eds. An introduction to biomaterials. Baca Raton, FL: CRC/Taylor & Francis, 2006.

2. Deutsch, M., Meinhart, J., Zilla, P., Howanietz, N., Gorlitzer, M., Froeschl, A., Stuempflen, A., Bezuidenhout, D., and Grabenwoeger, M. Long-term experience in autologous in vitro endothelialization of infrainguinal ePTFE grafts. J Vasc Surg 49, 352, 2009.

3. Swartz, D.D., Russell, J.A., and Andreadis, S.T. Engineering of fibrin-based functional and implantable small-diameter blood vessels. American journal of physiology 288, H1451, 2005.

4. Isenberg, B.C., Williams, C., and Tranquillo, R.T. Endothelialization and flow conditioning of fibrin-based media-equivalents. Annals of biomedical engineering 34, 971, 2006.

5. Lin, Y., Weisdorf, D.J., Solovey, A., and Hebbel, R.P. Origins of circulating endothelial cells and endothelial outgrowth from blood. The Journal of clinical investigation 105, 71, 2000.

6. Somani, A., Nguyen, J., Milbauer, L.C., Solovey, A., Sajja, S., and Hebbel, R.P. The establishment of murine blood outgrowth endothelial cells and observations relevant to gene therapy. Transl Res 150, 30, 2007.

7. Kladakis, S.M., and Nerem, R.M. Endothelial cell monolayer formation: effect of substrate and fluid shear stress. Endothelium 11, 29, 2004.

8. Levesque, M.J., and Nerem, R.M. The elongation and orientation of cultured endothelial cells in response to shear stress. Journal of biomechanical engineering 107, 341, 1985.

9. Nauman, E.A., Risic, K.J., Keaveny, T.M., and Satcher, R.L. Quantitative assessment of steady and pulsatile flow fields in a parallel plate flow chamber. Annals of biomedical engineering 27, 194, 1999.

10. Dye, J., Lawrence, L., Linge, C., Leach, L., Firth, J., and Clark, P. Distinct patterns of microvascular endothelial cell morphology are determined by extracellular matrix composition. Endothelium 11, 151, 2004.

11. Lafleur, M.A., Handsley, M.M., Knauper, V., Murphy, G., and Edwards, D.R. Endothelial tubulogenesis within fibrin gels specifically requires the activity of membrane-type-matrix metalloproteinases (MT-MMPs). Journal of cell science 115, 3427, 2002.

12. Chiu, J.J., Usami, S., and Chien, S. Vascular endothelial responses to altered shear stress: pathologic implications for atherosclerosis. Annals of medicine 41, 19, 2009.

13. Fries, J.W., Williams, A.J., Atkins, R.C., Newman, W., Lipscomb, M.F., and Collins, T. Expression of VCAM-1 and E-selectin in an in vivo model of endothelial activation. The American journal of pathology 143, 725, 1993.

14. Kaplanski, G., Marin, V., Fabrigoule, M., Boulay, V., Benoliel, A.M., Bongrand, P., Kaplanski, S., and Farnarier, C. Thrombin-activated human endothelial cells support monocyte adhesion in vitro following expression of intercellular adhesion molecule-1 (ICAM-1; CD54) and vascular cell adhesion molecule-1 (VCAM-1; CD106). Blood 92, 1259, 1998.

15. Chiu, J.J., Lee, P.L., Chen, C.N., Lee, C.I., Chang, S.F., Chen, L.J., Lien, S.C., Ko, Y.C., Usami, S., and Chien, S. Shear stress increases ICAM-1 and decreases VCAM-

1 and E-selectin expressions induced by tumor necrosis factor-[alpha] in endothelial cells. Arteriosclerosis, thrombosis, and vascular biology 24, 73, 2004.

16. Conte, M.S. The ideal small arterial substitute: a search for the Holy Grail? Faseb J 12, 43, 1998.

17. Nerem, R.M., and Seliktar, D. Vascular tissue engineering. Annu Rev Biomed Eng 3, 225, 2001.

18. Grassl, E.D., Oegema, T.R., and Tranquillo, R.T. Fibrin as an alternative biopolymer to type-I collagen for the fabrication of a media equivalent. Journal of biomedical materials research 60, 607, 2002.

19. Grassl, E.D., Oegema, T.R., and Tranquillo, R.T. A fibrin-based arterial media equivalent. Journal of biomedical materials research 66, 550, 2003.

20. Long, J.L., and Tranquillo, R.T. Elastic fiber production in cardiovascular tissue-equivalents. Matrix Biol 22, 339, 2003.

21. Neidert, M.R., Lee, E.S., Oegema, T.R., and Tranquillo, R.T. Enhanced fibrin remodeling in vitro with TGF-beta1, insulin and plasmin for improved tissue-equivalents. Biomaterials 23, 3717, 2002.

22. Williams, C., Johnson, S.L., Robinson, P.S., and Tranquillo, R.T. Cell sourcing and culture conditions for fibrin-based valve constructs. Tissue engineering 12, 1489, 2006.

23. Grouf, J.L., Throm, A.M., Balestrini, J.L., Bush, K.A., and Billiar, K.L. Differential effects of EGF and TGF-beta1 on fibroblast activity in fibrin-based tissue equivalents. Tissue engineering 13, 799, 2007.

24. Albelda, S.M., Daise, M., Levine, E.M., and Buck, C.A. Identification and characterization of cell-substratum adhesion receptors on cultured human endothelial cells. The Journal of clinical investigation 83, 1992, 1989.

25. Brown, M.A., Wallace, C.S., Anamelechi, C.C., Clermont, E., Reichert, W.M., and Truskey, G.A. The use of mild trypsinization conditions in the detachment of endothelial cells to promote subsequent endothelialization on synthetic surfaces. Biomaterials 28, 3928, 2007.

Chapter 4: Adult Blood Outgrowth Endothelial Cells in Vascular Tissue Engineering

4.1 Introduction

Human blood outgrowth endothelial cells (HBOECs) are a promising cell source for vascular tissue engineering. These cells can be isolated by outgrowth of circulating endothelial progenitor cells (EPCs) from a patient blood sample (1) and thus could provide a convenient source of autologous endothelial cells for seeding on tissue-engineered vessels prior to implantation. HBOECs, also called endothelial colony forming cells (ECFCs) and late outgrowth EPCs, have been shown to uniformly express endothelial cell markers, form tubular structures de novo, have typical endothelial cell morphology, and a robust proliferative capacity, expanding from 20 cells to 10^{19} cells in 9 weeks (1). HBOECs are negative for hematopoietic cell markers CD45, CD14 and CD115 and do not phagocytize bacteria (1-4). This is in contrast to other putative EPCs, termed early outgrowth endothelial cells or colony forming unit endothelial cells (CFU-ECs), which do not form vessels in vivo, will ingest bacteria, and express hematopoietic, as well as endothelial, cell markers (3). These CFU-ECs are likely of hematopoietic

origin (3, 5-8), but may express endothelial cell markers due to the uptake of platelet microparticles by mononuclear cells (9). This distinction between various cells termed EPCs in the literature is an important one, as unlike CFU-ECs, HBOECs have the potential to provide a highly proliferative, autologous endothelial cell source for vascular grafts.

Endothelial cells make up the interface between the bloodstream and vascular tissue and play a crucial role in vascular protection, prevention of thrombosis, regulation of nutrient delivery, control of vessel diameter and tone, and hemostasis. These properties of the endothelium appear to be highly influenced by the mechanical environment, with extensive evidence indicating an important role for mechanical factors in influencing endothelial cell structure, growth, and function. Shear stress on the endothelium is critical for maintenance of a thromboresistant surface, control of vessel diameter and vascular permeability, and even endothelial cell survival (10-12).

These essential functions of the endothelium must be fulfilled by a successful vascular graft. Indeed, several mechanisms of small diameter graft failure, such as thrombosis and inflammation, are most likely caused by a lack of a properly formed endothelium (11). For this reason, rigorous assessment of HBOECs is required to ensure successful use of these cells for vascular grafts. The endothelial layer needs to be confluent and remain adherent under normal physiological shear stresses, acting as a barrier between the blood and the procoagulant, sub-endothelial surface. Furthermore, these cells need to be in a non-activated, quiescent state, producing protective molecules that suppress platelet adhesion and activation, such as prostacyclin (PGI_2) and nitric

oxide (NO), anticoagulation factors, such as thrombomodulin (TM), and fibrinolytic factors. In conjunction with this phenotype, HBOECs should show limited expression of proinflammatory molecules, such as intercellular adhesion molecule-1 (ICAM-1), vascular cell adhesion molecule-1 (VCAM-1), P-Selectin, and E-Selectin (11, 13).

In vitro and *in vivo* studies have examined EPCs derived by a variety of methods for seeding on synthetic grafts (14-17), decellularized grafts (18) and tissue-engineered blood vessels (19, 20). Fewer studies have examined the specific HBOEC population for this same purpose (21, 22). However, these initial reports are promising as good HBOEC retention is reported on synthetic materials. 80% of ovine BOECs were retained on cholesterol-modified polyurethane after 2 hours of flow exposure at 75 dynes/cm^2 (22). BOECs derived from cord blood have been shown to adhere on fibronectin or smooth muscle cell (SMC) monolayers at supraphysiological shear stresses (up to 300 dynes/cm^2) for short durations and align with flow after 48 hours of shear stress exposure at a physiological shear stress (15 dynes/cm^2) (23). Importantly, HBOECs have been successfully isolated from patients with coronary artery disease (CAD) (24), indicating that isolation of adult HBOECs may be a viable option for seeding of vascular grafts for bypass surgery.

To examine the suitability of adult HBOECs for use in vascular tissue engineering, the shear stress responsiveness of these cells was examined on bioartificial tissue formed from neonatal human dermal fibroblasts entrapped in tubular fibrin gels. During four weeks in culture, the HDFs degrade the initial fibrin scaffold and deposit new extracellular matrix (ECM), producing bioartificial tissue. The tissue strengthens and

stiffens over time, producing a matrix that more closely mimics native vascular tissue (25-27). Immunohistochemistry was used to identify predominate ECM on the surface of the bioartificial tissue, as well as ECM deposited by the HBOECs post-seeding. Cell density, elongation, alignment, NO production, and expression of the proinflammatory molecules ICAM-1 and VCAM-1 by HBOECs under shear stress were compared to human umbilical vein endothelial cells (HUVECs) to determine if HBOEC flow responses were similar to mature endothelial cells. A whole blood assay was used to examine platelet adhesion to HBOEC- and HUVEC-seeded constructs pre-exposed to shear stress.

4.2 Materials and Methods

4.2.1 Cell Source

HBOECs were isolated and expanded from the peripheral blood of healthy, human volunteers, as previously described (28). The protocol for blood collection was approved by the University of Minnesota Institutional Review Board. The cells were maintained in endothelial growth medium (EGM; EBM-2 medium with EGM Singlequot supplement kit; Clonetics) supplemented with 8% additional fetal bovine serum (FBS; Hyclone), and 1% penicillin/streptomycin (Invitrogen). HBOECs were plated onto rat tail collagen I (BD Biosciences) and subcultured at 80-90% confluence using 0.05% trypsin EDTA (Gibco Invitrogen Co.). Flow cytometry of HBOEC isolations ensured positive staining for endothelial cell markers, including VE-Cadherin and P1H12, and negative staining for CD14 and CD45. These cells also displayed the characteristic cobblestone morphology of ECs, formed tubules in Matrigel, and took up acetylated low density

lipoprotein (acLDL; Biomedical Technologies, Inc). HBOECs were used from passage 8-12 for all experiments. For comparison, human umbilical vein endothelial cells (HUVECs; Clonetics) were maintained in the same culture medium and used from passage 4-6.

Neonatal human dermal fibroblasts (HDFs; Clonetics) were maintained in 50:50 DMEM/F12 medium (Invitrogen; Calsbad, CA) supplemented with 10% fetal bovine serum (FBS, Hyclone), 100 U/ml penicillin (Invitrogen), 100 μg/ml streptomycin (Invitrogen), and 2.5 μg/ml amphotericin-β (Invitrogen). HDFs were plated at 8,500 cells/cm^2, passaged at 100% confluence, and used at passage 9.

4.2.2 Fibrin-based Vascular Graft Fabrication

Tubular fibrin constructs were made as previously reported (29). Briefly, HDFs suspended in DMEM were mixed into a solution of bovine fibrinogen (Sigma) in 20 mM Hepes-buffered saline. A mixture of bovine thrombin (Sigma) and calcium chloride in DMEM was then added to the suspension, mixed well, and injected into tubular glass molds measuring 8 cm long and 9 mm in inner diameter and containing 2 mm glass rods with stoppers on either end. The glass rods had been coated in 5% Pluronics F127 (Sigma) for three hours to reduce adhesion between the fibrin gel and the mandrel. Final gel component concentrations were 3.3 mg/ml fibrin, 500,000 HDF/ml, 0.2 U/ml thrombin and 1.2 mM $CaCl_2$. The solution was allowed to gel at 37ºC for 30 minutes, at which time the outer mold was removed and the constructs placed in DMEM supplemented with 10% FBS, 10 U/ml penicillin, 100 μg/ml streptomycin, and 2.5 μg/ml amphotericin-β. 2 μg/ml insulin and 50 μg/ml ascorbic acid were added to the medium to

enhance fibrin gel remodeling into tissue. Construct medium was changed 3 times per week until use at 4 weeks. Vascular constructs at 4 weeks were 3-4 cm long and 2 mm in diameter, with a wall thickness of approximately 200 μm.

4.2.3 HBOEC and HUVEC Seeding on Bioartificial Tissue

After 4 weeks, remodeled fibrin tissue constructs were slit axially and placed lumenal surface down on a polycarbonate sheet using a method adapted from Kladakis et al.(30). A polycarbonate cap with a 3 mm high groove was placed around the piece of tissue and filled with a solution of 4% low gel temperature agarose (A0701; Sigma). The agarose was allowed to gel and then the polycarbonate sheet was removed, exposing the lumenal surface of the construct (Figure 4.1A). A Teflon ring was placed around the cap to form a well for cell culture medium. HBOECs or HUVECs were labeled with 2.5 μM CellTracker Green (Invitrogen) and then were seeded on the lumenal surface of the tissue constructs. The cells were seeded slowly, drop-wise onto the tissue at a concentration of $2x10^6$ cells/ml so as to achieve a seeding of 100,000 cells/cm^2. One hour after seeding the tissue was rinsed with HBSS to remove non-adherent cells and 4 ml of EGM medium was added to each well. For TNF-α activation or shear stress experiments, cells were allowed to adhere for 24 hours prior to start of the experiment.

4.2.4 Cell Staining

HBOEC and HUVEC expression of thrombomodulin (TM), tissue factor (TF), endothelial nitric oxide synthase (eNOS), VCAM-1, ICAM-1 and VE-Cadherin was examined by immunocytochemistry. Cells seeded for 48 hours in EGM medium on tissue

culture plastic coated with type I rat tail collagen or whole tissue were rinsed with Hanks balanced salt solution (HBSS), fixed in 4% paraformaldehyde for 10 minutes, and blocked with 5% normal donkey serum for 1 hour at room temperature. Samples were incubated with mouse anti-human TM (5 μg/ml; American Diagnostica), goat anti-human TF (10 μg/ml; American Diagnostica), rabbit anti-human eNOS (4 μg/ml; Santa Cruz), mouse anti-human VCAM-1 (5 μg/ml; Chemicon), mouse anti-human ICAM-1 (5 μg/ml; Chemicon), goat anti-human VE-Cadherin (10 μg/ml; Santa Cruz) and isotype matched controls for 1 hour. After rinsing, Dylight 549 conjugated, host-matched secondary antibody (1:400; Jackson Immuno) was applied for 1 hour at room temperature. Hoechst 33342 (1 ug/ml; Invitrogen) was used for staining of nuclei. Images were captured using epi-fluorescent microscopy (Olympus IX700) and confocal microscopy (Olympus Fluoview 1000). Measurement of the integrated fluorescent density per image for VCAM-1 and ICAM-1 was obtained with ImageJ software (NIH), as were cell counts per image. The integrated density per cell was calculated for each image and background values of the matched species IgG controls were subtracted.

4.2.5 Vascular Graft ECM Characterization

Constructs for histology were fixed in 4% paraformaldehyde for 3 hours at 4C, followed by overnight infiltration with 30% sucrose and 5% dimethyl sulfoxide (DMSO) in phosphate buffered saline (PBS). Samples were frozen in OCT (Tissue-Tek, Torrance, CA), sectioned into 9 μm thick cross-sections and stained with Lillie's trichrome (31).

Construct sections were also stained for the presence of various ECM proteins by immunohistochemistry. Sections were incubated with rabbit anti-human collagen I (2

μg/ml; Novus Biologicals), collagen IV (6 μg/ml; Abcam), laminin (10 μg/ml; Abcam), and fibronectin (1 μg/ml; American Diagnostica), goat anti-human fibrinogen (2 μg/ml; American Diagnostica), and isotype matched controls in 5% normal donkey serum in PBS (Jackson Immuno) overnight. After rinsing, sections were incubated with Dylight 549 donkey anti-rabbit or anti-goat (1:400 dilution, Jackson Immuno) in PBS for 45 minutes and counterstained for 10 minutes with Hoechst 33342 (1 μg/ml; Invitrogen).

4.2.6 Shear Stress Experiments

The polycarbonate caps with the embedded tissue seeded with HBOECs or HUVECs (Figure 4.1A) were placed in parallel plate flow chambers (PPFCs) modified from the design of Sakariassen et al (Figure 4.1B) (32). The PPFC had a slot height of 0.5 mm, with a tapered inlet and outlet, reaching a final width of 1 cm. This chamber was redesigned from the chamber used in chapter 3 so that whole blood studies could also be run in the chamber. Thus, glass was removed from the system to limit platelet activation, the entire body is fabricated with polycarbonate, and inlet and outlet regions now allow for less turbulent flow of blood or cell culture medium.

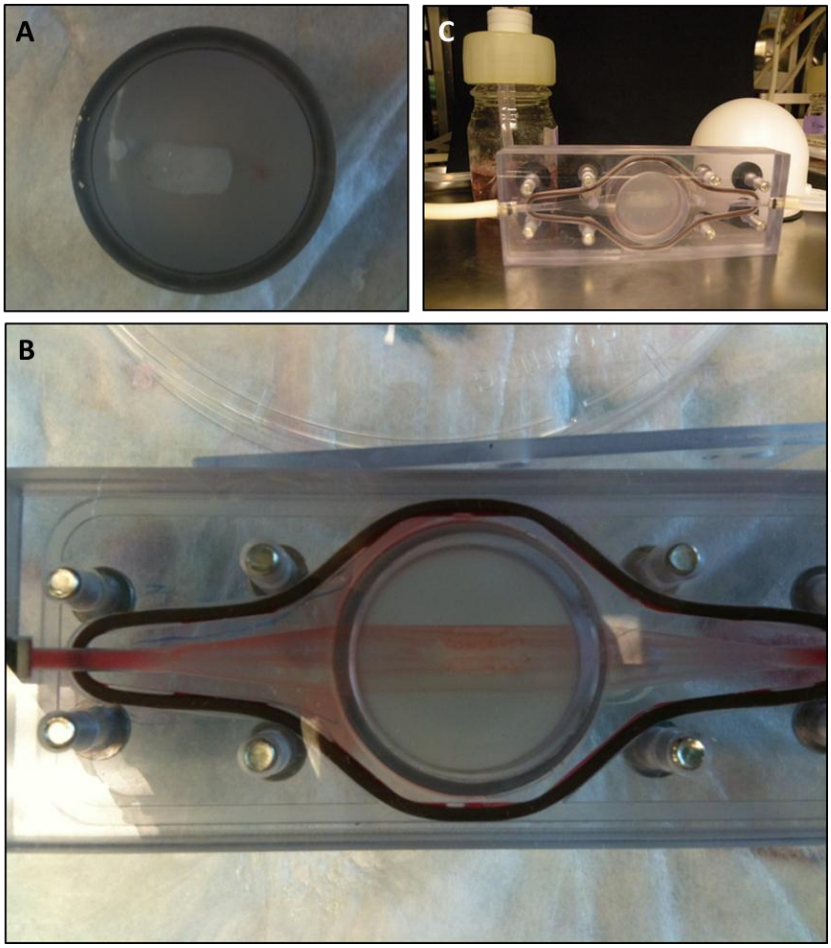

Figure 4.1: Parallel plate flow chamber for application of shear stress on HBOEC- and HUVEC-seeded bioartificial tissue. A) Polycarbonate cap used for embedding bioartificial tissue in agarose. This cap can then be placed in B) and utilized in C) a closed loop consisting of a medium reservoir, a peristaltic pump and a pulse dampener.

The chamber was assembled in a closed loop consisting of a medium reservoir allowing for gas exchange, a peristaltic pump (Cole-Parmer, Vernon Hills, Illinois), and a pulse dampener (Cole Parmer) (Figure 4.1C). The system was primed with the EGM medium prior to placing the tissue within the system and then the flow rate was increased 0.5 dyne/cm^2 every minute, starting at 3 dynes/cm^2 and increasing to 15 dynes/cm^2. Steady laminar shear stress was applied for 24 hours and then the constructs were harvested for analysis. In the case of TNF-α exposure, 10 U/ml TNF-α was added to static and flow samples at the time flow was started.

For short duration shear stress experiments, the shear stress was ramped as described; however, at 0, 1, 5, 10, 15 and 25 dynes/cm^2 the shear stress was held for 20 minutes and then the construct surface was imaged. HBOECs were seeded on bioartificial tissue and Type I collagen-coated tissue culture plastic (TCP) for 24 hours prior to application of shear stress. 12 images per sample were obtained of the CellTracker Green-labeled HBOECs using an Olympus IX70 inverted microscope. Images were thresholded at a fixed level and analyzed with ImageJ software (NIH) for % area coverage of the tissue surface. Unseeded TCP and bioartificial tissue were used as negative controls.

4.2.7 Cell Retention, Orientation and Alignment

HBOECs and HUVECs were stained and imaged for VE-Cadherin and Hoechst as described above. Confocal images were taken at 20x and 40x to eliminate imaging of Hoechst staining of the HDF nuclei. The number of nuclei per image were counted using ImageJ software and normalized to the area of the image to give a cell density. To

quantitate cell orientation and alignment, ImageJ software was used to outline each cell, based on the VE-Cadherin staining, and calculate the area, perimeter, major axis, minor axis, and angle of the major axis (cell alignment) with the flow direction. The shape index was calculated using:

$$Shape\ Index = \frac{4\pi Area}{Perimeter^2}$$

The shape index is a measure of the elongation of a cell and is equal to one for a circle and zero for a line. Decreasing values thus indicate that cells are becoming more elongated.

4.2.8 Scanning Electron Microscopy

Samples for scanning electron microscopy (SEM) were prepared using the fixation procedure of Ishihara et al.(33), with minor alterations for our tissue engineered constructs. Briefly, samples were removed from the PPFC, rinsed quickly with 37C Hanks balanced salt solution (HBSS), and then fixed with cold 3% glutaraldehyde for 2 hours, washed with cold 5% sucrose for 1 hour and post-fixed with 1% osmium tetroxide, all on ice and in 0.1 M sodium cacodylate pH 7.3. After graded ethanol dehydration, samples were CO_2 critical point dried, ion sputter coated with platinum to ~2 nm, and viewed in a Hitachi S-4700 or S-900 at 3.0 kV.

4.2.9 NO Production

Medium samples were collected from HUVEC and HBOEC seeding bioartificial tissue after 24 hours of static culture of exposure to 15 dynes/cm^2 shear stress. Samples were frozen at -80C, lyophilized, and reconstituted at 2.5x the initial concentration. A

commercially available kit was used to convert nitrate to nitrite, followed by the spectrophotometric quantitation of nitrite levels using Griess Reagent (Calbiochem, San Diego, CA).

4.2.10 Whole Blood Assay

A platelet adhesion assay was performed with 1 U/ml heparinized whole blood in the PPFCs described above. Whole blood was collected from healthy, consenting donors under University of Minnesota Institutional Review Board approval and used at 37C within 2 hours of the blood draw. The system was primed with HBSS at 37C prior to loading with whole blood. The initial 5-10 ml of blood was discarded to remove any blood that had mixed with the HBSS and then the system was run as a closed loop at a shear rate of 400 s^{-1}. After 20 minutes of whole blood exposure, HBSS was run through the system for 2 minutes to remove unbound platelets and leukocytes. The samples were removed from the flow chamber and fixed with 4% PFA for 10 minutes and then rinsed with HBSS. The tissue was simultaneously stained for EC junctions with goat anti-human VE-Cadherin and platelets with mouse anti-human GP-1b (1 μg/ml; Abcam) for 1 hour at room temperature. After rinsing with PBS, Dylight 549 donkey anti-mouse and Dylight 649 donkey anti-goat secondary antibody (1:400; Jackson Immuno) were applied for 45 minutes, followed by staining with Hoechst 33342 for 10 minutes. Samples were imaged on an Olympus Fluoview 1000 confocal microscope and platelet and leukocyte coverage quantified using ImageJ software. Images were converted to binary images by use of a fixed threshold. These images were used to calculate the area coverage of platelets or leukocytes. Values were normalized to the HBOEC static group.

4.2.11 Statistical Analysis

Statistical analysis was performed using GraphPad Prism software for Windows (GraphPad Software, Inc., San Diego, CA). One-way and multivariate ANOVA with Bonferroni *post hoc* analysis was conducted to evaluate significant differences between groups. A significance level of $\alpha=0.05$ was used for all tests. All graphs indicate mean ± standard error of the mean (SE).

4.3 Results

4.3.1 HBOECs formed a confluent monolayer on bioartificial tissue

HBOECs adhered to the bioartificial tissue and formed a confluent monolayer (Figure 4.2A-C). The cells had typical cobblestone morphology, stained for VE-Cadherin and maintained cell-to-cell contact (Figure 4.2B,C). The HBOECs also expressed thrombomodulin (Figure 4.2D), an important endothelial anticoagulant molecule, while showing limited tissue factor expression (Figure 4.2E) until exposed to the agonist TNF-α (Figure 4.2F). Staining throughout the thickness of the tissue showed that TNF-α stimulated TF expression by the HBOECs on the lumenal surface as well as by the underlying fibroblasts.

Non-endothelialized and HBOEC-seeded bioartificial tissue was stained for ECM molecules to assess the protein composition at the lumenal surface. The tissue was embedded in agarose with the lumenal surface exposed and cultured with or without HBOECs for 7 days. Immunostaining for fibrin, fibronectin, collagen I, collagen IV, and laminin highlighted the presence of all of these ECM proteins throughout the unseeded

(Figure 4.3A-E) and HBOEC-seeded tissue (Figure 4.3F-J). Residual fibrin, fibronectin and collagen I were present on the lumenal surface (Figure 4.3A-C); however, collagen IV and laminin staining was limited on the lumenal surface of the unseeded tissue (Figure 4.3D,E). This is in contrast to the HBOEC-seeded tissue, where a distinct band of collagen IV and laminin were present on the lumenal surface (Figure 4.3I,J). This alteration on the lumenal surface of the HBOEC-seeded tissue is indicative of new ECM deposition by the HBOECs.

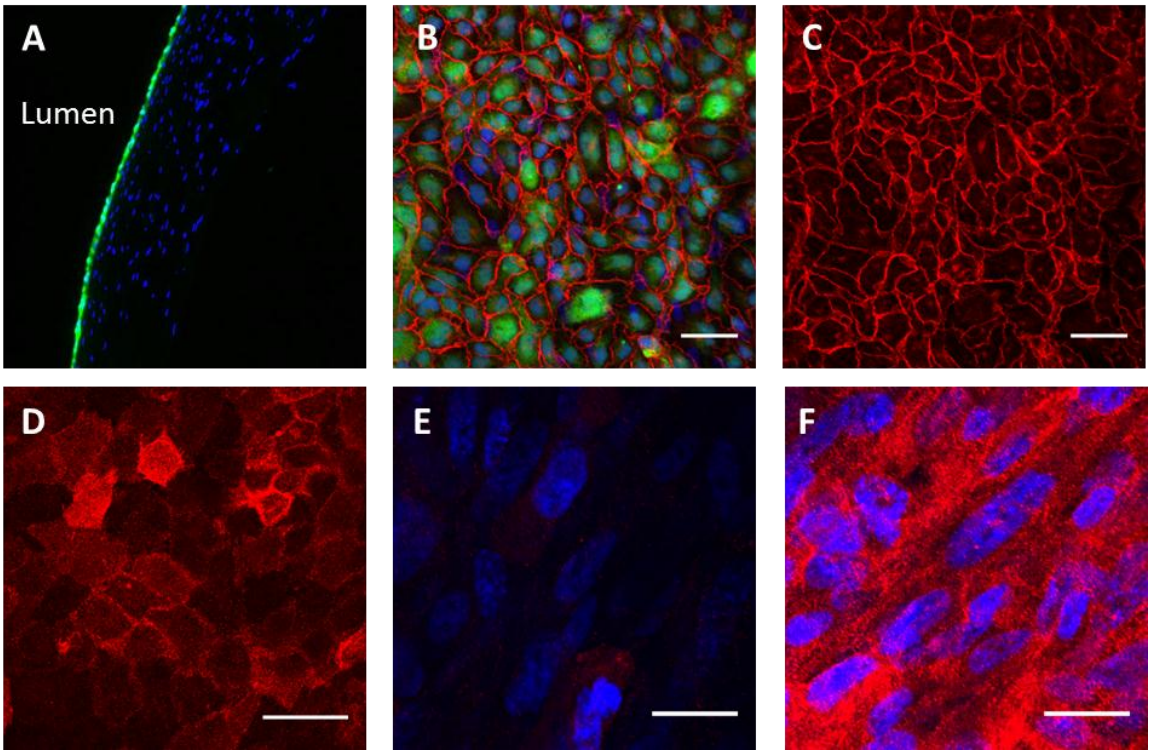

Figure 4.2: HBOECs seeded on bioartificial tissue. A) Cross sectional and B-C) *En face* images of CellTracker Green-labeled HBOECs seeding on bioartificial tissue show that the HBOECs form a confluent monolayer on the tissue surface. Nuclei of HBOEC and HDF in the tissue are stained blue and VE-Cadherin staining is pseudo-colored red. D) HBOECs on the bioartificial tissue express TM. E) TF expression by HBOEC on unstimulated tissue and F) after exposure to TNF-α. B-D) Scale bar = 50 μm. E-F) Scale bar = 25 μm.

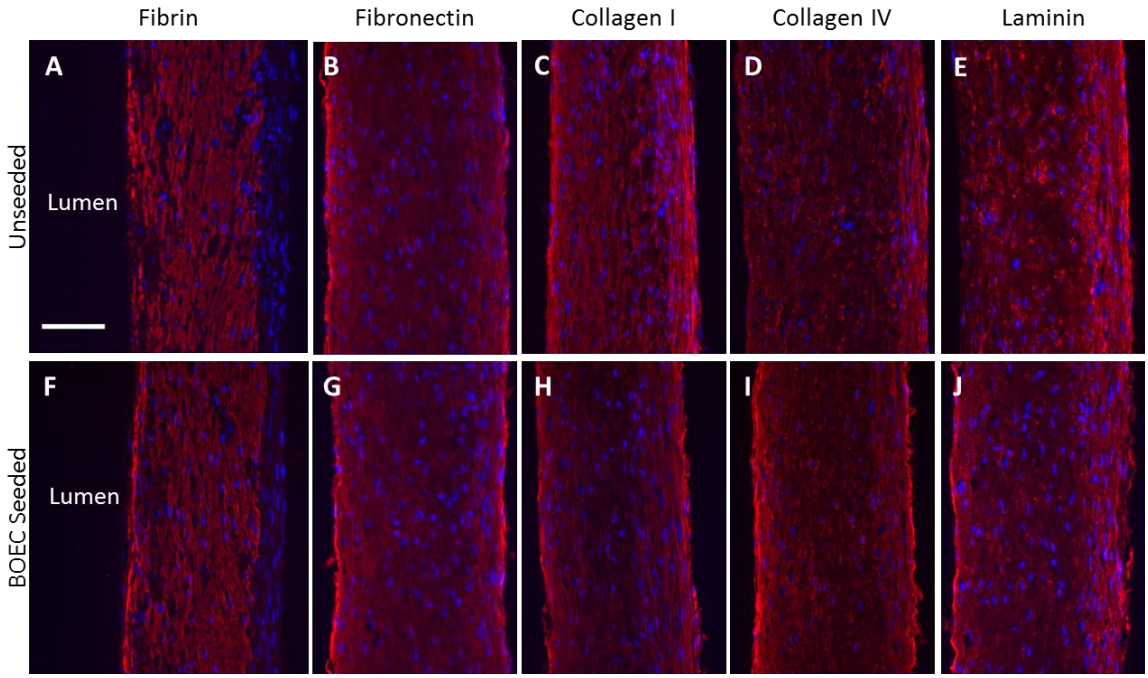

Figure 4.3: ECM staining of bioartificial tissue. A-E) Bioartificial tissue stained for ECM components. F-J) Bioartificial tissue seeded with HBOECs for 7 days prior to staining. A,F) Fibrin staining. B,G) Fibronectin staining. C,H) Collagen I staining. D,I) Collagen IV staining. E,J) Laminin staining. The lumenal surface is on the left side of each image, nuclei counterstained with Hoechst 33342. Scale bar = 100 μm.

4.3.2 HBOECs remained adherent on bioartificial tissue under physiological shear stress and elongate in the flow direction

HBOECs were seeded on collagen-coated TCP or bioartificial tissue and allowed to adhere for 24 hours. Surfaces were then exposed to increasing shear stress for 20 minute durations at each shear stress step (1, 5, 10, 15, 25 dynes/cm^2). HBOECs on collagen-coated TCP maintained 82.6 ± 1.2% surface coverage at 25 dynes/cm^2 (Figure 4.4). Surface coverage was improved by seeding on bioartificial tissue, with a surface coverage of 94.4 ± 0.6% at 25 dynes/cm^2. Surface coverage began to drop for HBOEC on TCP beginning at 15 dynes/cm^2, but was not significantly lower for HBOEC on bioartificial tissue until 25 dynes/cm^2.

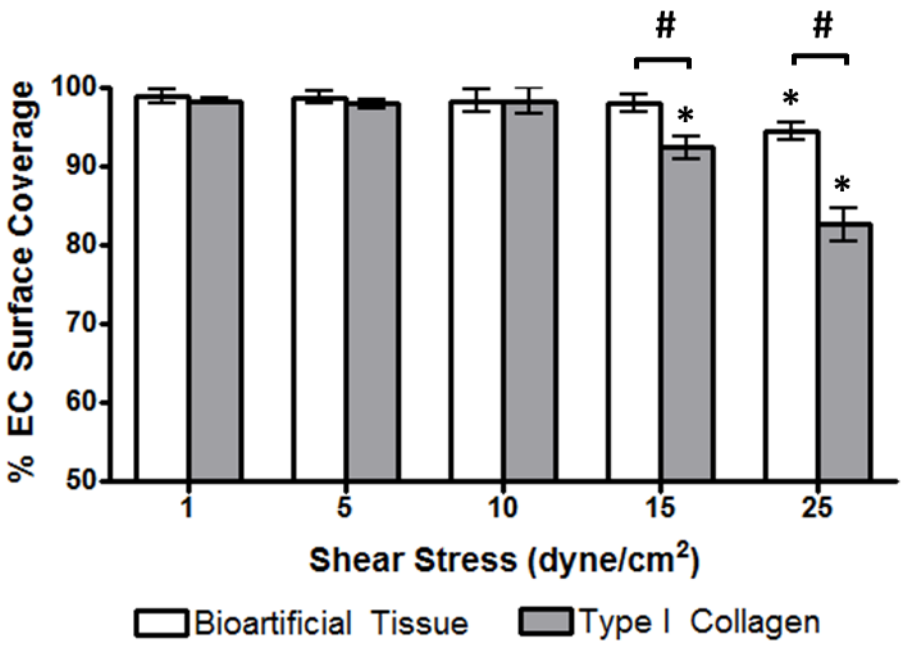

Figure 4.4: HBOEC retention under physiological shear stress for short durations. HBOECs were seeded on Type I collagen-coated TCP or bioartificial tissue and incrementally exposed to 1, 5, 10, 15, or 25 dynes/cm^2 for 20 minutes and HBOEC surface coverage calculated based on the CellTracker Green staining. Plot shows mean ± SE for n=3 samples. *Significant difference compared to 1 dynes/cm^2 samples on the same substrate ($p<0.05$). # Significant difference between HBOEC on TCP and bioartificial at the same shear stress.

To examine long term seeding on bioartificial tissue, HBOECs and HUVECs were seeded at a cell density near confluence and allowed to adhere for 24 hours. After 24 hours, seeded tissue was either maintained in static culture for another 24 hours (Figure 4.5A,C) or placed in a parallel plate flow chamber and laminar, steady shear stress applied at 15 dynes/cm^2 (Figure 4.5B,D). After 24 hours under flow, HBOECs and HUVECs had begun to elongate in the flow direction, as illustrated with VE-Cadherin staining. VE-Cadherin staining of the cell junctions was visible in all samples and confirmed that HBOEC and HUVEC under flow still maintain a confluent monolayer. Though the HBOECs and HUVECs exposed to flow showed a marked change in cell

morphology, the cell density was not significantly altered by application of shear stress (Figure 4.5E). HBOEC and HUVEC elongation and alignment were quantified for comparison by calculation of the cell shape index and alignment angle. These measurements confirmed that by 24 hours, HBOECs and HUVECs were elongating and aligning in the flow direction (Figure 4.5F,G). There was no significant difference between HBOECs and HUVECs in shape index or the strength of alignment with flow by 24 hours.

HBOECs statically cultured on bioartifical tissue formed a confluent monolayer of cobblestone morphology with bulging nuclei and perinuclear regions (Figure 4.6A). After exposure to flow the cells were beginning to elongate in the direction of flow (Figure 4.6B), while maintaining confluence and cell-cell overlapping at regions of tight junctions (34) (Figure 4.6C). Both the static and flow conditioned cells showed numerous microvilli and cytoplasmic filaments characteristic of endothelial cells (33).

In one set of experiments, HBOEC and HUVEC cell death was higher than usual for unknown reasons. However, an endothelial cell-specific phenomenon was noticeable in these cultures; HBOEC and HUVECs both maintained a confluent monolayer, rearranging underneath the dead cell to maintain endothelium integrity (Figure 4.7). HBOECs migrated or expanded underneath the dead cell and established tight junctions concurrent with dead cell detachment (Figure 4.7A,B). This EC-specific function has been shown for mature endothelial cells responding to injury (35, 36) and was visible in HUVEC cultures as well (Figure 4.7C,D). Reidy et al. show that as injured ECs retract

the adjoining cells migrate into the space, maintaining monolayer integrity and ensuring continuous coverage of the subendothelium (36).

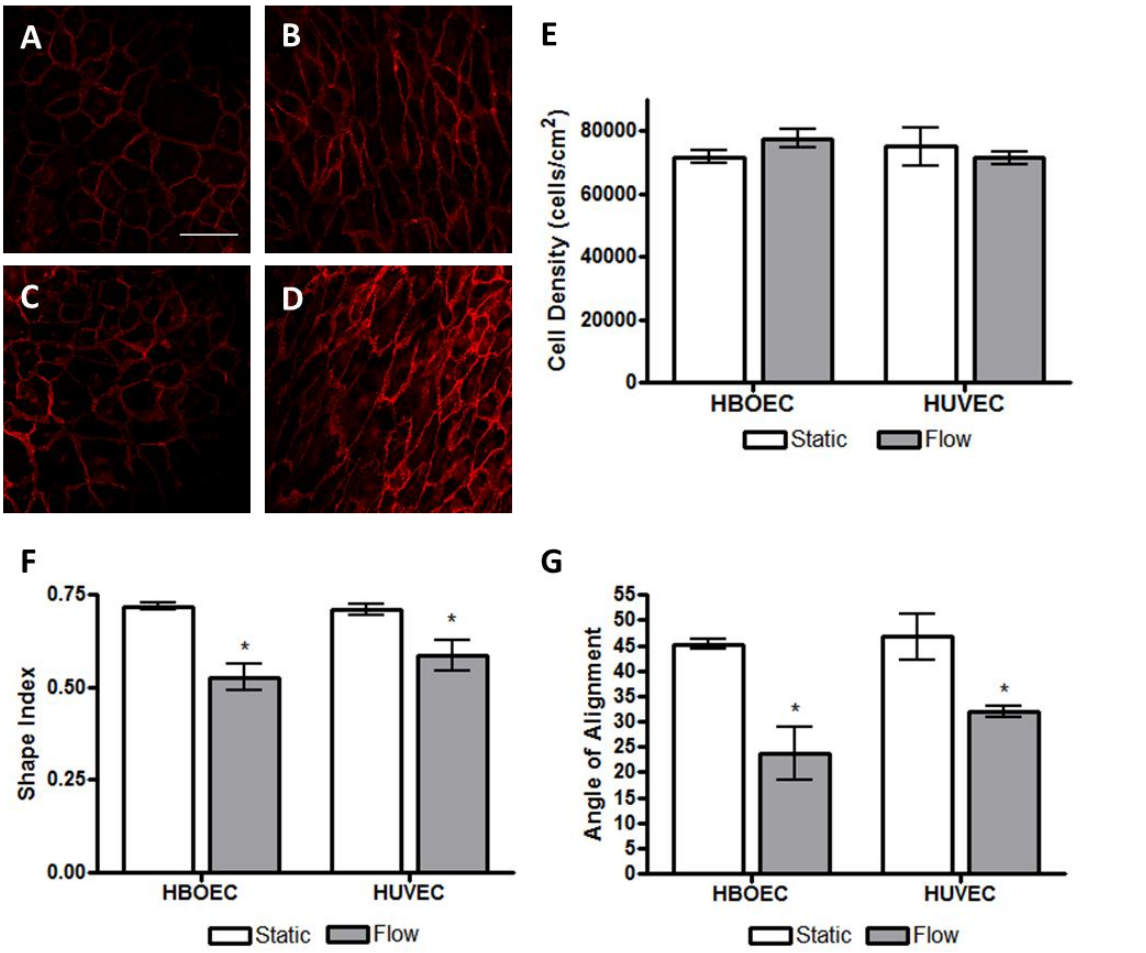

Figure 4.5: Retention, elongation, and alignment of HBOECs and HUVECs seeded on bioartificial tissue and exposed to shear stress. A-D) VE-Cadherin staining of A-B) HBOECs and C-D) HUVECs. A,C) Statically cultured cells. B,D) Cells cultured under 15 dynes/cm^2 for 24 hours. E) Cell density, F) elongation, and G) alignment of HBOECs and HUVECs after exposure to shear stress or static culture. The elongation is given as a shape index where 0 is a line and 1 is a circle. Cell alignment is given on a scale from perfectly aligned cells (0) to no alignment (45). *$p<0.05$ compared to static conditions. All plots show mean ± SE for n=3 independent experiments. Scale bar = 50 μm and applies to all images.

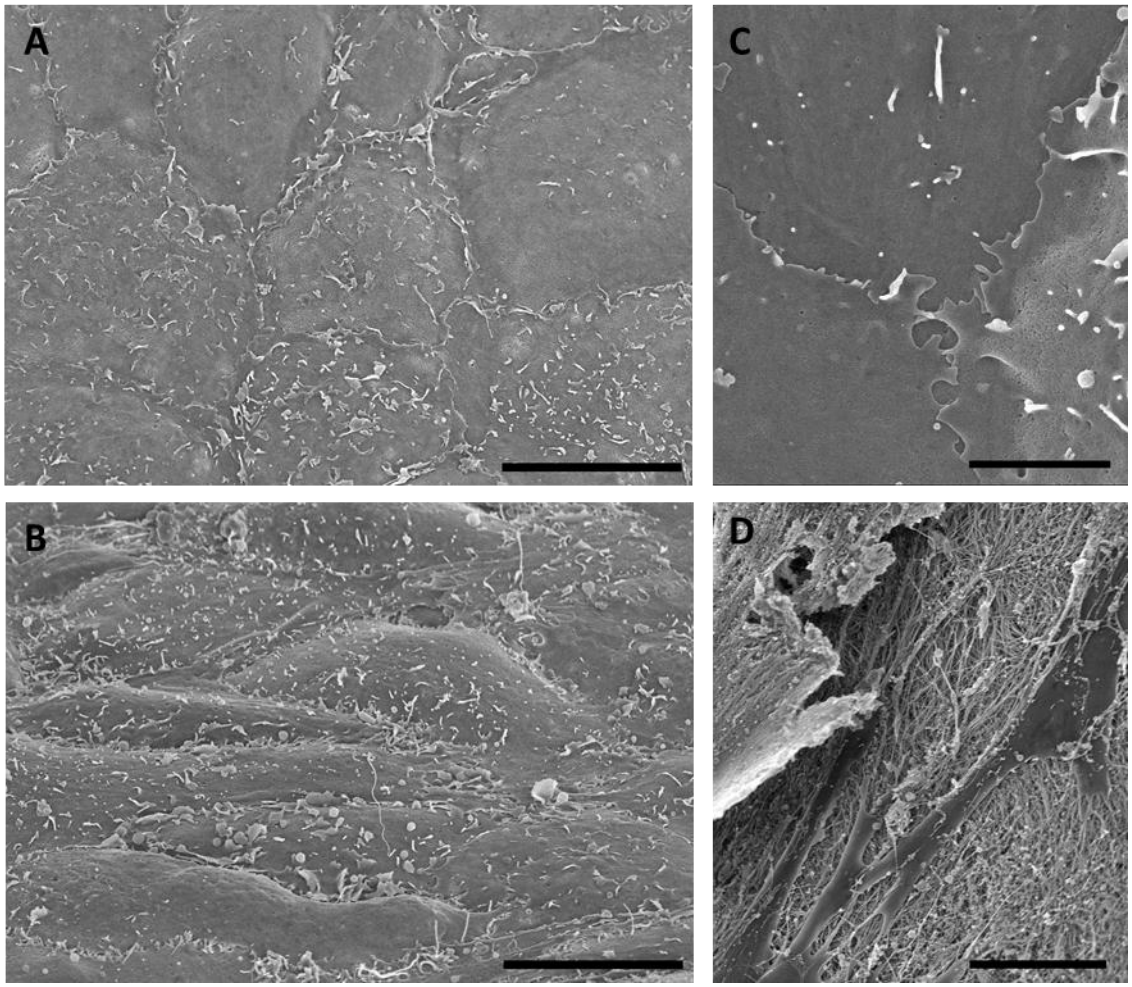

Figure 4.6: SEM of HBOECs on bioartificial tissue. HBOECs were A) cultured statically or B-C) exposed to 15 dynes/cm^2 shear stress for 24 hours. A) HBOECs cultured statically had distinct cell boundaries and prominent nuclei. B) HBOEC elongation occurred in the flow direction. C) High magnification image of HBOEC junctions after exposure to flow. D) Non-endothelialized section of bioartificial tissue showing smooth surface of fibroblasts and underlying ECM. A,B,D) Scale bar = 10 μm. C) Scale bar = 3 μm.

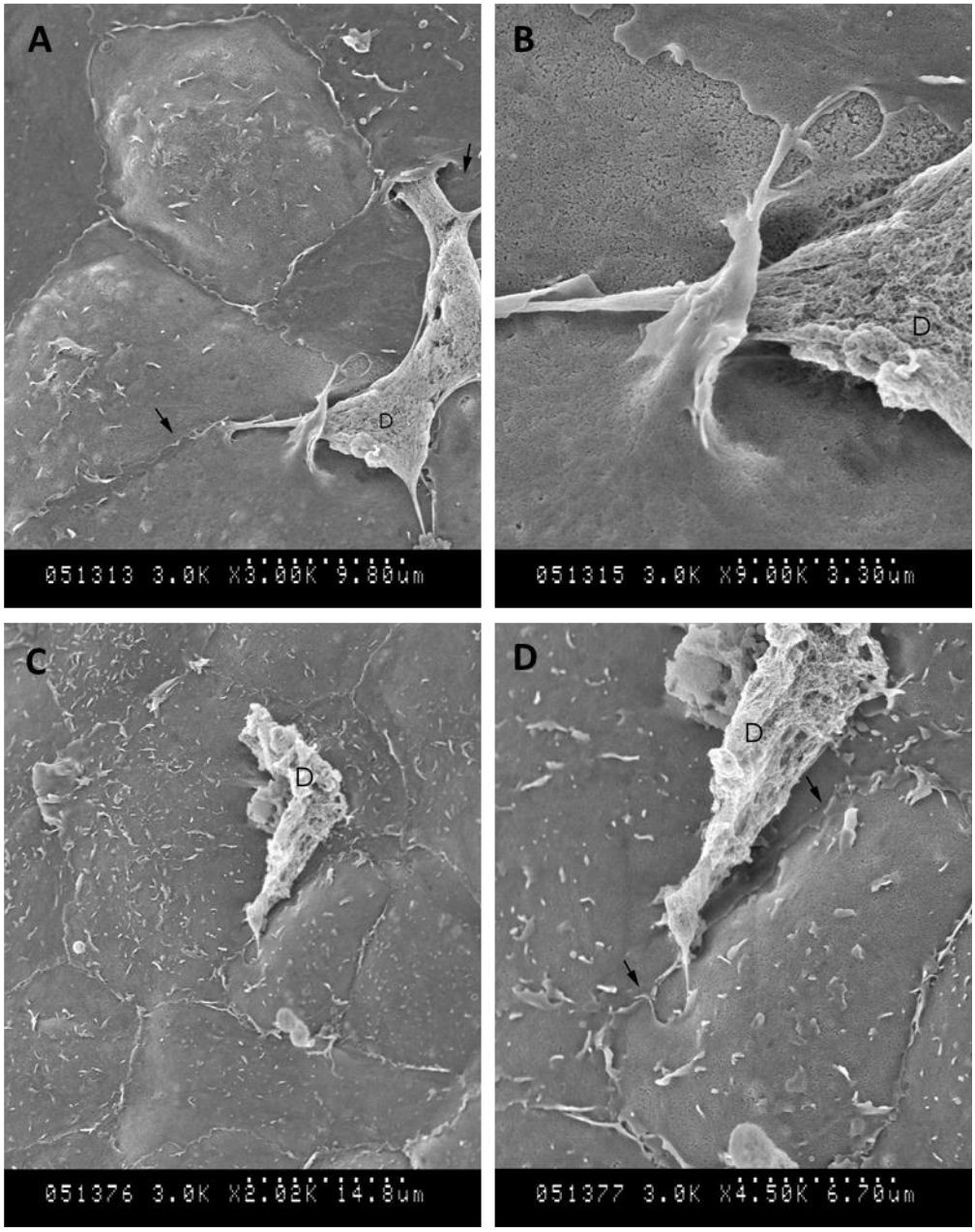

Figure 4.7: Maintenance of endothelial integrity. A) HBOECs with classic endothelial cobblestone morphology and dead cell, denoted "D". HBOECs have moved or expanded underneath the dead cell and are establishing tight junctions (arrows) concurrent with dead cell detachment. B) Newly forming filamentous connection, as seen in lower right in A. C) HUVECs with dead cell "D" showing same reorganizing behavior D) Higher magnification of C showing junctions in the area likely occupied by the dead cell before detachment.

4.3.3 Expression of proinflammatory molecules VCAM-1 and ICAM-1 can be modulated with shear stress and TNF-α stimulation

HBOEC expression of VCAM-1 and ICAM-1 after TNF-α stimulation was confirmed in static culture on collagen-coated TCP (Figure 4.8). This result agree with previous reports for the HBOEC response to TNF-α (1) and motivates our interest in examining VCAM-1 and ICAM-1 expression on bioartificial tissue as well as the potential for shear stress to modulate adhesion molecule expression.

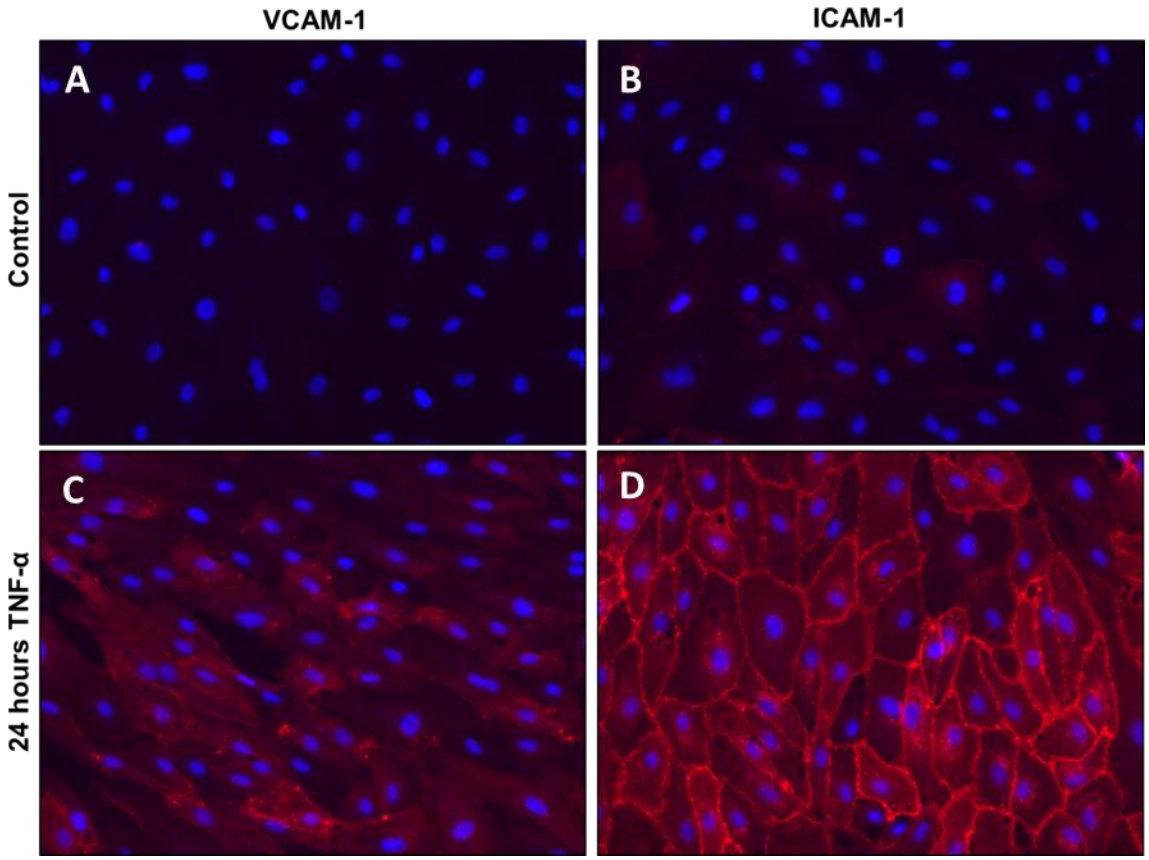

Figure 4.8: VCAM-1 and ICAM-1 expression on non-stimulated and TNF-α stimulated HBOECs cultured on collagen-coated TCP. A,C) VCAM-1 expression and B,D) ICAM-1 expression in A,B) unstimulated and C,D) TNF-α stimulated HBOECs.

Application of 15 dynes/cm^2 shear stress for 24 hours did not significantly alter VCAM-1 or ICAM-1 expression by HBOECs or HUVECs compared to static culture (Figure 4.9). Background due to non-specific binding of the VCAM-1 and ICAM-1 antibodies was subtracted from adhesion molecule expression during quantification by subtraction of mouse IgG control values, thus the values near zero indicate minimal expression of either VCAM-1 or ICAM-1, under static or shear stress culture, as these groups could not be distinguished statistically from the IgG controls.

To examine the responsiveness of the HBOECs to an inflammatory stimulus, 10 U/ml TNF-α was added to the cultures for 24 hours, during static culture or shear stress exposure. Addition of TNF-α increased VCAM-1 and ICAM-1 expression for both cell types, while shear stress was able to modulate this effect; shear stress conditioning combined with TNF-α stimulation decreased VCAM-1 and ICAM-1 expression compared to the static, TNF-α treated cells. VCAM-1 and ICAM-1 expression in the flow conditioned, TNF-α stimulated cells remained higher than the static or flow cultured, non-stimulated HBOECs and HUVECs. This indicates that HBOECs, like HUVECs, are responsive to biochemical inflammatory stimuli and modulate this response under steady laminar shear stress.

Based on multivariate ANOVA, the major source of variation in VCAM-1 and ICAM-1 expression was accounted for by the application of shear stress or TNF-α; however, cell type was a significant source of variability for VCAM-1 expression as well ($p<0.05$). VCAM-1 expression by HBOECs was elevated compared to HUVECs when

TNF-α was applied to statically cultured cells. Cell type was not a significant source of variability for ICAM expression.

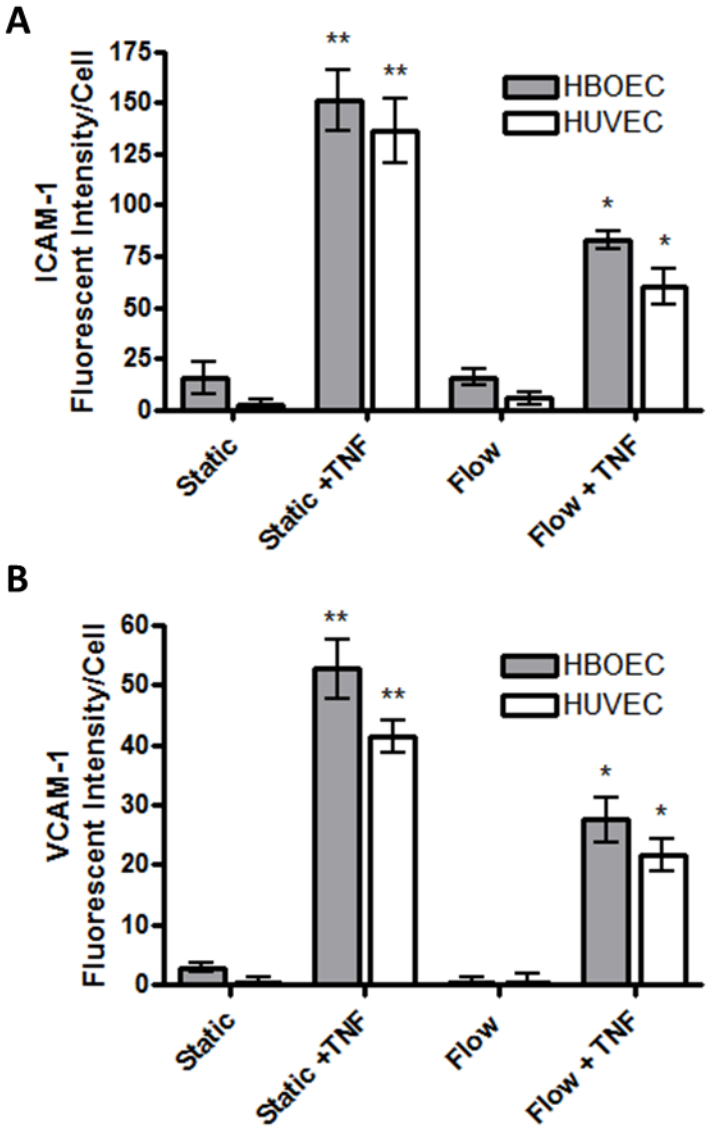

Figure 4.9: VCAM-1 and ICAM-1 expression by HBOECs and HUVECs seeded on bioartificial tissue and cultured under static or flow conditions for 24 hours, in the presence or absence of TNF-α. A) VCAM-1 Expression. B) ICAM-1 Expression. Plots show mean ± SE for n=3 tissue samples. *Significant increase over static and flow groups of the same cell type ($p<0.05$). **Significant increase over all other groups of the same cell type ($p<0.05$).

4.3.4 eNOS expression and NOx production were elevated by exposure to shear stress

After 24 hours of static culture or shear stress exposure at 15 dynes/cm^2, HBOECs seeded on the bioartificial tissue were stained for eNOS (Figure 4.10A-B). eNOS was localized to the HBOEC layer on the lumenal surface of the tissue. While eNOS staining of the statically cultured HBOECs was sporadic throughout the HBOEC layer (Figure 4.10A), flow conditioning increased the eNOS intensity and created a continuous band of eNOS throughout the HBOEC monolayer (Figure 4.10B).

To assess the effect of higher eNOS expression by HBOEC or HUVEC, NO production was measured for these same samples. NO production was measured via the quantitation of NO byproducts, nitrate and nitrite, in the cell culture medium after 24 hours of static culture or flow conditioning at 15 dynes/cm^2 (Figure 4.10C). Similar basal levels of NO were seen in HUVEC and HBOEC static culture. Nitric oxide production was elevated approximately 19-fold in HBOEC and HUVEC cultures when shear stress was applied for 24 hours.

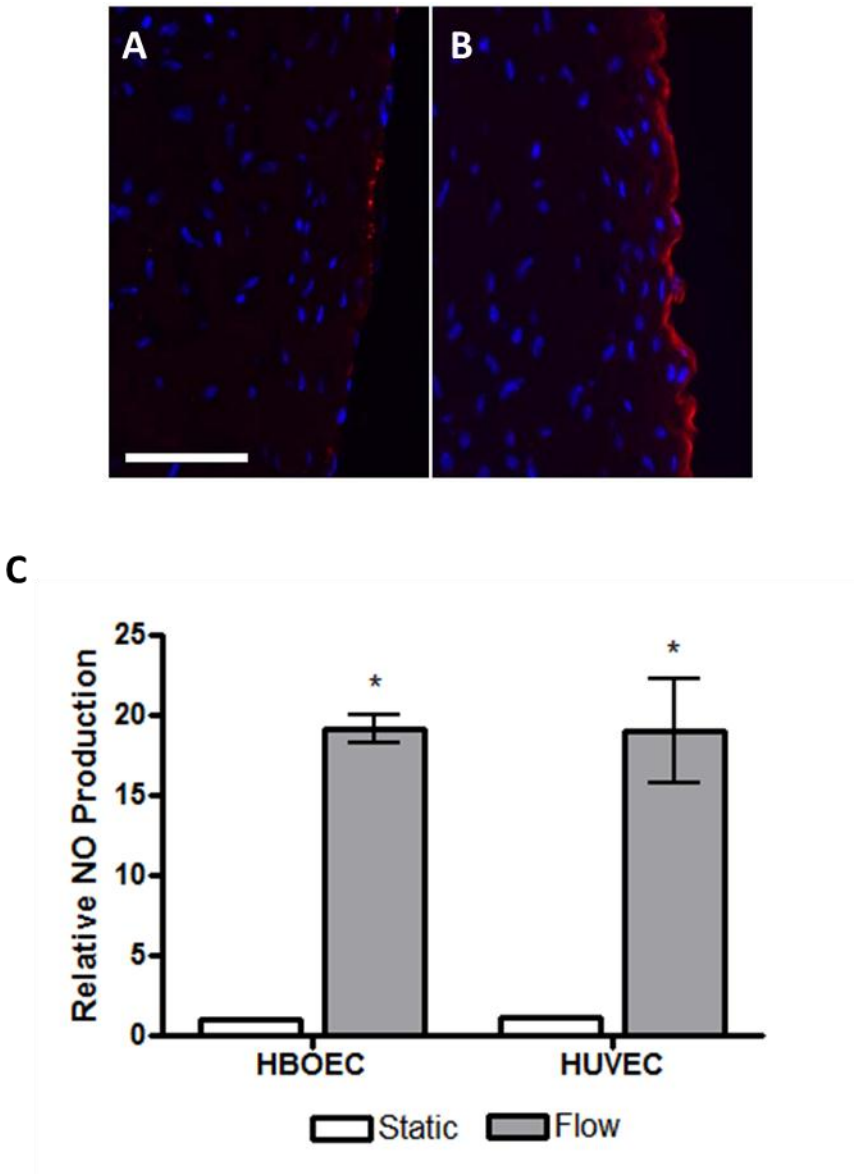

Figure 4.10: eNOS expression and NOx production by HBOEC and HUVEC seeded on bioartificial tissue and cultured under static and flow conditions for 24 hours. eNOS staining of HBOEC cross-sections after A) static culture or B) flow exposure. C) NO production was quantified by measurement of total nitrate and nitrite in the HBOEC and HUVEC culture medium. Values are normalized to the statically cultured HBOEC value. Plot shows mean ± SE for n=3 independent experiments. *NO production by HBOEC and HUVECs cultured under flow conditions increased compared to HBOEC static culture ($p<0.01$). Scale bar = 100 μm.

4.3.5 Platelet adhesion was lower following exposed to shear stress

As an *in vitro* method for examining the functional effect of HBOEC and HUVEC seeding on the bioartificial tissue, endothelialized and non-seeded tissue was exposed to 1 U/ml heparinized whole blood in PPFCs for 20 minutes and platelet adhesion to the exposed surfaces was then quantified (Figure 4.11A,B). Activation of HBOECs with TNF-α for 4 hours prior to application of the whole blood increased platelet adhesion to the surface (Figure 4.11A). Platelet surface coverage was higher on non-seeded tissue (11.0±2.8%) than on HBOEC-seeded tissue (0.5±0.1%) or HUVEC-seeded tissue (0.5±0.1%). Thus, HBOECs, like HUVECs, show decreased platelet adhesion compared to unseeded tissue.

A subset of the HBOEC- and HUVEC-seeded tissue was exposed to 15 dynes/cm^2 shear stress for 24 hours prior to whole blood exposure. Pre-conditioning of the HBOECs and HUVECs with shear stress decreased platelet adhesion compared to the statically cultured cells. Higher platelet adhesion on the static samples could be due to application of shear stress for the first time during the whole blood study. This loss might not occur for HBOECs or HUVECs that were pre-exposed to shear stress prior to the whole blood study. The alternative is that shear stress modulates the phenotype of the endothelial cells, decreasing platelet adhesion.

To examine the likelihood of these two possibilities, tissue samples were stained *en face* or after sectioning for VE-Cadherin and the platelet marker, GP-1b (Figure 4.11C-E). Images indicated monolayer coverage after whole blood exposure for samples that were both statically cultured and shear-conditioned prior to the whole blood assay.

Platelet binding most often appeared co-localized with the VE-Cadherin stain (Figure 4.11C). Platelets adhered near the junctions of cells, primarily as individual platelets (Figure 4.11C,D) and occasionally as small aggregates (Figure 4.11E).

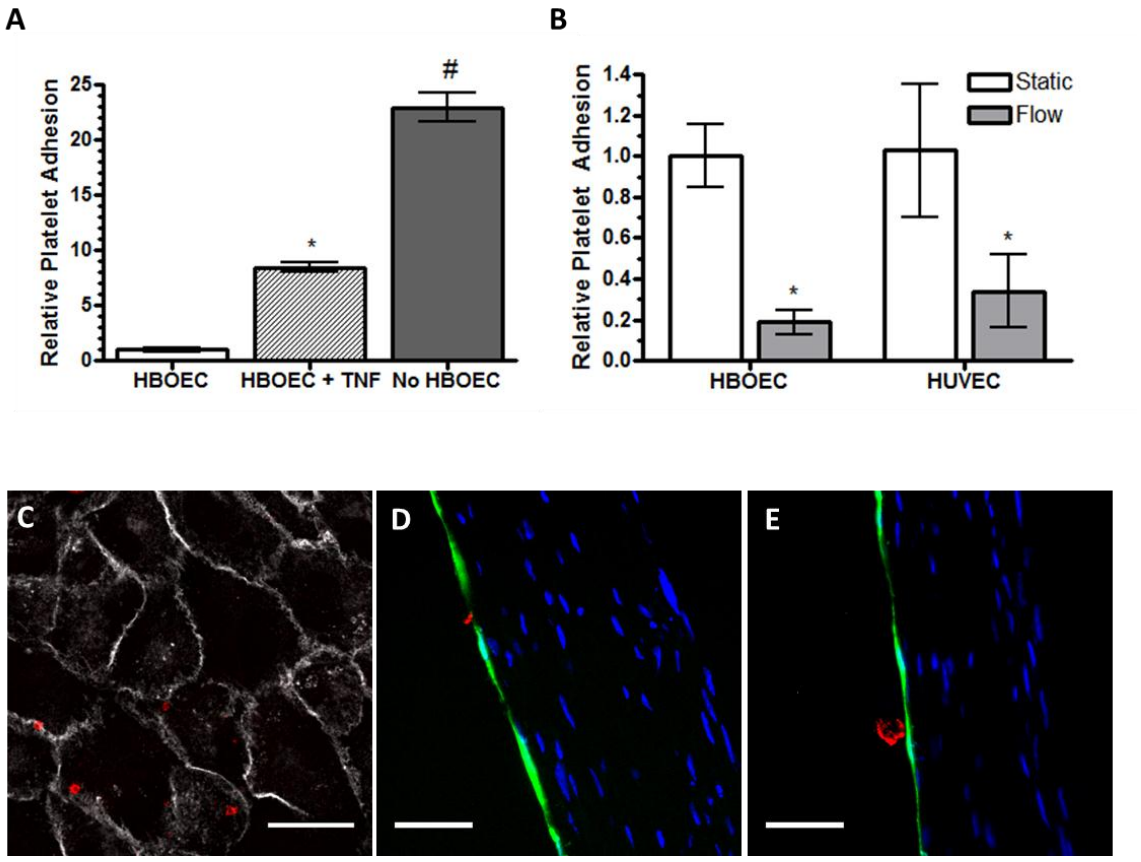

Figure 4.11: Platelet adhesion on HBOEC- and HUVEC-seeded bioartificial tissue pre-conditioned with 15 dynes/cm2 shear stress for 24 hours. A) Normalized platelet coverage. HBOEC-seeded tissue was compared to HBOEC-seeded tissue that was pre-exposed to TNF-α for 4 hours or non-seeded tissue. All groups were normalized to the statically cultured HBOEC group. *$p<0.001$ compared to unstimulated HBOEC. #$p<0.001$ compared to stimulated and non-stimulated HBOEC-seeded tissue. B) HBOEC- and HUVEC-seeded tissue was statically cultured or exposed to 15 dynes/cm^2 shear stress for 24 hours prior to whole blood exposure. *$p<0.05$ compared to the statically cultured cells of the same EC type. C) En face image of platelet localization. Scale bar = 25 μm. Images of cross-sections showing D) platelet localization and E) platelet aggregation on the surface of statically cultured HBOECs. Scale bar = 50 μm. Plots show mean ± SE for one representative experiment with n=3 tissue samples.

4.4 Discussion

The fabrication of a small-diameter vascular graft will require the incorporation of a non-thrombogenic lumenal surface, most likely through the formation of a functional neoendothelium, in order to obviate the need for anti-coagulation therapy. HBOECs are a promising cell source for this application, as they can be easily and non-invasively isolated, are highly proliferative, and do not suffer from smooth muscle cell contamination issues. The successful use of HBOECs for vascular tissue engineering will require 1) formation of a confluent monolayer on the tissue surface, 2) retention of the HBOEC under physiological shear stress, and 3) presentation of a non-thrombogenic and anti-inflammatory phenotype. As with native endothelium, responsiveness of the HBOEC to physiological shear stress will likely be necessary for the maintenance of a thromboresistant phenotype.

To address these requirements, bioartificial tissue was fabricated for HBOEC seeding. Tubular fibrin gels with entrapped HDF were allowed to remodel for 4 weeks as the HDFs degraded the fibrin and deposited new ECM, including fibronectin, laminin, and collagen I and IV, as shown in this study. The lumenal surface of the tissue stained positively for fibrin, fibronectin, and collagen I; however, collagen IV and laminin were primarily localized on the ablumenal surface. Fibronectin (37-40), laminin (37, 41, 42), collagen I (37, 38, 42), and fibrin (42-44) are all adhesion proteins that have been utilized to improve retention of ECs on vascular grafts, suggesting that a cell-produced matrix rich with these components would be conducive to EC adhesion and retention. Previous work with fibrin grafts made with SMCs had different localization of these adhesion

proteins; fibronectin and laminin were present on the lumenal surface, with collagen I primarily localized on the ablumenal surface (29).

HBOECs were seeded on the lumenal surface of HDF remodeled tissue, where the cells deposited new ECM, which appeared as localized bands of the basement membrane proteins collagen IV and laminin on the lumenal surface of the tissue. These bands were not present in the non-endothelialized tissue. The deposition of laminin and collagen IV was shown after 7 days of HBOEC culture since increases in fluorescent intensity at the lumenal surface were not obvious by the 2 day time point. While all of the flow studies were started after only 24 hours of seeding, these staining results do show that HBOECs are depositing collagen IV and laminin on bioartificial tissue over the course of the first week.

HBOEC adhesion and morphology was assessed on the bioartificial tissue. By 24 hours post-seeding, HBOECs formed a confluent monolayer of cells, with cell-to-cell junction formation, as assessed by VE-Cadherin staining and SEM. SEM of the BOECs after static culture or 24 hours of shear stress on the bioartificial tissue illustrates alignment of the HBOECs with flow, as well as maintenance of a confluent monolayer and cell-cell overlap at regions of tight junctions. The morphology is similar to that reported for other EC types reported in the literature (45), including the presence of cilia on the cell surface (33).

To assess HBOEC retention and alignment under flow conditions, a shear stress of 15 dynes/cm^2 was applied to mimic physiological arterial flow. When exposed to 15 dynes/cm^2 shear stress for 24 hours, HBOECs remained adherent, maintained a similar

cell density and VE-Cadherin staining, and elongated and aligned with flow. These results compared well with the HUVEC control cells used in these experiments, as well as with cell retention reported for cord blood-derived OECs (23) and short duration, high shear stress experiments with HBOECs (21, 22, 24).

While HBOECs grown as monolayers on collagen-coated tissue culture plastic show limited expression of the proinflammatory markers ICAM-1 and VCAM-1 (1), expression of these markers may be altered depending on the underlying matrix as well as the presence of secondary cell types. SMC-EC co-culture has been shown to increase gene and protein expression of activation markers such as VCAM-1, ICAM-1, and E-selectin, while shear stress modulates this expression (46, 47). Shear stress also alters activation marker expression in TNF-α stimulated and unstimulated EC monolayers (48-52). Like mature ECs, HBOECs upregulate VCAM-1 and ICAM-1 when exposed to TNF-α, a proinflammatory cytokine (53). Similar to results found with HBOECs seeded on type I collagen (1), HBOECs seeded on bioartificial tissue express low levels of VCAM-1 and ICAM-1 until exposed to TNF-α. However, TNF-α stimulated ICAM-1 and VCAM-1 expression was diminished by shear stress when TNF-α was administered during flow conditioning. These studies demonstrate that shear stress conditioning may be useful in decreasing surface expression of various procoagulation molecules on HBOECs, thereby promoting an anti-inflammatory phenotype, as reported for other ECs.

Shear stress can also be used to increase eNOS expression and NO production in mature ECs (54-56). NO promotes blood vessel vasodilation, inhibits platelet adhesion and aggregation, and is constitutively expressed in native ECs, primarily through eNOS

activity (57-59). Thus, production of NO is a necessary phenotype for functional HBOECs seeded on bioartificial tissue. Similar basal levels of NO were produced by HUVECs and HBOECs cultured statically. We have shown that HBOECs increased total NO production when cultured with steady laminar shear stress for 24 hours, as did the HUVEC control cells. This correlates with increased staining for eNOS in tissue cross-sections.

Though assessment of HBOEC retention and function *in vivo* will be necessary for a full consideration of HBOEC function, *in vitro* studies allowed comparison of HUVECs and HBOECs for a number of quantifiable parameters. As a functional test, we developed a whole blood study to examine platelet adhesion under flow. Though the ideal *in vitro* whole blood experiment would be performed with non-anticoagulated blood drawn directly into the flow chamber from the donor, that setup requires that blood be drawn from the donor for the full duration of the experiment and limits the flow rate that can be applied. Thus, most platelet adhesion studies with whole blood rely on the use of anticoagulated blood, often with heparin as the anticoagulant of choice. Platelet adhesion to a number of surfaces is Mg^{2+}-dependent, which rules out the use of citrated blood (60). A sub-therapeutic level of heparin, which prevented clotting during collection but enabled clotting on extended exposure to bioartificial tissue or collagen surfaces, was used for these studies.

Bioartificial tissue seeded with HBOECs or HUVECs or left unseeded was exposed to whole blood at a shear rate of 400 s^{-1} to mimic blood flow in human arteries. This equates to a wall shear stress of approximately 15 dynes/cm^2. Platelet coverage was

dramatically reduced on HBOEC-seeded bioartificial tissue as compared to non-seeded tissue. HBOECs and HUVECs had similar levels of platelet coverage, both when statically cultured and when pre-conditioned with shear stress for 24 hours prior to whole blood exposure. Pre-conditioning of the HBOECs or HUVECs with 15 dynes/cm^2 shear stress for 24 hours reduced platelet adhesion compared to statically cultured samples. Though a limited loss of statically cultured HBOECs or HUVECs during exposure to whole blood could not be fully ruled out, fluorescent micrographs indicated that monolayer coverage by the HBOECs and HUVECs was preserved.

Two likely possibilities exist for the decreased platelet adhesion on shear stress pre-conditioned surfaces. Pre-conditioning may have improved monolayer integrity, while blood flow over statically cultured HBOECs and HUVECs may have disrupted the endothelium, exposing the subendothelial matrix and increasing platelet adhesion on these substrates. However, increased thromboresistance of ECs under shear stress may also be responsible for decreased platelet adhesion. We have shown that HBOECs and HUVECs exposed to shear stress express higher levels of NO, while other groups have reported increased EC expression of PGI_2, NO, thrombomodulin, and tissue plasminogen activator, and decreased expression of plasminogen activator inhibitor type-1 with shear stress (61). Lund et al. showed that HBOECs have lower tissue factor and higher eNOS gene expression when exposed to shear stress (62). This switch to a more thromboresistant phenotype with shear stress exposure could account for the decreased platelet adhesion on the shear stress pre-conditioned surfaces. Either of these possibilities, however, leads to the same conclusion: that pre-conditioning with shear

stress has the potential to improve the functional outcome with HBOEC and HUVEC neoendothelium.

Methods to improve HBOEC adhesion and function upon implantation will be important benchmarks in developing a functional tissue-engineered vascular graft. As shear stress has been shown to have important effects on EC phenotype, adhesion, and function, shear stress preconditioning may represent another strategy for utilizing HBOECs successfully in endothelium formation. Shear stress preconditioning of EC-seeded vascular grafts prior to implantation or exposure to high flow rates has been shown to improve EC adherence and phenotype (63-66). Our results with HBOECs seeded on bioartificial tissue indicate that 1) HBOECs are shear stress responsive and 2) HBOECs can be pre-conditioned with shear stress *in vitro* to increase NO production and decrease platelet adhesion.

These results illustrate the potential utility for HBOECs in vascular tissue engineering, as not only do the cells adhere to the bioartificial tissue and remain adherent under physiological shear stress, they also exhibit low expression of activation markers and reduced platelet binding compared to unseeded tissue. Furthermore, exposure to shear stress decreased ICAM-1 and VCAM-1 expression on TNF-α stimulated HBOECs, increased eNOS expression and NO production, and decreased platelet adhesion during whole blood flow. These outcomes indicate that HBOECs are shear stress responsive and are functionally similar to HUVECs in their response to shear stress and their ability to limit platelet binding to a bioartificial vascular graft.

4.5 References

1. Lin, Y., Weisdorf, D.J., Solovey, A., and Hebbel, R.P. Origins of circulating endothelial cells and endothelial outgrowth from blood. The Journal of clinical investigation 105, 71, 2000.

2. Ingram, D.A., Caplice, N.M., and Yoder, M.C. Unresolved questions, changing definitions, and novel paradigms for defining endothelial progenitor cells. Blood 106, 1525, 2005.

3. Yoder, M.C., Mead, L.E., Prater, D., Krier, T.R., Mroueh, K.N., Li, F., Krasich, R., Temm, C.J., Prchal, J.T., and Ingram, D.A. Redefining endothelial progenitor cells via clonal analysis and hematopoietic stem/progenitor cell principals. Blood 109, 1801, 2007.

4. Hirschi, K.K., Ingram, D.A., and Yoder, M.C. Assessing identity, phenotype, and fate of endothelial progenitor cells. Arteriosclerosis, thrombosis, and vascular biology 28, 1584, 2008.

5. Rehman, J., Li, J., Orschell, C.M., and March, K.L. Peripheral blood "endothelial progenitor cells" are derived from monocyte/macrophages and secrete angiogenic growth factors. Circulation 107, 1164, 2003.

6. Zhang, S.J., Zhang, H., Wei, Y.J., Su, W.J., Liao, Z.K., Hou, M., Zhou, J.Y., and Hu, S.S. Adult endothelial progenitor cells from human peripheral blood maintain monocyte/macrophage function throughout in vitro culture. Cell research 16, 577, 2006.

7. Harraz, M., Jiao, C., Hanlon, H.D., Hartley, R.S., and Schatteman, G.C. CD34-blood-derived human endothelial cell progenitors. Stem cells (Dayton, Ohio) 19, 304, 2001.

8. Rohde, E., Malischnik, C., Thaler, D., Maierhofer, T., Linkesch, W., Lanzer, G., Guelly, C., and Strunk, D. Blood monocytes mimic endothelial progenitor cells. Stem cells (Dayton, Ohio) 24, 357, 2006.

9. Prokopi, M., Pula, G., Mayr, U., Devue, C., Gallagher, J., Xiao, Q., Boulanger, C.M., Westwood, N., Urbich, C., Willeit, J., Steiner, M., Breuss, J., Xu, Q., Kiechl, S., and Mayr, M. Proteomic analysis reveals presence of platelet microparticles in endothelial progenitor cell cultures. Blood 114, 723, 2009.

10. Davies, P.F. Flow-mediated endothelial mechanotransduction. Physiological reviews 75, 519, 1995.

11. Wu, K.K., and Thiagarajan, P. Role of endothelium in thrombosis and hemostasis. Annual review of medicine 47, 315, 1996.

12. Gimbrone, M.A., Jr., Topper, J.N., Nagel, T., Anderson, K.R., and Garcia-Cardena, G. Endothelial dysfunction, hemodynamic forces, and atherogenesis. Annals of the New York Academy of Sciences 902, 230, 2000.

13. McGuigan, A.P., and Sefton, M.V. The influence of biomaterials on endothelial cell thrombogenicity. Biomaterials 28, 2547, 2007.

14. He, H., Shirota, T., Yasui, H., and Matsuda, T. Canine endothelial progenitor cell-lined hybrid vascular graft with nonthrombogenic potential. The Journal of thoracic and cardiovascular surgery 126, 455, 2003.

15. Shirota, T., He, H., Yasui, H., and Matsuda, T. Human endothelial progenitor cell-seeded hybrid graft: proliferative and antithrombogenic potentials in vitro and fabrication processing. Tissue engineering 9, 127, 2003.

16. Griese, D.P., Ehsan, A., Melo, L.G., Kong, D., Zhang, L., Mann, M.J., Pratt, R.E., Mulligan, R.C., and Dzau, V.J. Isolation and transplantation of autologous circulating endothelial cells into denuded vessels and prosthetic grafts: implications for cell-based vascular therapy. Circulation 108, 2710, 2003.

17. Allen, J.B., Khan, S., Lapidos, K.A., and Ameer, G.A. Toward engineering a human neoendothelium with circulating progenitor cells. Stem cells (Dayton, Ohio) 28, 318, 2010.

18. Kaushal, S., Amiel, G.E., Guleserian, K.J., Shapira, O.M., Perry, T., Sutherland, F.W., Rabkin, E., Moran, A.M., Schoen, F.J., Atala, A., Soker, S., Bischoff, J., and Mayer, J.E., Jr. Functional small-diameter neovessels created using endothelial progenitor cells expanded ex vivo. Nature medicine 7, 1035, 2001.

19. Schmidt, D., Asmis, L.M., Odermatt, B., Kelm, J., Breymann, C., Gossi, M., Genoni, M., Zund, G., and Hoerstrup, S.P. Engineered living blood vessels: functional endothelia generated from human umbilical cord-derived progenitors. The Annals of thoracic surgery 82, 1465, 2006.

20. Aper, T., Schmidt, A., Duchrow, M., and Bruch, H.P. Autologous blood vessels engineered from peripheral blood sample. Eur J Vasc Endovasc Surg 33, 33, 2007.

21. Thebaud, N.B., Bareille, R., Remy, M., Bourget, C., Daculsi, R., and Bordenave, L. Human progenitor-derived endothelial cells vs. venous endothelial cells for vascular tissue engineering: an in vitro study. Journal of tissue engineering and regenerative medicine 4, 473, 2010.

22. Stachelek, S.J., Alferiev, I., Connolly, J.M., Sacks, M., Hebbel, R.P., Bianco, R., and Levy, R.J. Cholesterol-modified polyurethane valve cusps demonstrate blood outgrowth endothelial cell adhesion post-seeding in vitro and in vivo. The Annals of thoracic surgery 81, 47, 2006.

23. Brown, M.A., Wallace, C.S., Angelos, M., and Truskey, G.A. Characterization of umbilical cord blood-derived late outgrowth endothelial progenitor cells exposed to laminar shear stress. Tissue Eng Part A 15, 3575, 2009.

24. Stroncek, J.D., Grant, B.S., Brown, M.A., Povsic, T.J., Truskey, G.A., and Reichert, W.M. Comparison of endothelial cell phenotypic markers of late-outgrowth endothelial progenitor cells isolated from patients with coronary artery disease and healthy volunteers. Tissue Eng Part A 15, 3473, 2009.

25. Grassl, E.D., Oegema, T.R., and Tranquillo, R.T. A fibrin-based arterial media equivalent. Journal of biomedical materials research 66, 550, 2003.

26. Syedain, Z.H., Weinberg, J.S., and Tranquillo, R.T. Cyclic distension of fibrin-based tissue constructs: evidence of adaptation during growth of engineered connective tissue. Proceedings of the National Academy of Sciences of the United States of America 105, 6537, 2008.

27. Ahmann, K.A., Weinbaum, J.S., Johnson, S.L., and Tranquillo, R.T. Fibrin Degradation Enhances Vascular Smooth Muscle Cell Proliferation and Matrix Deposition in Fibrin-Based Tissue Constructs Fabricated In Vitro. Tissue Eng Part A, 2010.

28. Lin, Y. Phenotypic characterization of outgrowth endothelial cells from cultures of peripheral blood and feasibility studies of using these cells in biomedical applications. 2003.

29. Isenberg, B.C., Williams, C., and Tranquillo, R.T. Endothelialization and flow conditioning of fibrin-based media-equivalents. Ann Biomed Eng 34, 971, 2006.

30. Kladakis, S.M., and Nerem, R.M. Endothelial cell monolayer formation: effect of substrate and fluid shear stress. Endothelium 11, 29, 2004.

31. Kiernan, J.A. Histological and histochemical methods : theory and practice. Oxford [U.K.] ; Boston: Butterworth-Heinemann, 1999.

32. Sakariassen, K.S., Aarts, P.A., de Groot, P.G., Houdijk, W.P., and Sixma, J.J. A perfusion chamber developed to investigate platelet interaction in flowing blood with human vessel wall cells, their extracellular matrix, and purified components. The Journal of laboratory and clinical medicine 102, 522, 1983.

33. Ishihara, T., Ferrans, V.J., Jones, M., Boyce, S.W., and Roberts, W.C. Occurrence and significance of endothelial cells in implanted porcine bioprosthetic valves. The American journal of cardiology 48, 443, 1981.

34. Bowman, P.D., Ennis, S.R., Rarey, K.E., Betz, A.L., and Goldstein, G.W. Brain microvessel endothelial cells in tissue culture: a model for study of blood-brain barrier permeability. Annals of neurology 14, 396, 1983.

35. Mohtai, M., and Yamamoto, T. Smooth muscle cell proliferation in the rat coronary artery induced by vitamin D. Atherosclerosis 63, 193, 1987.

36. Reidy, M.A., and Schwartz, S.M. Endothelial injury and regeneration. IV. Endotoxin: a nondenuding injury to aortic endothelium. Laboratory investigation; a journal of technical methods and pathology 48, 25, 1983.

37. Anderson, J.S., Price, T.M., Hanson, S.R., and Harker, L.A. In vitro endothelialization of small-caliber vascular grafts. Surgery 101, 577, 1987.

38. Kaehler, J., Zilla, P., Fasol, R., Deutsch, M., and Kadletz, M. Precoating substrate and surface configuration determine adherence and spreading of seeded endothelial cells on polytetrafluoroethylene grafts. J Vasc Surg 9, 535, 1989.

39. Kesler, K.A., Herring, M.B., Arnold, M.P., Glover, J.L., Park, H.M., Helmus, M.N., and Bendick, P.J. Enhanced strength of endothelial attachment on polyester elastomer and polytetrafluoroethylene graft surfaces with fibronectin substrate. J Vasc Surg 3, 58, 1986.

40. Seeger, J.M., and Klingman, N. Improved in vivo endothelialization of prosthetic grafts by surface modification with fibronectin. J Vasc Surg 8, 476, 1988.

41. Koveker, G.B., Graham, L.M., Burkel, W.E., Sell, R., Wakefield, T.W., Dietrich, K., and Stanley, J.C. Extracellular matrix preparation of expanded polytetrafluoroethylene grafts seeded with endothelial cells: influence on early platelet deposition, cellular growth, and luminal prostacyclin release. Surgery 109, 313, 1991.

42. Xiao, L., and Shi, D. Role of precoating in artificial vessel endothelialization. Chinese journal of traumatology = Zhonghua chuang shang za zhi / Chinese Medical Association 7, 312, 2004.

43. Gosselin, C., Vorp, D.A., Warty, V., Severyn, D.A., Dick, E.K., Borovetz, H.S., and Greisler, H.P. ePTFE coating with fibrin glue, FGF-1, and heparin: effect on retention of seeded endothelial cells. The Journal of surgical research 60, 327, 1996.

44. Zilla, P., Fasol, R., Preiss, P., Kadletz, M., Deutsch, M., Schima, H., Tsangaris, S., and Groscurth, P. Use of fibrin glue as a substrate for in vitro endothelialization of PTFE vascular grafts. Surgery 105, 515, 1989.

45. Jaffe, E.A., Nachman, R.L., Becker, C.G., and Minick, C.R. Culture of human endothelial cells derived from umbilical veins. Identification by morphologic and immunologic criteria. The Journal of clinical investigation 52, 2745, 1973.

46. Chiu, J.J., Chen, L.J., Lee, P.L., Lee, C.I., Lo, L.W., Usami, S., and Chien, S. Shear stress inhibits adhesion molecule expression in vascular endothelial cells induced by coculture with smooth muscle cells. Blood 101, 2667, 2003.

47. Chiu, J.J., Chen, L.J., Lee, C.I., Lee, P.L., Lee, D.Y., Tasi, M.C., Lin, C.W., Usami, S., and Chien, S. Mechanisms of induction of endothelial cell E-selectin expression by smooth muscle cells and its inhibition by shear stress. Blood, 2007.

48. Ohtsuka, A., Ando, J., Korenaga, R., Kamiya, A., Toyama-Sorimachi, N., and Miyasaka, M. The effect of flow on the expression of vascular adhesion molecule-1 by cultured mouse endothelial cells. Biochemical and biophysical research communications 193, 303, 1993.

49. Morigi, M., Zoja, C., Figliuzzi, M., Foppolo, M., Micheletti, G., Bontempelli, M., Saronni, M., Remuzzi, G., and Remuzzi, A. Fluid shear stress modulates surface expression of adhesion molecules by endothelial cells. Blood 85, 1696, 1995.

50. Sheikh, S., Rainger, G.E., Gale, Z., Rahman, M., and Nash, G.B. Exposure to fluid shear stress modulates the ability of endothelial cells to recruit neutrophils in response to tumor necrosis factor-alpha: a basis for local variations in vascular sensitivity to inflammation. Blood 102, 2828, 2003.

51. Chiu, J.J., Lee, P.L., Chen, C.N., Lee, C.I., Chang, S.F., Chen, L.J., Lien, S.C., Ko, Y.C., Usami, S., and Chien, S. Shear stress increases ICAM-1 and decreases VCAM-1 and E-selectin expressions induced by tumor necrosis factor-[alpha] in endothelial cells. Arteriosclerosis, thrombosis, and vascular biology 24, 73, 2004.

52. Chiu, J.J., Lee, P.L., Chang, S.F., Chen, L.J., Lee, C.I., Lin, K.M., Usami, S., and Chien, S. Shear stress regulates gene expression in vascular endothelial cells in response to tumor necrosis factor-alpha: a study of the transcription profile with complementary DNA microarray. Journal of biomedical science 12, 481, 2005.

53. Zhang, Y., Ingram, D.A., Murphy, M.P., Saadatzadeh, M.R., Mead, L.E., Prater, D.N., and Rehman, J. Release of proinflammatory mediators and expression of proinflammatory adhesion molecules by endothelial progenitor cells. American journal of physiology 296, H1675, 2009.

54. Kuchan, M.J., and Frangos, J.A. Role of calcium and calmodulin in flow-induced nitric oxide production in endothelial cells. The American journal of physiology 266, C628, 1994.

55. Kuchan, M.J., Jo, H., and Frangos, J.A. Role of G proteins in shear stress-mediated nitric oxide production by endothelial cells. The American journal of physiology 267, C753, 1994.

56. Yee, A., Bosworth, K.A., Conway, D.E., Eskin, S.G., and McIntire, L.V. Gene expression of endothelial cells under pulsatile non-reversing vs. steady shear stress; comparison of nitric oxide production. Ann Biomed Eng 36, 571, 2008.

57. Radomski, M.W., Palmer, R.M., and Moncada, S. Endogenous nitric oxide inhibits human platelet adhesion to vascular endothelium. Lancet 2, 1057, 1987.

58. de Graaf, J.C., Banga, J.D., Moncada, S., Palmer, R.M., de Groot, P.G., and Sixma, J.J. Nitric oxide functions as an inhibitor of platelet adhesion under flow conditions. Circulation 85, 2284, 1992.

59. Harrison, D.G., Widder, J., Grumbach, I., Chen, W., Weber, M., and Searles, C. Endothelial mechanotransduction, nitric oxide and vascular inflammation. Journal of internal medicine 259, 351, 2006.

60. de Groot, P.G., MJ, I.J., and Sixma, J.J. Platelet adhesion to the subendothelium under flow. Methods in molecular biology (Clifton, N.J 96, 159, 1999.

61. Traub, O., and Berk, B.C. Laminar shear stress: mechanisms by which endothelial cells transduce an atheroprotective force. Arteriosclerosis, thrombosis, and vascular biology 18, 677, 1998.

62. Lund, T., Hermansen, S.E., Andreasen, T.V., Olsen, J.O., Osterud, B., Myrmel, T., and Ytrehus, K. Shear stress regulates inflammatory and thrombogenic gene transcripts in cultured human endothelial progenitor cells. Thrombosis and haemostasis 104, 582, 2010.

63. Ott, M.J., and Ballermann, B.J. Shear stress-conditioned, endothelial cell-seeded vascular grafts: improved cell adherence in response to in vitro shear stress. Surgery 117, 334, 1995.

64. Ballermann, B.J., and Ott, M.J. Adhesion and differentiation of endothelial cells by exposure to chronic shear stress: a vascular graft model. Blood purification 13, 125, 1995.

65. Baguneid, M., Murray, D., Salacinski, H.J., Fuller, B., Hamilton, G., Walker, M., and Seifalian, A.M. Shear-stress preconditioning and tissue-engineering-based paradigms for generating arterial substitutes. Biotechnology and applied biochemistry 39, 151, 2004.

66. Yazdani, S.K., Tillman, B.W., Berry, J.L., Soker, S., and Geary, R.L. The fate of an endothelium layer after preconditioning. J Vasc Surg 51, 174, 2010.

Chapter 5: Discussion and Future Directions

5.1 Summary of Major Results

The comprehensive goal of this work was the *in vitro* fabrication and assessment of a completely biological, fibrin-based, small-diameter vascular graft. Two major areas were examined to achieve this goal: 1) controlled fibrin degradation and its possible role in improving new matrix deposition, cellularity, and ultimately, mechanical properties and 2) endothelialization of these grafts to form a complete vessel and ensure thromboresistance.

We hypothesized that controlling the rate of fibrin degradation could allow for better matrix formation in our media equivalents (MEs). Further, we were interested in possible effects that fibrin degradation products (FDPs) may have on the overall remodeling by vascular smooth muscle cells (vSMCs) in the ME. To this end, we examined collagen and elastin deposition and cellularity in small fibrin disc constructs and small-diameter MEs. In both cases, decreasing the concentration of ACA led to increased FDP in the medium and better biochemical and mechanical properties. FDP

were shown to be direct physiological stimulators of collagen deposition, a fact that can be exploited when fibrin degradation is controlled to allow high concentrations of FDP formation. This work was necessary for creation of MEs with good mechanical properties that allowed easy handling, as previous vSMC small-diameter vessels had inadequate mechanical properties and handling (1). Through semi-optimization of fibrin degradation, we were able to create better remodeled MEs that could be utilized for endothelial cell seeding experiments.

Endothelialization of small-diameter MEs is necessary for creation of a non-thrombogenic surface *in vitro*. This research sought to examine EC adhesion under physiological shear stress and the phenotype of ECs seeded on MEs. A novel EC type, blood outgrowth endothelial cells (BOECs), were chosen for these endeavors, as they can be isolated non-invasively and grown to cell numbers that far exceed the quantities needed for endothelialization of small-diameter vessels. Two BOEC species types were examined: 1) rat BOECs were utilized for development of a Fischer rat model and 2) human BOECs were employed in order to examine the phenotype of adult BOECs, particularly in regard to shear stress response and thrombogencity. RBOECs were shown to respond to a number of stimuli in a manner consistent with mature ECs. Further, they were adherent on vSMC MEs, could proliferation on this surface, and would remain adherent for 24 hours under low shear stress or short durations of high shear stress. However, mechanical properties for these vessels were still inferior to native vessels and RBOEC monolayers were not maintained under physiological shear stress for long durations.

By these standards, HBOEC seeding was more successful. HBOECs could be seeded on human dermal fibroblast (HDF) MEs to form confluent monolayers and would remain adherent under long durations of physiological shear stress. HBOECs were responsive to physiological shear stress; shear stress modulated VCAM-1 and ICAM-1 expression after TNF-α stimulation, increased eNOS expression and NO production, and decreased platelet adhesion on HBOEC-seeded MEs. These results indicate that HBOECs behave like mature ECs and support their application for tissue-engineered vascular grafts.

Together, these lines of research allowed for the formation of a functional, small-diameter vascular graft, while elucidating key aspects of the remodeling process and endothelial cell phenotype. However, considerable work still remains to be done to elucidate the full potential of these vascular grafts.

5.2 Fibrinolysis

In Chapter 2 of this work we were able to elucidate some of the key mechanisms of fibrin degradation, however only a semi-optimization of the MEs was performed. While low concentrations of the fibrinolysis inhibitor ACA lead to improved matrix remodeling, there was a limit to the magnitude that ACA could be reduced. Without ACA, the vSMC degrade the matrix in less than two days, and if the ACA concentration was too low the MEs became too thin to be practical for handling or eventual implantation. Thus a future optimization might examine the effect of increasing the initial fibrin concentration while decreasing the ACA concentration. This could allow increased FDP generation while maintaining the initial fibrin scaffold for a longer duration.

However, there is still likely to be an upper limit to initial fibrin concentrations at which vSMC are capable of adhering, spreading and remodeling the fibrin matrix, thus a careful balanced will likely need to be maintained.

For the fabrication of MEs with human cells, our lab utilizes human dermal fibrobasts (HDF) due to their high collagen deposition and repeatability of results. These cells are not as fibrinolytic as vSMCs and do not require the use of a fibrinolytic inhibitor to maintain the construct scaffold. However, the effects of ACA on these cells could be used to draw more general conclusions about fibrin degradation as they relate to multiple cell types. Doping with active plasmin (2), plasminogen activators, such as urokinase (uPA) or tissue plasminogen activator (tPA), or directly with FDP as in our studies, would be other methods to examine the effects of fibrin degradation or FDP concentrations on HDF MEs, with the hypothesis that increased FDP generation could lead to improved remodeling.

5.3 Methods to Improve Mechanical Properties

Experiments with chemical stimulation have repeatedly shown that, though mechanical properties can be improved with numerous supplements, static culture is not sufficient for fabrication of biopolymer constructs with mechanical properties of native vessels. However, recent work in our lab has shown that mechanical stimuli or ruthenium photo-crossing linking is capable of producing fibrin-based MEs with near-native mechanical properties. Using cyclic stretch, our lab has been able to achieve burst pressures of 1366 ± 177 mmHg with HDF MEs after 5 weeks of culture (3). Ruthenium crossing-linking of 9-11 week old MEs produced burst pressures of 980 ± 93 mmHg

compared to 317 ± 130 mmHg for the control MEs (Bjork et al, submitted). While both of these methods lead to constructs with high burst pressures, the matrix remodeling and quantity of residual fibrin will differ, as will the composition of the extracellular matrix (ECM) at the lumenal surface. In the case of cyclic distention, enhanced collagen deposition and maturity has been implicated in the improved mechanical properties. Also, the flow of medium on the lumenal surface, instead of static culture on a mandrel, will likely lead to increased remodeling on the lumenal surface. This is in contrast to the ruthenium cross-linking method, which thus far has utilized statically cultured HDF MEs, as used in Chapter 4, and thus would be less remodeled at the time of cross-linking unless longer static culture periods are used prior to cross-linking.

Using these methods for enhancing ME mechanical properties, combined with HBOEC seeding strategies from Chapter 4, would allow for the formation of a complete, tissue-engineered artery. However, the different lumenal matrix compositions of these MEs could alter HBOEC seeding on the surfaces, with 4-5 week old ruthenium cross-linked MEs the most similar to the MEs described in Chapter 4. Both types of enhanced-mechanical property MEs should be examined for HBOEC seeding, as either could be utilized for implantation. This will require, at minimum, a re-examination of HBOEC retention on these surfaces under shear stress, which can most easily be accomplished in the parallel plate flow chambers (PPFCs) designed in Chapters 3 and 4.

5.4 BOEC Sources

Thus far, HBOEC experiments have utilized cells from isolations of HBOECs from two healthy donors. Direct comparison of results with these isolations as well as others, at least in terms of HBOEC retention, would allow generalization of these finding to a broader population. Furthermore, future studies should examine adhesion under shear stress of HBOECs from patients with coronary artery disease (CAD). Though Stroncek et al. has shown similar isolation rates for healthy donors and CAD patients and good adhesion of these cells under flow (4), their sample size was low (n=13) and proliferative BOEC colonies were only isolated from approximately half of the patients. Improving this isolation rate would be necessary for making this a more universal approach. The CAD study isolated from a 50 ml blood sample, so a larger quantity of blood would hopefully improve the isolation rate.

5.5 Endothelialization of Tubular Constructs

Thus far, all HBOEC and RBOEC studies were done on MEs that were slit axially and laid flat prior to seeding. This allowed for real-time visualization of BOEC adhesion and morphology and allowed us to isolate the effects of a well-defined wall shear stress from other mechanical effects due to flow through a distensible, tubular ME. However, the seeding of tubular constructs will be necessary for implant studies and will require different methods for seeding. We have been able to seed HBOECs on tubular NHDF MEs using a method developed by our lab (1) and modified for this purpose (Figure 5.1). MEs were fabricated as described in Chapter 4, cultured for 4 weeks, then mounted on

hose barbs on a brace and a suspension of CellTracker Green-labeled HBOECs at 2 x 10^6 cells/ml was injected into the ME. This equates to approximately 200,000 HBOECs/cm^2. The ME was then capped at both ends, placed in a 50 ml conical, and rotated at 2 rpm for 1 hour (CELLroll; Intergra Biosciences). After 1 hour, the caps were removed and a syringe pump was used to flush the ME lumen, removing non-adherent cells, at a rate of 1 ml/min for 2 minutes with EGM medium. After rinsing, the ME was left uncapped and returned to the 50 ml conical and cultured vertically.

After 24 hours of culture, MEs were harvested using a modified fixation method. MEs were flushed with HBSS for 1 minute at a rate of 1 ml/min using a syringe pump and then perfusion fixed with cold 4% PFA, again using the syringe pump, at a rate of 1 ml/min for 10 minutes. After fixation, MEs were rinsed with PBS and slit open using a dissection microscope. MEs were then stained for cell nuclei and VE-Cadherin as in Chapter 4.

Good monolayer coverage with HBOECs was achieved using this method (Figure 5.2). Imaging of CellTracker Green showed spread, adherent HBOECs on the tissue, while staining for VE-Cadherin showed junction formation with these cells. Without the rinse at 1 hour or with 4 hour seeding times instead of 1 hour, clumps of HBOECs were visible on the tissue (Figure 5.3). Thus, the optimization of this protocol was important to formation of a HBOEC monolayer. HBOECs demonstrate a tendency to aggregate over time, likely due to the lack of available matrix for adhesion given the excess of HBOECs utilized to ensure full surface coverage.

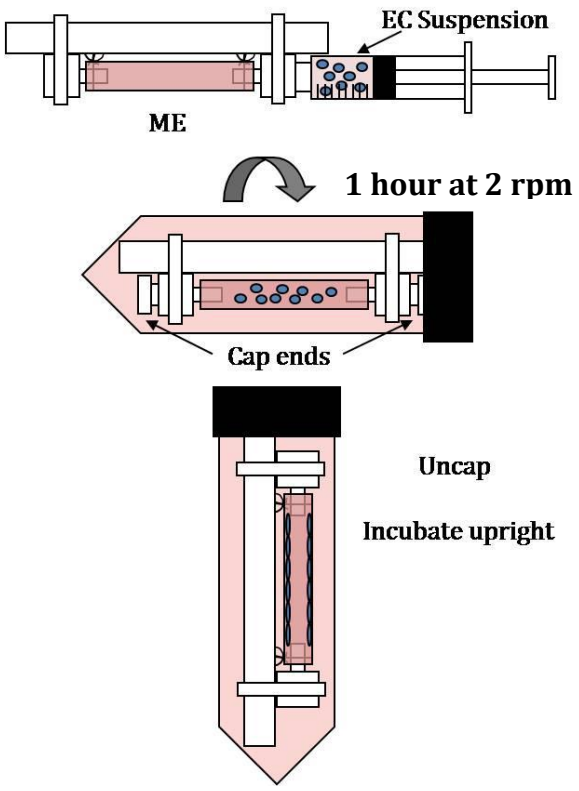

Figure 5.1: Method for seeding endothelial cells on tubular vascular grafts. Modified from method and figure by B. Isenberg (1).

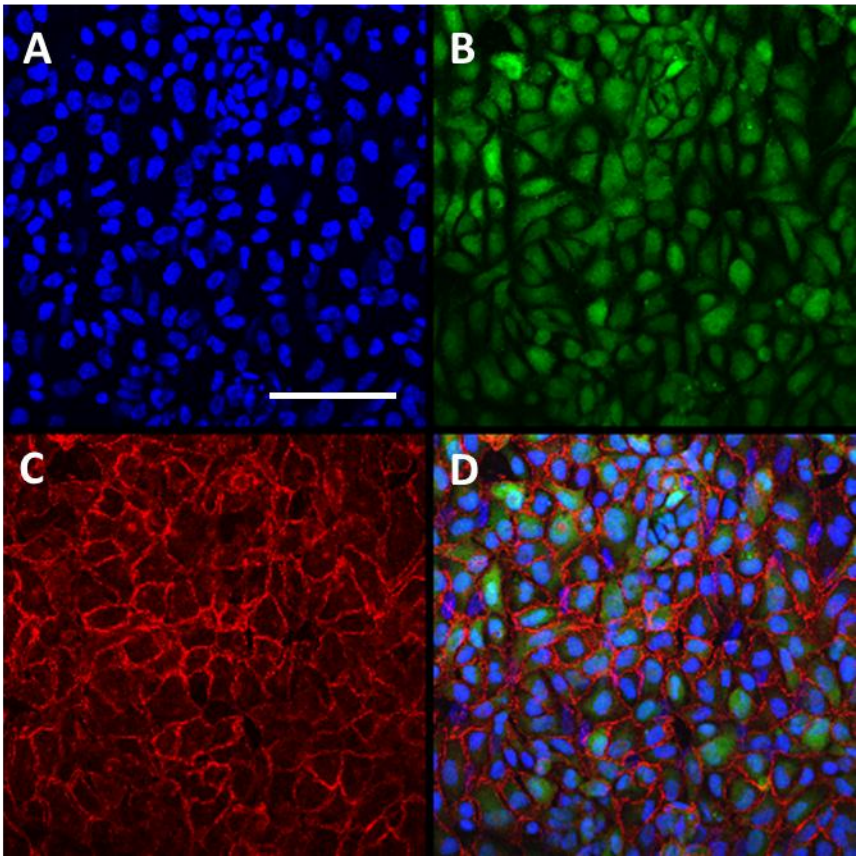

Figure 5.2: HBOEC seeding on tubular vascular grafts by rotation for 1 hour. HBOECs were seeded by rotation for 1 hour at 2 rpm, followed by rinsing with cell culture medium to remove non-adherent HBOECs. Images were taken 24 hours after seeding. A confluent monolayer of HBOECs is visible on the ME surface. A) Hoechst stain for cell nuclei. B) CellTracker Green-labeled HBOECs. C) VE-Cadherin staining of cell junctions. D) Composite image. Scale bar = 100 μm.

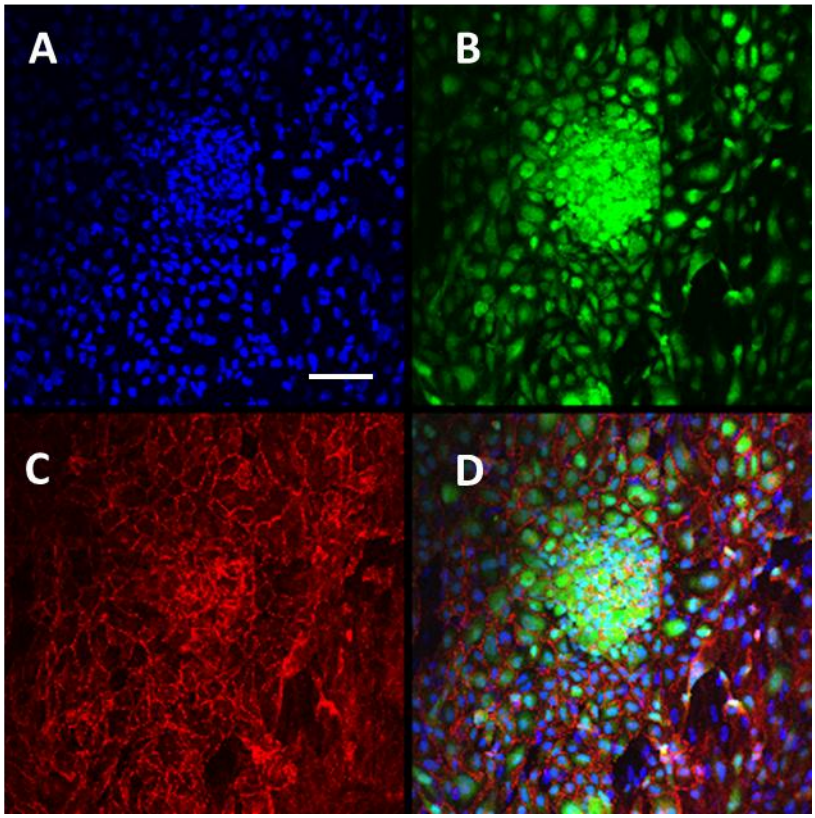

Figure 5.3: HBOEC seeding on tubular vascular grafts for 4 hours. HBOECs were seeded by rotation for 4 hours at 2 rpm, followed by rinsing with cell culture medium to remove non-adherent HBOECs. Using an extended seeding time, large aggregates of HBOECs were visible on the ME surface. A) Hoechst stain showing cell nuclei. B) CellTracker Green-labeled HBOECs. C) VE-Cadherin staining of cell junctions. D) Composite image. Scale bar = 100 μm.

5.6 Implantation Considerations

A next logical step for this research involves the use of implant studies. These will be necessary to determine full functionality, including adequate burst pressures, limitation of intimal hyperplasia and dilation, and thromboresistance, and will allow for an examination of matrix remodeling *in vivo*. Choice of appropriate animal models will be necessary; however, a variety of factors will impact this decision. Species-dependent differences in endothelial and blood cells make autologous implantation with non-human cells an incomplete picture (5) and require that MEs with appropriate mechanical properties be made from dermal fibroblasts or SMCs from multiple species; however, use of human cells likely will require immunosuppressant drugs or use of immunodeficient animals.

Studies with non-endothelialized, mechanically-conditioned, HDF-embedded MEs implanted interpositionally in the infrarenal aorta of nude rats are currently underway. With these initial studies we can examine graft incorporation into the host tissue, as well as watch for lumen narrowing, aneurysm formation, intact anastomoses, and blood infiltration into the graft tissue. Seeding with HBOECs prior to implantation would allow for examination of HBOEC adhesion *in vivo*. However, the approximately 1 cm long graft is short enough that endothelial cell repopulation from the anastomoses is likely (5). This makes it necessary for the HBOECs to be differentiated from the host ECs, through pre-labeling, transfection with green fluorescent protein, or immunostaining for human EC-specific antigens.

For large animal studies, our lab has previous experience in the sheep model. Sheep have been described as having a coagulation system that is closer to human than either dogs or pigs. The ovine carotid artery is also readily accessible and similar in diameter to human peripheral arteries, satisfying the requirement for a small-diameter implant location. In addition, implantation of conduits in the neck of sheep is well tolerated, with minimal postoperative morbidity (5).

In preparation for sheep implant studies, our lab has been investigating ovine vascular SMCs for fabrication of MEs. To complement this work, ovine BOECs were examined for adhesion under shear stress. OBOECs were seeded on NHDF MEs, as described in Chapter 4, and culture for 24 hours prior to exposure to short durations of shear stress, a method also described in Chapter 4. OBOECs were exposed to shear stresses up to 80 dynes/cm^2 for 20 minutes without a significant cell loss (Figure 5.4). Confluent monolayers of OBOECs were also maintained after 24 hours at 15 dynes/cm^2 shear stress. Seeding and shear stress retention on the MEs optimized for sheep implant will still be necessary; however, these are promising initial findings, as the OBOECs remained adherent on the bioartificial tissue at shear stresses above arterial physiological shear stress.

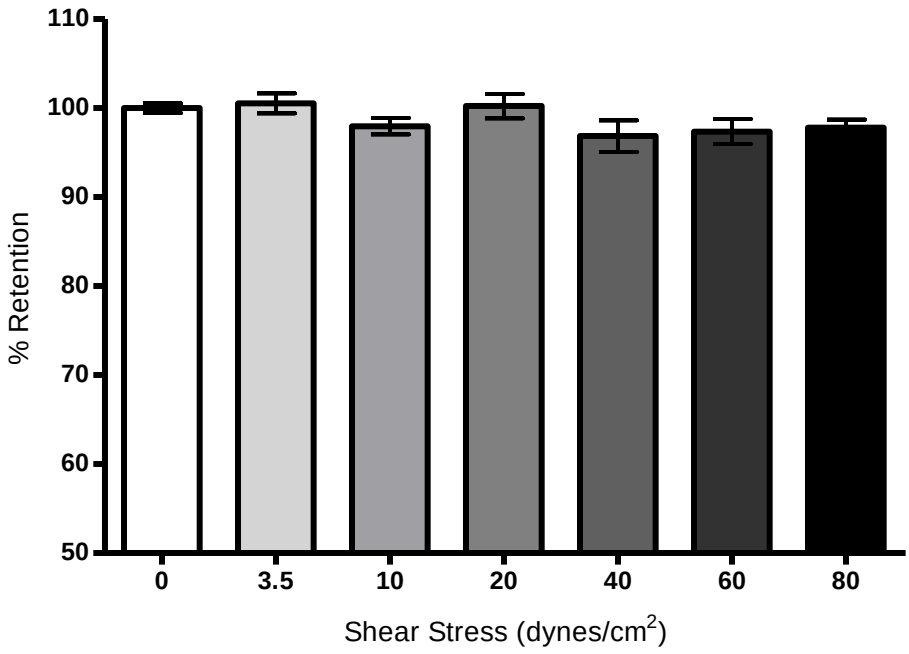

Figure 5.4: Ovine BOECs cultured on bioartificial tissue exposed to short durations of shear stress up to 80 dynes/cm^2. Mean ± standard error of the mean (SE) for n=3 samples.

With each model, a different maximum and mean shear stress will be imposed on the neoendothelium, dependent on the vessel size and rate of blood flow. Assuming the graft diameter is appropriately matched, Table 5.1 lists the mean wall shear stress that would be imposed for each species. For similar vessels, these values vary predominately based on the size of the animal (6), from a wall shear stress of 70 dynes/cm^2 in the rat infrarenal aorta to 8.4 dynes/cm^2 for the sheep femoral artery. Assurance that BOECs remain adherent at the appropriate shear stress, at least for short durations, will be necessary prior to implantation. For sheep femoral artery implant, we have already been able to show that OBOECs are retained under physiological shear stress, however for the rat implant model, the mean wall shear stress is higher than we have examined for rat or

human BOECs. The maximum wall shear stress due to pulsatile flow in the rat aorta would reach shear stresses even higher, thus *in vitro* examination of, and optimization for, BOEC retention would be required to ensure maintenance of the endothelium immediately upon implant.

Table 5.1: Mean shear stress for human arteries and implant model vessels.

Vessel	Species	Mean Wall Shear Stress (dyne/cm^2)
Coronary Artery	Human	10-20, mean ~16 (7)
Infrarenal Aorta	Human	4.8 ± 0.3 (6)
	Rat	70.5 ± 6.7 (6)
	Mouse	87.6 ± 8.3 (6)
Common Carotid Artery	Sheep	8.4 (5)
	Baboon	12.6 (5)
Common Femoral Artery	Sheep	11.2 (5)

All flow experiments in these studies utilized steady, laminar shear stress. Steady or pulsatile laminar shear stress is considered to be atheroprotective, while reversing, oscillatory, or low shear stress is believe to be atherogenic (8, 9). Steady shear stress stimulates many of the same endothelial cell responses as pulsatile stress, however there are some qualitative and quantitative differences (10-13). Thus, application of pulsatile, non-reversing flow *in vitro* represents another method to improve BOEC phenotype; however, the relevance of these *in vitro* studies to an implant model may be limited. Endothelial cells respond quickly to changes in shear stress, thus maintenance of a confluent monolayer during implant may be the most important outcome to be gained from pre-conditioning studies. Thus, either steady or pulsatile flow could be used for pre-conditioning as long as a confluent monolayer can be maintained when the cells are implanted. *In vitro* systems can be utilized to mimic the pulsatile shear stress, as well as

cyclic stretch, experienced by grafts at implant, and thus serve as an indicator for BOEC adhesion after implant. Our lab bioreactors (1, 3) could be modified for this purpose, and utilized to examined BOEC adhesion, as well as allow for pre-conditioning of tubular constructs leading up to implantation.

All shear stress experiments thus far have instituted a ramping period such that the shear stress is increased incrementally to the final set point. Multiple groups report that ECs perform better functionally and are more likely to remain adherent when slowly ramped to physiological shear stress or when pre-conditioned with shear stress prior to implant (14-17). Thus, the ramping period currently instituted may be necessary for BOEC retention. To test this, ramping can be compared to an immediate step increase in shear stress to the physiological shear stress. This will mimic the implant conditions, where after surgical implant blood flow is re-established quickly at the physiological flow rate, as the clamp is removed. The adhesion of BOECs exposed to a single step increase, from static to physiological shear stress, will be an indicator of whether BOEC-seeded MEs can be implanted after static culture of the BOECs. If significant cell loss is noted, pre-conditioning with flow and an incremental ramping of the shear stress will be necessary prior to implant.

5.7 Conclusions

This dissertation outlines methods, results and analysis in the creation of a complete, bioartificial artery through the controlled degradation of an initial fibrin scaffold combined with successful seeding and retention of BOECs on this tissue. *In vitro* results indicate the neoendothelium is functional, thromboresistant, and remains adherent

under physiological shear stress. Utilizing these results and methods in combination with mechanical strengthening methods recently outlined by our lab, we have the potential to achieve functional, small-diameter grafts that could withstand arterial implant.

5.8 References

1. Isenberg, B.C., Williams, C., and Tranquillo, R.T. Endothelialization and flow conditioning of fibrin-based media-equivalents. Annals of biomedical engineering 34, 971, 2006.

2. Neidert, M.R., Lee, E.S., Oegema, T.R., and Tranquillo, R.T. Enhanced fibrin remodeling in vitro with TGF-beta1, insulin and plasmin for improved tissue-equivalents. Biomaterials 23, 3717, 2002.

3. Syedain, Z.H., Meier, L.A., Bjork, J.W., Lee, A., and Tranquillo, R.T. Implantable arterial grafts from human fibroblasts and fibrin using a multi-graft pulsed flow-stretch bioreactor with noninvasive strength monitoring. Biomaterials, 2010.

4. Stroncek, J.D., Grant, B.S., Brown, M.A., Povsic, T.J., Truskey, G.A., and Reichert, W.M. Comparison of endothelial cell phenotypic markers of late-outgrowth endothelial progenitor cells isolated from patients with coronary artery disease and healthy volunteers. Tissue engineering 15, 3473, 2009.

5. Byrom, M.J., Bannon, P.G., White, G.H., and Ng, M.K. Animal models for the assessment of novel vascular conduits. J Vasc Surg 52, 176, 2010.

6. Greve, J.M., Les, A.S., Tang, B.T., Draney Blomme, M.T., Wilson, N.M., Dalman, R.L., Pelc, N.J., and Taylor, C.A. Allometric scaling of wall shear stress from mice to humans: quantification using cine phase-contrast MRI and computational fluid dynamics. American journal of physiology 291, H1700, 2006.

7. Fung, Y.C. Biomechanics : mechanical properties of living tissues. New York: Springer-Verlag, 1993.

8. Traub, O., and Berk, B.C. Laminar shear stress: mechanisms by which endothelial cells transduce an atheroprotective force. Arteriosclerosis, thrombosis, and vascular biology 18, 677, 1998.

9. Chiu, J.J., Usami, S., and Chien, S. Vascular endothelial responses to altered shear stress: pathologic implications for atherosclerosis. Annals of medicine 41, 19, 2009.

10. Yee, A., Bosworth, K.A., Conway, D.E., Eskin, S.G., and McIntire, L.V. Gene expression of endothelial cells under pulsatile non-reversing vs. steady shear stress; comparison of nitric oxide production. Annals of biomedical engineering 36, 571, 2008.

11. Frangos, J.A., Eskin, S.G., McIntire, L.V., and Ives, C.L. Flow effects on prostacyclin production by cultured human endothelial cells. Science (New York, N.Y 227, 1477, 1985.

12. Helmlinger, G., Berk, B.C., and Nerem, R.M. Calcium responses of endothelial cell monolayers subjected to pulsatile and steady laminar flow differ. The American journal of physiology 269, C367, 1995.

13. Hsieh, H.J., Li, N.Q., and Frangos, J.A. Pulsatile and steady flow induces c-fos expression in human endothelial cells. Journal of cellular physiology 154, 143, 1993.

14. Ballermann, B.J., and Ott, M.J. Adhesion and differentiation of endothelial cells by exposure to chronic shear stress: a vascular graft model. Blood purification 13, 125, 1995.

15. Ott, M.J., and Ballermann, B.J. Shear stress-conditioned, endothelial cell-seeded vascular grafts: improved cell adherence in response to in vitro shear stress. Surgery 117, 334, 1995.

16. Yazdani, S.K., Tillman, B.W., Berry, J.L., Soker, S., and Geary, R.L. The fate of an endothelium layer after preconditioning. J Vasc Surg 51, 174.

17. Dardik, A., Liu, A., and Ballermann, B.J. Chronic in vitro shear stress stimulates endothelial cell retention on prosthetic vascular grafts and reduces subsequent in vivo neointimal thickness. J Vasc Surg 29, 157, 1999.

Bibliography

Ahmann, K.A., Weinbaum, J.S., Johnson, S.L., and Tranquillo, R.T. Fibrin Degradation Enhances Vascular Smooth Muscle Cell Proliferation and Matrix Deposition in Fibrin-Based Tissue Constructs Fabricated In Vitro. Tissue engineering, 2010.

Albelda, S.M., Daise, M., Levine, E.M., and Buck, C.A. Identification and characterization of cell-substratum adhesion receptors on cultured human endothelial cells. The Journal of clinical investigation 83, 1992, 1989.

Allen, J.B., Khan, S., Lapidos, K.A., and Ameer, G.A. Toward engineering a human neoendothelium with circulating progenitor cells. Stem cells (Dayton, Ohio) 28, 318, 2010.

Anderson, J.S., Price, T.M., Hanson, S.R., and Harker, L.A. In vitro endothelialization of small-caliber vascular grafts. Surgery 101, 577, 1987.

Ando, J., Tsuboi, H., Korenaga, R., Takada, Y., Toyama-Sorimachi, N., Miyasaka, M., and Kamiya, A. Down-regulation of vascular adhesion molecule-1 by fluid shear stress in cultured mouse endothelial cells. Annals of the New York Academy of Sciences 748, 148, 1995.

Anonick, P.K., Vasudevan, J., and Gonias, S.L. Antifibrinolytic activities of alpha-N-acetyl-L-lysine methyl ester, epsilon-aminocaproic acid, and tranexamic acid. Importance of kringle interactions and active site inhibition. Arterioscler Thromb 12, 708, 1992.

Aper, T., Schmidt, A., Duchrow, M., and Bruch, H.P. Autologous blood vessels engineered from peripheral blood sample. Eur J Vasc Endovasc Surg 33, 33, 2007.

Arts, C.H., Blankensteijn, J.D., Heijnen-Snyder, G.J., Verhagen, H.J., Hedeman Joosten, P.P., Sixma, J.J., Eikelboom, B.C., and de Groot, P.G. Reduction of non-endothelial cell contamination of microvascular endothelial cell seeded grafts decreases thrombogenicity and intimal hyperplasia. Eur J Vasc Endovasc Surg 23, 404, 2002.

Baguneid, M., Murray, D., Salacinski, H.J., Fuller, B., Hamilton, G., Walker, M., and Seifalian, A.M. Shear-stress preconditioning and tissue-engineering-based paradigms for generating arterial substitutes. Biotechnology and applied biochemistry 39, 151, 2004.

Bakker, A.H., Weening-Verhoeff, E.J., and Verheijen, J.H. The role of the lysyl binding site of tissue-type plasminogen activator in the interaction with a forming fibrin clot. The Journal of biological chemistry 270, 12355, 1995.

Ballermann, B.J., and Ott, M.J. Adhesion and differentiation of endothelial cells by exposure to chronic shear stress: a vascular graft model. Blood purification 13, 125, 1995.

Bank, A.J., Wang, H., Holte, J.E., Mullen, K., Shammas, R., and Kubo, S.H. Contribution of collagen, elastin, and smooth muscle to in vivo human brachial artery wall stress and elastic modulus. Circulation 94, 3263, 1996.

Barocas, V.H., Girton, T.S., and Tranquillo, R.T. Engineered alignment in media equivalents: magnetic prealignment and mandrel compaction. Journal of biomechanical engineering 120, 660, 1998.

Bensaid, W., Triffitt, J.T., Blanchat, C., Oudina, K., Sedel, L., and Petite, H. A biodegradable fibrin scaffold for mesenchymal stem cell transplantation. Biomaterials 24, 2497, 2003.

Bergh, N., Ulfhammer, E., Glise, K., Jern, S., and Karlsson, L. Influence of TNF-alpha and biomechanical stress on endothelial anti- and prothrombotic genes. Biochemical and biophysical research communications 385, 314, 2009.

Bian, W., and Bursac, N. Engineered skeletal muscle tissue networks with controllable architecture. Biomaterials 30, 1401, 2009.

Birukov, K.G., Shirinsky, V.P., Stepanova, O.V., Tkachuk, V.A., Hahn, A.W., Resink, T.J., and Smirnov, V.N. Stretch affects phenotype and proliferation of vascular smooth muscle cells. Molecular and cellular biochemistry 144, 131, 1995.

Bos, G.W., Poot, A.A., Beugeling, T., van Aken, W.G., and Feijen, J. Small-diameter vascular graft prostheses: current status. Arch Physiol Biochem 106, 100, 1998.

Bowman, P.D., Ennis, S.R., Rarey, K.E., Betz, A.L., and Goldstein, G.W. Brain microvessel endothelial cells in tissue culture: a model for study of blood-brain barrier permeability. Annals of neurology 14, 396, 1983.

Brown, M.A., Wallace, C.S., Anamelechi, C.C., Clermont, E., Reichert, W.M., and Truskey, G.A. The use of mild trypsinization conditions in the detachment of endothelial cells to promote subsequent endothelialization on synthetic surfaces. Biomaterials 28, 3928, 2007.

Brown, M.A., Wallace, C.S., Angelos, M., and Truskey, G.A. Characterization of umbilical cord blood-derived late outgrowth endothelial progenitor cells exposed to laminar shear stress. Tissue engineering 15, 3575, 2009.

Byrom, M.J., Bannon, P.G., White, G.H., and Ng, M.K. Animal models for the assessment of novel vascular conduits. J Vasc Surg 52, 176, 2010.

Campbell, P.G., Novak, J.F., Yanosick, T.B., and McMaster, J.H. Involvement of the plasmin system in dissociation of the insulin-like growth factor-binding protein complex. Endocrinology 130, 1401, 1992.

Cederholm-Williams, S.A. Concentration of plasminogen and antiplasmin in plasma and serum. Journal of clinical pathology 34, 979, 1981.

Chiu, J.J., Chen, L.J., Lee, C.I., Lee, P.L., Lee, D.Y., Tasi, M.C., Lin, C.W., Usami, S., and Chien, S. Mechanisms of induction of endothelial cell E-selectin expression by smooth muscle cells and its inhibition by shear stress. Blood, 2007.

Chiu, J.J., Chen, L.J., Lee, P.L., Lee, C.I., Lo, L.W., Usami, S., and Chien, S. Shear stress inhibits adhesion molecule expression in vascular endothelial cells induced by coculture with smooth muscle cells. Blood 101, 2667, 2003.

Chiu, J.J., Lee, P.L., Chang, S.F., Chen, L.J., Lee, C.I., Lin, K.M., Usami, S., and Chien, S. Shear stress regulates gene expression in vascular endothelial cells in response to tumor necrosis factor-alpha: a study of the transcription profile with complementary DNA microarray. Journal of biomedical science 12, 481, 2005.

Chiu, J.J., Lee, P.L., Chen, C.N., Lee, C.I., Chang, S.F., Chen, L.J., Lien, S.C., Ko, Y.C., Usami, S., and Chien, S. Shear stress increases ICAM-1 and decreases VCAM-1 and E-selectin expressions induced by tumor necrosis factor-[alpha] in endothelial cells. Arteriosclerosis, thrombosis, and vascular biology 24, 73, 2004.

Chiu, J.J., Usami, S., and Chien, S. Vascular endothelial responses to altered shear stress: pathologic implications for atherosclerosis. Annals of medicine 41, 19, 2009.

Chiu, J.J., Wung, B.S., Shyy, J.Y., Hsieh, H.J., and Wang, D.L. Reactive oxygen species are involved in shear stress-induced intercellular adhesion molecule-1 expression in endothelial cells. Arteriosclerosis, thrombosis, and vascular biology 17, 3570, 1997.

Christensen, U. Allosteric effects of some antifibrinolytic amino acids on the catalytic activity of human plasmin. Biochimica et biophysica acta 526, 194, 1978.

Clark, R.A. Fibrin is a many splendored thing. J Invest Dermatol 121, xxi, 2003.

Conte, M.S. The ideal small arterial substitute: a search for the Holy Grail? Faseb J 12, 43, 1998.

Costa, M.A., and Simon, D.I. Molecular basis of restenosis and drug-eluting stents. Circulation 111, 2257, 2005.

Cox, S., Cole, M., and Tawil, B. Behavior of human dermal fibroblasts in three-dimensional fibrin clots: dependence on fibrinogen and thrombin concentration. Tissue engineering 10, 942, 2004.

Cummings, C.L., Gawlitta, D., Nerem, R.M., and Stegemann, J.P. Properties of engineered vascular constructs made from collagen, fibrin, and collagen-fibrin mixtures. Biomaterials 25, 3699, 2004.

Dardik, A., Liu, A., and Ballermann, B.J. Chronic in vitro shear stress stimulates endothelial cell retention on prosthetic vascular grafts and reduces subsequent in vivo neointimal thickness. J Vasc Surg 29, 157, 1999.

Davies, P.F. Flow-mediated endothelial mechanotransduction. Physiological reviews 75, 519, 1995.

Davis, M.E., Grumbach, I.M., Fukai, T., Cutchins, A., and Harrison, D.G. Shear stress regulates endothelial nitric-oxide synthase promoter activity through nuclear factor kappaB binding. The Journal of biological chemistry 279, 163, 2004.

de Graaf, J.C., Banga, J.D., Moncada, S., Palmer, R.M., de Groot, P.G., and Sixma, J.J. Nitric oxide functions as an inhibitor of platelet adhesion under flow conditions. Circulation 85, 2284, 1992.

de Groot, P.G., MJ, I.J., and Sixma, J.J. Platelet adhesion to the subendothelium under flow. Methods in molecular biology (Clifton, N.J 96, 159, 1999.

Deutsch, M., Meinhart, J., Zilla, P., Howanietz, N., Gorlitzer, M., Froeschl, A., Stuempflen, A., Bezuidenhout, D., and Grabenwoeger, M. Long-term experience in autologous in vitro endothelialization of infrainguinal ePTFE grafts. J Vasc Surg 49, 352, 2009.

Dombi, G.W., Haut, R.C., and Sullivan, W.G. Correlation of high-speed tensile strength with collagen content in control and lathyritic rat skin. The Journal of surgical research 54, 21, 1993.

Dye, J., Lawrence, L., Linge, C., Leach, L., Firth, J., and Clark, P. Distinct patterns of microvascular endothelial cell morphology are determined by extracellular matrix composition. Endothelium 11, 151, 2004.

Frangos, J.A., Eskin, S.G., McIntire, L.V., and Ives, C.L. Flow effects on prostacyclin production by cultured human endothelial cells. Science (New York, N.Y 227, 1477, 1985.

Fries, J.W., Williams, A.J., Atkins, R.C., Newman, W., Lipscomb, M.F., and Collins, T. Expression of VCAM-1 and E-selectin in an in vivo model of endothelial activation. The American journal of pathology 143, 725, 1993.

Fung, Y.C. Biomechanics : mechanical properties of living tissues. New York: Springer-Verlag, 1993.

George, S.J., Johnson, J.L., Smith, M.A., Angelini, G.D., and Jackson, C.L. Transforming growth factor-beta is activated by plasmin and inhibits smooth muscle cell death in human saphenous vein. Journal of vascular research 42, 247, 2005.

George, S.J., Johnson, J.L., Smith, M.A., and Jackson, C.L. Plasmin-mediated fibroblast growth factor-2 mobilisation supports smooth muscle cell proliferation in human saphenous vein. Journal of vascular research 38, 492, 2001.

Gimbrone, M.A., Jr., Topper, J.N., Nagel, T., Anderson, K.R., and Garcia-Cardena, G. Endothelial dysfunction, hemodynamic forces, and atherogenesis. Annals of the New York Academy of Sciences 902, 230, 2000.

Gosselin, C., Vorp, D.A., Warty, V., Severyn, D.A., Dick, E.K., Borovetz, H.S., and Greisler, H.P. ePTFE coating with fibrin glue, FGF-1, and heparin: effect on retention of seeded endothelial cells. The Journal of surgical research 60, 327, 1996.

Grabowski, E.F., Reininger, A.J., Petteruti, P.G., Tsukurov, O., and Orkin, R.W. Shear stress decreases endothelial cell tissue factor activity by augmenting secretion of tissue factor pathway inhibitor. Arteriosclerosis, thrombosis, and vascular biology 21, 157, 2001.

Grassl, E.D., Oegema, T.R., and Tranquillo, R.T. Fibrin as an alternative biopolymer to type-I collagen for the fabrication of a media equivalent. Journal of biomedical materials research 60, 607, 2002.

Grassl, E.D., Oegema, T.R., and Tranquillo, R.T. A fibrin-based arterial media equivalent. Journal of biomedical materials research 66, 550, 2003.

Green, K.A., Almholt, K., Ploug, M., Rono, B., Castellino, F.J., Johnsen, M., Bugge, T.H., Romer, J., and Lund, L.R. Profibrinolytic effects of metalloproteinases during skin wound healing in the absence of plasminogen. J Invest Dermatol 128, 2092, 2008.

Greve, J.M., Les, A.S., Tang, B.T., Draney Blomme, M.T., Wilson, N.M., Dalman, R.L., Pelc, N.J., and Taylor, C.A. Allometric scaling of wall shear stress from mice to humans: quantification using cine phase-contrast MRI and computational fluid dynamics. American journal of physiology 291, H1700, 2006.

Griese, D.P., Ehsan, A., Melo, L.G., Kong, D., Zhang, L., Mann, M.J., Pratt, R.E., Mulligan, R.C., and Dzau, V.J. Isolation and transplantation of autologous circulating endothelial cells into denuded vessels and prosthetic grafts: implications for cell-based vascular therapy. Circulation 108, 2710, 2003.

Grouf, J.L., Throm, A.M., Balestrini, J.L., Bush, K.A., and Billiar, K.L. Differential effects of EGF and TGF-beta1 on fibroblast activity in fibrin-based tissue equivalents. Tissue engineering 13, 799, 2007.

Harraz, M., Jiao, C., Hanlon, H.D., Hartley, R.S., and Schatteman, G.C. CD34- blood-derived human endothelial cell progenitors. Stem cells (Dayton, Ohio) 19, 304, 2001.

Harrison, D.G., Widder, J., Grumbach, I., Chen, W., Weber, M., and Searles, C. Endothelial mechanotransduction, nitric oxide and vascular inflammation. Journal of internal medicine 259, 351, 2006.

He, H., Shirota, T., Yasui, H., and Matsuda, T. Canine endothelial progenitor cell-lined hybrid vascular graft with nonthrombogenic potential. The Journal of thoracic and cardiovascular surgery 126, 455, 2003.

Helmlinger, G., Berk, B.C., and Nerem, R.M. Calcium responses of endothelial cell monolayers subjected to pulsatile and steady laminar flow differ. The American journal of physiology 269, C367, 1995.

Henninger, D.D., Panes, J., Eppihimer, M., Russell, J., Gerritsen, M., Anderson, D.C., and Granger, D.N. Cytokine-induced VCAM-1 and ICAM-1 expression in different organs of the mouse. J Immunol 158, 1825, 1997.

Herring, M.B. Endothelial cell seeding. J Vasc Surg 13, 731, 1991.

Hiles, M.C., Badylak, S.F., Lantz, G.C., Kokini, K., Geddes, L.A., and Morff, R.J. Mechanical properties of xenogeneic small-intestinal submucosa when used as an aortic graft in the dog. Journal of biomedical materials research 29, 883, 1995.

Hirai, J., and Matsuda, T. Self-organized, tubular hybrid vascular tissue composed of vascular cells and collagen for low-pressure-loaded venous system. Cell Transplant 4, 597, 1995.

Hirschi, K.K., Ingram, D.A., and Yoder, M.C. Assessing identity, phenotype, and fate of endothelial progenitor cells. Arteriosclerosis, thrombosis, and vascular biology 28, 1584, 2008.

Hoerstrup, S.P., Zund, G., Sodian, R., Schnell, A.M., Grunenfelder, J., and Turina, M.I. Tissue engineering of small caliber vascular grafts. Eur J Cardiothorac Surg 20, 164, 2001.

Hong, H., and Stegemann, J.P. 2D and 3D collagen and fibrin biopolymers promote specific ECM and integrin gene expression by vascular smooth muscle cells. Journal of biomaterials science 19, 1279, 2008.

Hsieh, H.J., Li, N.Q., and Frangos, J.A. Pulsatile and steady flow induces c-fos expression in human endothelial cells. Journal of cellular physiology 154, 143, 1993.

Hunter, C.J., and Levenston, M.E. Maturation and integration of tissue-engineered cartilages within an in vitro defect repair model. Tissue engineering 10, 736, 2004.

Huynh, T., Abraham, G., Murray, J., Brockbank, K., Hagen, P.O., and Sullivan, S. Remodeling of an acellular collagen graft into a physiologically responsive neovessel. Nat Biotechnol 17, 1083, 1999.

Ingram, D.A., Caplice, N.M., and Yoder, M.C. Unresolved questions, changing definitions, and novel paradigms for defining endothelial progenitor cells. Blood 106, 1525, 2005.

Ingram, D.A., Mead, L.E., Tanaka, H., Meade, V., Fenoglio, A., Mortell, K., Pollok, K., Ferkowicz, M.J., Gilley, D., and Yoder, M.C. Identification of a novel hierarchy of endothelial progenitor cells using human peripheral and umbilical cord blood. Blood 104, 2752, 2004.

Isenberg, B.C., and Tranquillo, R.T. Long-term cyclic distention enhances the mechanical properties of collagen-based media-equivalents. Annals of biomedical engineering 31, 937, 2003.

Isenberg, B.C., Williams, C., and Tranquillo, R.T. Endothelialization and flow conditioning of fibrin-based media-equivalents. Annals of biomedical engineering 34, 971, 2006.

Isenberg, B.C., Williams, C., and Tranquillo, R.T. Small-diameter artificial arteries engineered in vitro. Circulation research 98, 25, 2006.

Ishihara, T., Ferrans, V.J., Jones, M., Boyce, S.W., and Roberts, W.C. Occurrence and significance of endothelial cells in implanted porcine bioprosthetic valves. The American journal of cardiology 48, 443, 1981.

Itosaka, H., Kuroda, S., Shichinohe, H., Yasuda, H., Yano, S., Kamei, S., Kawamura, R., Hida, K., and Iwasaki, Y. Fibrin matrix provides a suitable scaffold for bone marrow stromal cells transplanted into injured spinal cord: A novel material for CNS tissue engineering. Neuropathology, 2008.

Jaffe, E.A., Nachman, R.L., Becker, C.G., and Minick, C.R. Culture of human endothelial cells derived from umbilical veins. Identification by morphologic and immunologic criteria. The Journal of clinical investigation 52, 2745, 1973.

Jeong, S.I., Kwon, J.H., Lim, J.I., Cho, S.W., Jung, Y., Sung, W.J., Kim, S.H., Kim, Y.H., Lee, Y.M., Kim, B.S., Choi, C.Y., and Kim, S.J. Mechano-active tissue engineering

of vascular smooth muscle using pulsatile perfusion bioreactors and elastic PLCL scaffolds. Biomaterials 26, 1405, 2005.

Jockenhoevel, S., Zund, G., Hoerstrup, S.P., Chalabi, K., Sachweh, J.S., Demircan, L., Messmer, B.J., and Turina, M. Fibrin gel -- advantages of a new scaffold in cardiovascular tissue engineering. Eur J Cardiothorac Surg 19, 424, 2001.

Kaehler, J., Zilla, P., Fasol, R., Deutsch, M., and Kadletz, M. Precoating substrate and surface configuration determine adherence and spreading of seeded endothelial cells on polytetrafluoroethylene grafts. J Vasc Surg 9, 535, 1989.

Kaplanski, G., Marin, V., Fabrigoule, M., Boulay, V., Benoliel, A.M., Bongrand, P., Kaplanski, S., and Farnarier, C. Thrombin-activated human endothelial cells support monocyte adhesion in vitro following expression of intercellular adhesion molecule-1 (ICAM-1; CD54) and vascular cell adhesion molecule-1 (VCAM-1; CD106). Blood 92, 1259, 1998.

Kaushal, S., Amiel, G.E., Guleserian, K.J., Shapira, O.M., Perry, T., Sutherland, F.W., Rabkin, E., Moran, A.M., Schoen, F.J., Atala, A., Soker, S., Bischoff, J., and Mayer, J.E., Jr. Functional small-diameter neovessels created using endothelial progenitor cells expanded ex vivo. Nature medicine 7, 1035, 2001.

Kesler, K.A., Herring, M.B., Arnold, M.P., Glover, J.L., Park, H.M., Helmus, M.N., and Bendick, P.J. Enhanced strength of endothelial attachment on polyester elastomer and polytetrafluoroethylene graft surfaces with fibronectin substrate. J Vasc Surg 3, 58, 1986.

Key, N.S., Vercellotti, G.M., Winkelmann, J.C., Moldow, C.F., Goodman, J.L., Esmon, N.L., Esmon, C.T., and Jacob, H.S. Infection of vascular endothelial cells with herpes simplex virus enhances tissue factor activity and reduces thrombomodulin expression. Proceedings of the National Academy of Sciences of the United States of America 87, 7095, 1990.

Khan, O.F., and Sefton, M.V. Endothelial cell behaviour within a microfluidic mimic of the flow channels of a modular tissue engineered construct. Biomedical microdevices.

Kiernan, J.A. Histological and histochemical methods : theory and practice. Oxford [U.K.] ; Boston: Butterworth-Heinemann, 1999.

Kim, B.S., and Mooney, D.J. Engineering smooth muscle tissue with a predefined structure. Journal of biomedical materials research 41, 322, 1998.

Kim, B.S., Nikolovski, J., Bonadio, J., and Mooney, D.J. Cyclic mechanical strain regulates the development of engineered smooth muscle tissue. Nat Biotechnol 17, 979, 1999.

Kim, B.S., Nikolovski, J., Bonadio, J., Smiley, E., and Mooney, D.J. Engineered smooth muscle tissues: regulating cell phenotype with the scaffold. Experimental cell research 251, 318, 1999.

Kim, Y.J., Sah, R.L., Doong, J.Y., and Grodzinsky, A.J. Fluorometric assay of DNA in cartilage explants using Hoechst 33258. Analytical biochemistry 174, 168, 1988.

Kladakis, S.M., and Nerem, R.M. Endothelial cell monolayer formation: effect of substrate and fluid shear stress. Endothelium 11, 29, 2004.

Koveker, G.B., Graham, L.M., Burkel, W.E., Sell, R., Wakefield, T.W., Dietrich, K., and Stanley, J.C. Extracellular matrix preparation of expanded polytetrafluoroethylene grafts seeded with endothelial cells: influence on early platelet deposition, cellular growth, and luminal prostacyclin release. Surgery 109, 313, 1991.

Kuchan, M.J., and Frangos, J.A. Role of calcium and calmodulin in flow-induced nitric oxide production in endothelial cells. The American journal of physiology 266, C628, 1994.

Kuchan, M.J., Jo, H., and Frangos, J.A. Role of G proteins in shear stress-mediated nitric oxide production by endothelial cells. The American journal of physiology 267, C753, 1994.

Kupcsik, L., Alini, M., and Stoddart, M.J. Epsilon-aminocaproic acid is a useful fibrin degradation inhibitor for cartilage tissue engineering. Tissue engineering 15, 2309, 2009.

L'Heureux, N., Dusserre, N., Konig, G., Victor, B., Keire, P., Wight, T.N., Chronos, N.A., Kyles, A.E., Gregory, C.R., Hoyt, G., Robbins, R.C., and McAllister, T.N. Human tissue-engineered blood vessels for adult arterial revascularization. Nature medicine 12, 361, 2006.

L'Heureux, N., Germain, L., Labbe, R., and Auger, F.A. In vitro construction of a human blood vessel from cultured vascular cells: a morphologic study. J Vasc Surg 17, 499, 1993.

L'Heureux, N., Paquet, S., Labbe, R., Germain, L., and Auger, F.A. A completely biological tissue-engineered human blood vessel. Faseb J 12, 47, 1998.

L'Heureux, N., Stoclet, J.C., Auger, F.A., Lagaud, G.J., Germain, L., and Andriantsitohaina, R. A human tissue-engineered vascular media: a new model for pharmacological studies of contractile responses. Faseb J 15, 515, 2001.

Lafleur, M.A., Handsley, M.M., Knauper, V., Murphy, G., and Edwards, D.R. Endothelial tubulogenesis within fibrin gels specifically requires the activity of membrane-type-matrix metalloproteinases (MT-MMPs). Journal of cell science 115, 3427, 2002.

Lantz, G.C., Badylak, S.F., Coffey, A.C., Geddes, L.A., and Blevins, W.E. Small intestinal submucosa as a small-diameter arterial graft in the dog. J Invest Surg 3, 217, 1990.

Lantz, G.C., Badylak, S.F., Hiles, M.C., Coffey, A.C., Geddes, L.A., Kokini, K., Sandusky, G.E., and Morff, R.J. Small intestinal submucosa as a vascular graft: a review. J Invest Surg 6, 297, 1993.

Levesque, M.J., and Nerem, R.M. The elongation and orientation of cultured endothelial cells in response to shear stress. Journal of biomechanical engineering 107, 341, 1985.

Lin, Y. Phenotypic characterization of outgrowth endothelial cells from cultures of peripheral blood and feasibility studies of using these cells in biomedical applications, University of Minnesota, 2003.

Lin, Y., Weisdorf, D.J., Solovey, A., and Hebbel, R.P. Origins of circulating endothelial cells and endothelial outgrowth from blood. The Journal of clinical investigation 105, 71, 2000.

Lloyd-Jones, D., Adams, R.J., Brown, T.M., Carnethon, M., Dai, S., De Simone, G., Ferguson, T.B., Ford, E., Furie, K., Gillespie, C., Go, A., Greenlund, K., Haase, N., Hailpern, S., Ho, P.M., Howard, V., Kissela, B., Kittner, S., Lackland, D., Lisabeth, L., Marelli, A., McDermott, M.M., Meigs, J., Mozaffarian, D., Mussolino, M., Nichol, G., Roger, V.L., Rosamond, W., Sacco, R., Sorlie, P., Roger, V.L., Thom, T., Wasserthiel-Smoller, S., Wong, N.D., and Wylie-Rosett, J. Heart disease and stroke statistics--2010 update: a report from the American Heart Association. Circulation 121, e46.

Long, J.L., and Tranquillo, R.T. Elastic fiber production in cardiovascular tissue-equivalents. Matrix Biol 22, 339, 2003.

Lund, T., Hermansen, S.E., Andreasen, T.V., Olsen, J.O., Osterud, B., Myrmel, T., and Ytrehus, K. Shear stress regulates inflammatory and thrombogenic gene transcripts in cultured human endothelial progenitor cells. Thrombosis and haemostasis 104, 582, 2010.

Malek, A.M., Jackman, R., Rosenberg, R.D., and Izumo, S. Endothelial expression of thrombomodulin is reversibly regulated by fluid shear stress. Circulation research 74, 852, 1994.

Matsumoto, Y., Kawai, Y., Watanabe, K., Sakai, K., Murata, M., Handa, M., Nakamura, S., and Ikeda, Y. Fluid shear stress attenuates tumor necrosis factor-alpha-induced tissue factor expression in cultured human endothelial cells. Blood 91, 4164, 1998.

McAllister, T.N., Maruszewski, M., Garrido, S.A., Wystrychowski, W., Dusserre, N., Marini, A., Zagalski, K., Fiorillo, A., Avila, H., Manglano, X., Antonelli, J., Kocher, A., Zembala, M., Cierpka, L., de la Fuente, L.M., and L'Heureux, N. Effectiveness of haemodialysis access with an autologous tissue-engineered vascular graft: a multicentre cohort study. Lancet 373, 1440, 2009.

McGuigan, A.P., and Sefton, M.V. The influence of biomaterials on endothelial cell thrombogenicity. Biomaterials 28, 2547, 2007.

Mohtai, M., and Yamamoto, T. Smooth muscle cell proliferation in the rat coronary artery induced by vitamin D. Atherosclerosis 63, 193, 1987.

Mol, A., van Lieshout, M.I., Dam-de Veen, C.G., Neuenschwander, S., Hoerstrup, S.P., Baaijens, F.P., and Bouten, C.V. Fibrin as a cell carrier in cardiovascular tissue engineering applications. Biomaterials 26, 3113, 2005.

Morigi, M., Zoja, C., Figliuzzi, M., Foppolo, M., Micheletti, G., Bontempelli, M., Saronni, M., Remuzzi, G., and Remuzzi, A. Fluid shear stress modulates surface expression of adhesion molecules by endothelial cells. Blood 85, 1696, 1995.

Myers, P.R., Wright, T.F., Tanner, M.A., and Adams, H.R. EDRF and nitric oxide production in cultured endothelial cells: direct inhibition by E. coli endotoxin. The American journal of physiology 262, H710, 1992.

Nagel, T., Resnick, N., Atkinson, W.J., Dewey, C.F., Jr., and Gimbrone, M.A., Jr. Shear stress selectively upregulates intercellular adhesion molecule-1 expression in cultured human vascular endothelial cells. The Journal of clinical investigation 94, 885, 1994.

Naito, M., Stirk, C.M., Smith, E.B., and Thompson, W.D. Smooth muscle cell outgrowth stimulated by fibrin degradation products. The potential role of fibrin fragment E in restenosis and atherogenesis. Thrombosis research 98, 165, 2000.

Nauman, E.A., Risic, K.J., Keaveny, T.M., and Satcher, R.L. Quantitative assessment of steady and pulsatile flow fields in a parallel plate flow chamber. Annals of biomedical engineering 27, 194, 1999.

Neidert, M.R., Lee, E.S., Oegema, T.R., and Tranquillo, R.T. Enhanced fibrin remodeling in vitro with TGF-beta1, insulin and plasmin for improved tissue-equivalents. Biomaterials 23, 3717, 2002.

Nerem, R.M., and Seliktar, D. Vascular tissue engineering. Annu Rev Biomed Eng 3, 225, 2001.

Niklason, L.E., Abbott, W., Gao, J., Klagges, B., Hirschi, K.K., Ulubayram, K., Conroy, N., Jones, R., Vasanawala, A., Sanzgiri, S., and Langer, R. Morphologic and mechanical characteristics of engineered bovine arteries. J Vasc Surg 33, 628, 2001.

Niklason, L.E., Gao, J., Abbott, W.M., Hirschi, K.K., Houser, S., Marini, R., and Langer, R. Functional arteries grown in vitro. Science (New York, N.Y 284, 489, 1999.

Nishida, K., Harrison, D.G., Navas, J.P., Fisher, A.A., Dockery, S.P., Uematsu, M., Nerem, R.M., Alexander, R.W., and Murphy, T.J. Molecular cloning and characterization of the constitutive bovine aortic endothelial cell nitric oxide synthase. The Journal of clinical investigation 90, 2092, 1992.

Ogawa, S., Clauss, M., Kuwabara, K., Shreeniwas, R., Butura, C., Koga, S., and Stern, D. Hypoxia induces endothelial cell synthesis of membrane-associated proteins. Proceedings of the National Academy of Sciences of the United States of America 88, 9897, 1991.

Ohtsuka, A., Ando, J., Korenaga, R., Kamiya, A., Toyama-Sorimachi, N., and Miyasaka, M. The effect of flow on the expression of vascular adhesion molecule-1 by cultured mouse endothelial cells. Biochemical and biophysical research communications 193, 303, 1993.

Osathanon, T., Linnes, M.L., Rajachar, R.M., Ratner, B.D., Somerman, M.J., and Giachelli, C.M. Microporous nanofibrous fibrin-based scaffolds for bone tissue engineering. Biomaterials 29, 4091, 2008.

Osawa, M., Masuda, M., Kusano, K., and Fujiwara, K. Evidence for a role of platelet endothelial cell adhesion molecule-1 in endothelial cell mechanosignal transduction: is it a mechanoresponsive molecule? The Journal of cell biology 158, 773, 2002.

Ott, M.J., and Ballermann, B.J. Shear stress-conditioned, endothelial cell-seeded vascular grafts: improved cell adherence in response to in vitro shear stress. Surgery 117, 334, 1995.

Patel, S.D., Waltham, M., Wadoodi, A., Burnand, K.G., and Smith, A. The role of endothelial cells and their progenitors in intimal hyperplasia. Therapeutic advances in cardiovascular disease 4, 129.

Pelaez, D., Huang, C.Y., and Cheung, H.S. Cyclic Compression Maintains Viability and Induces Chondrogenesis of Human Mesenchymal Stem Cells in Fibrin Gel Scaffolds. Stem cells and development, 2008.

Prokopi, M., Pula, G., Mayr, U., Devue, C., Gallagher, J., Xiao, Q., Boulanger, C.M., Westwood, N., Urbich, C., Willeit, J., Steiner, M., Breuss, J., Xu, Q., Kiechl, S., and Mayr, M. Proteomic analysis reveals presence of platelet microparticles in endothelial progenitor cell cultures. Blood 114, 723, 2009.

Radomski, M.W., Palmer, R.M., and Moncada, S. Endogenous nitric oxide inhibits human platelet adhesion to vascular endothelium. Lancet 2, 1057, 1987.

Ravi, S., Qu, Z., and Chaikof, E.L. Polymeric materials for tissue engineering of arterial substitutes. Vascular 17 Suppl 1, S45, 2009.

Rehman, J., Li, J., Orschell, C.M., and March, K.L. Peripheral blood "endothelial progenitor cells" are derived from monocyte/macrophages and secrete angiogenic growth factors. Circulation 107, 1164, 2003.

Reidy, M.A., and Schwartz, S.M. Endothelial injury and regeneration. IV. Endotoxin: a nondenuding injury to aortic endothelium. Laboratory investigation; a journal of technical methods and pathology 48, 25, 1983.

Rijken, D.C., and Lijnen, H.R. New insights into the molecular mechanisms of the fibrinolytic system. J Thromb Haemost 7, 4, 2009.

Roach, M.R., and Burton, A.C. The reason for the shape of the distensibility curves of arteries. Canadian journal of biochemistry and physiology 35, 681, 1957.

Robinson, P.S., Johnson, S.L., Evans, M.C., Barocas, V.H., and Tranquillo, R.T. Functional tissue-engineered valves from cell-remodeled fibrin with commissural alignment of cell-produced collagen. Tissue engineering 14, 83, 2008.

Rohde, E., Malischnik, C., Thaler, D., Maierhofer, T., Linkesch, W., Lanzer, G., Guelly, C., and Strunk, D. Blood monocytes mimic endothelial progenitor cells. Stem cells (Dayton, Ohio) 24, 357, 2006.

Ross, J.J., and Tranquillo, R.T. ECM gene expression correlates with in vitro tissue growth and development in fibrin gel remodeled by neonatal smooth muscle cells. Matrix Biol 22, 477, 2003.

Rowe, S.L., and Stegemann, J.P. Interpenetrating collagen-fibrin composite matrices with varying protein contents and ratios. Biomacromolecules 7, 2942, 2006.

Sakariassen, K.S., Aarts, P.A., de Groot, P.G., Houdijk, W.P., and Sixma, J.J. A perfusion chamber developed to investigate platelet interaction in flowing blood with human vessel wall cells, their extracellular matrix, and purified components. The Journal of laboratory and clinical medicine 102, 522, 1983.

Schmidt, C.E., and Baier, J.M. Acellular vascular tissues: natural biomaterials for tissue repair and tissue engineering. Biomaterials 21, 2215, 2000.

Schmidt, D., Asmis, L.M., Odermatt, B., Kelm, J., Breymann, C., Gossi, M., Genoni, M., Zund, G., and Hoerstrup, S.P. Engineered living blood vessels: functional endothelia generated from human umbilical cord-derived progenitors. The Annals of thoracic surgery 82, 1465, 2006.

Seeger, J.M., and Klingman, N. Improved in vivo endothelialization of prosthetic grafts by surface modification with fibronectin. J Vasc Surg 8, 476, 1988.

Seliktar, D., Black, R.A., Vito, R.P., and Nerem, R.M. Dynamic mechanical conditioning of collagen-gel blood vessel constructs induces remodeling in vitro. Annals of biomedical engineering 28, 351, 2000.

Seliktar, D., Nerem, R.M., and Galis, Z.S. The role of matrix metalloproteinase-2 in the remodeling of cell-seeded vascular constructs subjected to cyclic strain. Annals of biomedical engineering 29, 923, 2001.

Sheikh, S., Rainger, G.E., Gale, Z., Rahman, M., and Nash, G.B. Exposure to fluid shear stress modulates the ability of endothelial cells to recruit neutrophils in response to tumor necrosis factor-alpha: a basis for local variations in vascular sensitivity to inflammation. Blood 102, 2828, 2003.

Shin'oka, T., Imai, Y., and Ikada, Y. Transplantation of a tissue-engineered pulmonary artery. The New England journal of medicine 344, 532, 2001.

Shinoka, T., Shum-Tim, D., Ma, P.X., Tanel, R.E., Isogai, N., Langer, R., Vacanti, J.P., and Mayer, J.E., Jr. Creation of viable pulmonary artery autografts through tissue engineering. The Journal of thoracic and cardiovascular surgery 115, 536, 1998.

Shirota, T., He, H., Yasui, H., and Matsuda, T. Human endothelial progenitor cell-seeded hybrid graft: proliferative and antithrombogenic potentials in vitro and fabrication processing. Tissue engineering 9, 127, 2003.

Solan, A., Mitchell, S., Moses, M., and Niklason, L. Effect of pulse rate on collagen deposition in the tissue-engineered blood vessel. Tissue engineering 9, 579, 2003.

Solovey, A., Lin, Y., Browne, P., Choong, S., Wayner, E., and Hebbel, R.P. Circulating activated endothelial cells in sickle cell anemia. The New England journal of medicine 337, 1584, 1997.

Somani, A., Nguyen, J., Milbauer, L.C., Solovey, A., Sajja, S., and Hebbel, R.P. The establishment of murine blood outgrowth endothelial cells and observations relevant to gene therapy. Transl Res 150, 30, 2007.

Spencer, F.C. The internal mammary artery: the ideal coronary bypass graft? The New England journal of medicine 314, 50, 1986.

Spicer, P.P., and Mikos, A.G. Fibrin glue as a drug delivery system. J Control Release, 2010.

Spotnitz, W.D. Fibrin sealant: past, present, and future: a brief review. World journal of surgery 34, 632, 2010.

Stachelek, S.J., Alferiev, I., Connolly, J.M., Sacks, M., Hebbel, R.P., Bianco, R., and Levy, R.J. Cholesterol-modified polyurethane valve cusps demonstrate blood outgrowth endothelial cell adhesion post-seeding in vitro and in vivo. The Annals of thoracic surgery 81, 47, 2006.

Starcher, B. A ninhydrin-based assay to quantitate the total protein content of tissue samples. Analytical biochemistry 292, 125, 2001.

Stegemann, H., and Stalder, K. Determination of hydroxyproline. Clinica chimica acta; international journal of clinical chemistry 18, 267, 1967.

Stern, D.M., Kaiser, E., and Nawroth, P.P. Regulation of the coagulation system by vascular endothelial cells. Haemostasis 18, 202, 1988.

Stroncek, J.D., Grant, B.S., Brown, M.A., Povsic, T.J., Truskey, G.A., and Reichert, W.M. Comparison of endothelial cell phenotypic markers of late-outgrowth endothelial progenitor cells isolated from patients with coronary artery disease and healthy volunteers. Tissue engineering 15, 3473, 2009.

Sumpio, B.E., Banes, A.J., Link, W.G., and Johnson, G., Jr. Enhanced collagen production by smooth muscle cells during repetitive mechanical stretching. Arch Surg 123, 1233, 1988.

Sun, Z., Chen, Y.H., Wang, P., Zhang, J., Gurewich, V., Zhang, P., and Liu, J.N. The blockage of the high-affinity lysine binding sites of plasminogen by EACA significantly inhibits prourokinase-induced plasminogen activation. Biochimica et biophysica acta 1596, 182, 2002.

Swartz, D.D., Russell, J.A., and Andreadis, S.T. Engineering of fibrin-based functional and implantable small-diameter blood vessels. American journal of physiology 288, H1451, 2005.

Syedain, Z.H., Meier, L.A., Bjork, J.W., Lee, A., and Tranquillo, R.T. Implantable arterial grafts from human fibroblasts and fibrin using a multi-graft pulsed flow-stretch bioreactor with noninvasive strength monitoring. Biomaterials, 2010.

Syedain, Z.H., Weinberg, J.S., and Tranquillo, R.T. Cyclic distension of fibrin-based tissue constructs: evidence of adaptation during growth of engineered connective tissue. Proceedings of the National Academy of Sciences of the United States of America 105, 6537, 2008.

Takada, Y., Shinkai, F., Kondo, S., Yamamoto, S., Tsuboi, H., Korenaga, R., and Ando, J. Fluid shear stress increases the expression of thrombomodulin by cultured human endothelial cells. Biochemical and biophysical research communications 205, 1345, 1994.

Tawil, B. Fibrin and Its Applications. In: Guelcher, S.A., and Hollinger, J.O., eds. An introduction to biomaterials. Baca Raton, FL: CRC/Taylor & Francis, 2006.

Taylor, S.J., and Sakiyama-Elbert, S.E. Effect of controlled delivery of neurotrophin-3 from fibrin on spinal cord injury in a long term model. J Control Release 116, 204, 2006.

Thebaud, N.B., Bareille, R., Remy, M., Bourget, C., Daculsi, R., and Bordenave, L. Human progenitor-derived endothelial cells vs. venous endothelial cells for vascular tissue engineering: an in vitro study. Journal of tissue engineering and regenerative medicine 4, 473, 2010.

Thomas, A.C., Campbell, G.R., and Campbell, J.H. Advances in vascular tissue engineering. Cardiovasc Pathol 12, 271, 2003.

Thompson, W.D., Evans, A.T., and Campbell, R. The control of fibrogenesis: stimulation and suppression of collagen synthesis in the chick chorioallantoic membrane with fibrin degradation products, wound extracts and proteases. The Journal of pathology 148, 207, 1986.

Traub, O., and Berk, B.C. Laminar shear stress: mechanisms by which endothelial cells transduce an atheroprotective force. Arteriosclerosis, thrombosis, and vascular biology 18, 677, 1998.

Ugwu, F., Lemmens, G., Collen, D., and Lijnen, H.R. Matrix metalloproteinase deficiencies do not impair cell-associated fibrinolytic activity. Thrombosis research 102, 61, 2001.

Wake, M.C., Gupta, P.K., and Mikos, A.G. Fabrication of pliable biodegradable polymer foams to engineer soft tissues. Cell Transplant 5, 465, 1996.

Weinbaum, J.S., Qi, J., and Tranquillo, R.T. Monitoring Collagen Transcription by Vascular Smooth Muscle Cells in Fibrin-Based Tissue Constructs. Tissue engineering, 2009.

Weinberg, C.B., and Bell, E. A blood vessel model constructed from collagen and cultured vascular cells. Science (New York, N.Y 231, 397, 1986.

Williams, C., Johnson, S.L., Robinson, P.S., and Tranquillo, R.T. Cell sourcing and culture conditions for fibrin-based valve constructs. Tissue engineering 12, 1489, 2006.

Wilson, G.J., Courtman, D.W., Klement, P., Lee, J.M., and Yeger, H. Acellular matrix: a biomaterials approach for coronary artery bypass and heart valve replacement. The Annals of thoracic surgery 60, S353, 1995.

Wu, K.K., and Thiagarajan, P. Role of endothelium in thrombosis and hemostasis. Annual review of medicine 47, 315, 1996.

Xiao, L., and Shi, D. Role of precoating in artificial vessel endothelialization. Chinese journal of traumatology = Zhonghua chuang shang za zhi / Chinese Medical Association 7, 312, 2004.

Yan, D., Urano, T., Takada, Y., and Takada, A. Dissociation of alpha 2-plasmin-inhibitor-plasmin complex and regeneration of plasmin activity by SDS treatment. Thrombosis research 69, 491, 1993.

Yao, L., Swartz, D.D., Gugino, S.F., Russell, J.A., and Andreadis, S.T. Fibrin-based tissue-engineered blood vessels: differential effects of biomaterial and culture parameters on mechanical strength and vascular reactivity. Tissue engineering 11, 991, 2005.

Yazdani, S.K., Tillman, B.W., Berry, J.L., Soker, S., and Geary, R.L. The fate of an endothelium layer after preconditioning. J Vasc Surg 51, 174.

Yazdani, S.K., Tillman, B.W., Berry, J.L., Soker, S., and Geary, R.L. The fate of an endothelium layer after preconditioning. J Vasc Surg 51, 174, 2010.

Ye, Q., Zund, G., Benedikt, P., Jockenhoevel, S., Hoerstrup, S.P., Sakyama, S., Hubbell, J.A., and Turina, M. Fibrin gel as a three dimensional matrix in cardiovascular tissue engineering. Eur J Cardiothorac Surg 17, 587, 2000.

Yee, A., Bosworth, K.A., Conway, D.E., Eskin, S.G., and McIntire, L.V. Gene expression of endothelial cells under pulsatile non-reversing vs. steady shear stress; comparison of nitric oxide production. Annals of biomedical engineering 36, 571, 2008.

Yee, K.O., Rooney, M.M., Giachelli, C.M., Lord, S.T., and Schwartz, S.M. Role of beta1 and beta3 integrins in human smooth muscle cell adhesion to and contraction of fibrin clots in vitro. Circulation research 83, 241, 1998.

Yoder, M.C., Mead, L.E., Prater, D., Krier, T.R., Mroueh, K.N., Li, F., Krasich, R., Temm, C.J., Prchal, J.T., and Ingram, D.A. Redefining endothelial progenitor cells via clonal analysis and hematopoietic stem/progenitor cell principals. Blood 109, 1801, 2007.

Zavoico, G.B., Ewenstein, B.M., Schafer, A.I., and Pober, J.S. IL-1 and related cytokines enhance thrombin-stimulated PGI2 production in cultured endothelial cells without affecting thrombin-stimulated von Willebrand factor secretion or platelet-activating factor biosynthesis. J Immunol 142, 3993, 1989.

Zhang, G., Hu, Q., Braunlin, E.A., Suggs, L.J., and Zhang, J. Enhancing efficacy of stem cell transplantation to the heart with a PEGylated fibrin biomatrix. Tissue engineering 14, 1025, 2008.

Zhang, S.J., Zhang, H., Wei, Y.J., Su, W.J., Liao, Z.K., Hou, M., Zhou, J.Y., and Hu, S.S. Adult endothelial progenitor cells from human peripheral blood maintain monocyte/macrophage function throughout in vitro culture. Cell research 16, 577, 2006.

Zhang, Y., Ingram, D.A., Murphy, M.P., Saadatzadeh, M.R., Mead, L.E., Prater, D.N., and Rehman, J. Release of proinflammatory mediators and expression of proinflammatory adhesion molecules by endothelial progenitor cells. American journal of physiology 296, H1675, 2009.

Zilla, P., Fasol, R., Preiss, P., Kadletz, M., Deutsch, M., Schima, H., Tsangaris, S., and Groscurth, P. Use of fibrin glue as a substrate for in vitro endothelialization of PTFE vascular grafts. Surgery 105, 515, 1989.

Appendix A: Methods

A.1 Cell Culture

A.1.1 Porcine Valve Interstitial Cells (PVIC)

Medium: DMEM/F12 with 10% FBS, 1% Antibiotic/Antimycotic
To split cells

1. Split cells when they are 80-90% confluent.
2. Remove medium and discard.
3. Rinse flask with PBS (without calcium or magnesium), using approximately 10 ml per T175.
4. Add 5ml of 0.25% trypsin warmed to 37C for each T175 flask.
5. Place flask in incubator, wait about a minute, remove and check for cell rounding and release with microscope. Tap flask gently to finish releasing cells, if necessary.
6. Add 1 ml FBS per T175 flask (20% volume of trypsin) to neutralize. Rinse and collect cells into 50 cc conical.
7. Pellet cells at 220 x g for 5 minutes.
8. Resuspend cells in medium. Usually resuspending in 3ml per T175 harvested gives a final concentration above 3M/ml.
9. Remove 50 µl of cells and place into microfuge tube containing 200 µl of a trypan blue solution. Count cells in hemocytometer.
10. Plate cells at 1 M per T175, using 30 ml media per flask.

A.1.2 Neonatal Human Dermal Fibroblasts (nhDF)

Medium: DMEM/F12 with 15% FBS, 1% Pen/Strep
To split cells

Cells are ready to be split when cells are 100% confluent, usually after 4 days.

1. Remove medium and discard.
2. Rinse flask with PBS (without Ca and Mg), using about 10 ml per T175.
3. Add 5 ml of 0.25% trypsin at 37C to each T175 flask.
4. Incubate cells with trypsin until they have detached from flask surfrace.
5. Add 1 cc FBS per T175 to neutralize. Collect cells into a 50 cc conical. Rinse flask with PBS and transfer the rinse to the same 50cc conical.
6. Pellet cells at 220 x g for 5 minutes.
7. Resuspend cells in media. Use about 3 ml of media per T175.
8. Remove 50 µl of cells and place into microfuge tube containing 200 µl of a trypan blue solution. Count cells in hemocytometer.
9. Plate cells at 1.5 M per T175, using 30 ml medium per T175 flask.

A.1.3 Neonatal Rat Smooth Muscle Cells (nrSMC)

Medium: DMEM/F12 with 15% FBS and 1% P/S

Thawing

1. Thaw 4M nrSMCs from liquid nitrogen storage. Thaw in the 37C bath immediately and remove from bath as soon as thawed.
2. Dilute 4M cells into 30ml of nrSMC medium pre-warmed to 37C and transfer to a T175 flask.
3. Change the medium on the cells at 24 hours.

Passaging

Cells are ready to be split when 90-100% confluent, usually every 3-4 days.

1. Remove medium from flasks. Wash each flask 2 times with 10 ml PBS.
2. Add 5 ml warm 0.05% Trypsin/EDTA to each T175 flask.
3. Transfer flasks to the 37˚C incubator for 2-3 minutes until cells are free floating. Monitor detachment with the cell culture microscope.
4. Add 1 ml FBS to each flask to deactivate trypsin. Collect cells into 50 ml conical tube.
5. Rinse flasks sequentially twice with PBS. Collect rinses into the same 50 ml conical tube.
6. Centrifuge cells at 220 x g for 5 minutes.
7. Resuspend cells in appropriate medium and count.
8. Replate cells at 3.5 M/T175 flask (20,000/cm2).
9. Culture medium should be changed every 2 days, with the first (usually only) media change occurring 2 days after plating.

Freezing cells

nrSMCs are frozen in 50% culture medium, 45% FBS and 5% DMSO. Cells are routinely frozen in 1 ml aliquots containing 2M cells/ml.

1. Pre-label 1 ml NUNC vials for cell storage and place on ice. Key information: Cell type, isolation, passage number, cells/vial, date frozen, initials.
2. Make up "freezing media": 10% DMSO in FBS and place on ice.
3. Harvest cells and resuspend at 4 x 10^6 cells / ml in cell culture medium.
4. Gradually add equal volume of "freezing media" to the cell solution and keep on ice. Immediately aliquot into freezing vials, 1 ml/vial.
5. Place vials in freezing container (Mr. Frosty) and put at -80˚C overnight.
6. Transfer vials to liquid nitrogen storage.

A.1.4 Rat Vascular Endothelial Cells (Source: VEC Technologies)

Medium: VEC Medium (VEC Technologies). Add 1% Pen/Strep to bottle if it is not included.

Prepare 0.2% Gelatin-coated flasks

1. Warm gelatin to 37˚C.
2. Add gelatin to flask, shake back and forth gently to coat the bottom completely, then remove excess gelatin.
3. Allow to dry for at least 30 minutes.

Splitting rvECs

1. Warm VEC EC medium, HBSS and 0.25% Trypsin in 37˚C bath. Total trypsin needed per flask: T25 = 1ml, T75 = 2ml, T175 = 5ml
2. Wash flasks twice with HBSS without Ca and Mg.
   *Note: Washing with PBS will cause cells to detach immediately.
3. Wash flasks once with 0.25% trypsin/EDTA (T25 = 0.5ml, T75 = 2ml, T175 = 2.5ml). Let trypsin flow down bottom of flask, then take off immediately.
4. Add 0.25% Trypsin/EDTA to detach cells. (T25 = 0.5ml, T75 = 2ml, T175 = 2.5ml). Rock flask to coat surface. Cells will begin to detach immediately. Check under microscope. If cells are not floating, monitor progress and gently rock flask until they are fully detached.
5. Immediately add 37˚C VEC EC medium to the flask, collect cells into centrifuge tube. Wash flask with additional medium and collect this medium as well.
6. Plate into gelatin-coated flasks, splitting 1:2 or 1:3. Total amount of medium/ flask: T25 = 5ml, T75 = 15ml, T175 = 30ml.

A.1.5 Rat Blood Outgrowth Endothelial Cells (Source: Dr Robert Hebbel's Lab)

Medium

500 ml EBM-2 basal medium (Clonetics #CC-3156)
EBM-2 Singlequots (Clonetics #CC-4176)
0.123 g Dibutyryl cyclic AMP (Sigma #D-0627)
40 ml FBS (heat inactivated; GIBCO #10082-147)
5 ml antibiotic-antimycotic (A/A)

To make medium

1. Add 0.123 g cAMP into 500 ml of warm EBM-2 basal medium. Mix well.
2. Sterile filter the medium through a 500ml filter unit (0.2 μm)
3. Add EBM-2 SingleQuots, including the 10 ml aliquot of FBS, 40 ml of additional FBS, and 5ml A/A to the filtered EBM-2 medium.

Rat tail Collagen Type I Solution Preparation

1. Determine the amount of collagen required to make 500ml of a 0.05mg/ml Collagen solution.
2. Add 0.575 ml of glacial acetic acid to Milli-Q (appropriate amount to make 500ml of solution. Ie 500ml – volume of collagen that will be added later).
3. Mix well and sterile filter.
4. Add respective amount of collagen type 1 for a final concentration of 0.05 mg/ml, mix well and store at 4C. *Keep the stock collagen solution on ice the entire time.

Prepare Collagen-coated flasks

1. Add 0.05 mg/ml collagen solution the flasks (7ml for T75, 12 ml for T175). Incubate overnight at 37C.
2. After the overnight coating aspirate the collagen and rinse the flasks with HBSS without Ca+, Mg2+ twice.
3. The coated flask can now be used for cell culture or can be stored at 4C for up to 3 weeks. Store dry (ie aspirate last HBSS rinse and store as is).

Splitting rBOECs

1. Rinse flask twice with HBSS without Ca+, Mg2+ or phenol red at RT.
2. Add 0.25% Trypsin-EDTA for a quick rinse (30-60 sec). Add 2 ml per T75 or 5 ml per T175.
3. Aspirate off the trypsin rinse and add 0.25% trypsin to detach cells. Add 3 ml per T75 or 5 ml per T175. Incubate at 37C, examining cells after 2 minutes. Leave trypsin on for up to 5 minutes. Some agitation/knocking of flask is required to loosen the cells.
4. Add FBS to quench the trypsin (0.5 ml for T75, 1 ml for T175) and then transfer the cells to a 50cc conical.
5. Rinse 1-2 times with HBSS and add rinses to the 50cc conical.
6. Pellet cells at 220 x g for 5 minutes. Then resuspend in rBOEC medium.
7. Count cells and replate at 1 M cells/T75 in 10 ml of rBOEC medium.

A.1.6 Human/Ovine Blood Outgrowth Endothelial Cells (Source: Dr. Robert Hebbel's Lab)

Medium

500 ml EBM-2 basal medium (Clonetics #CC-3156)
EBM-2 SingleQuots (Clonetics #CC-4176)
40 ml FBS (heat inactivated; GIBCO #10082-147)
5 ml pen/strep (Invitrogen)

Splitting hBOEC or oBOECs

1. Rinse T75 flask twice with HBSS without Ca+/Mg2+ or phenol red (Gibco 14175)
2. Add 0.05% Trypsin-EDTA (3 ml for T75, 5 ml for T175) for approximately 2 minutes, incubating at 37C. Monitor for cell detachment.
3. Add FBS (0.5 ml for T75, 1 ml for T175) to quench the trypsin and pipette cell solution up and down on flask surface then transfer the solution to a 50cc conical.
4. Rinse flask with HBSS (6.5 ml for T75, 9 ml for T175) and transfer this to the 50cc conical as well.
5. Spin down cells and resuspend in BOEC medium using 1 ml of BOEC medium per T75 and 2 ml per T175. Replate on collagen-coated flasks at approximately 40,000 cell/cm^2.

A.2 Construct Fabrication and Culture

A.2.1 Media Equivalents

Mandrel Materials

10 cm section of glass outer shell *(reusable)*
8 cm long glass rod (2 cm)
Rubber stoppers from ½ cc syringe *(Kendall monoject insulin syringes – ½ cc)*
Rubber stoppers from 3 cc syringe *(Kendall monoject luer lock syringes – 3cc)*
¼ inch wide Teflon tape
½ inch wide Teflon tape
10 cm section of glass outer shell *(reusable)*
Contrex EZ powdered enzymatic detergent *(Decon Labs Inc.)*
Branson GP "pink" formulated cleaning concentrate *(Branson)*

Prepare ME mandrels

1. Sonicate the mandrel materials and rubber stoppers in the Contrex solution for 30 minutes w/ heat. Note: do not put too many stoppers in a jar for sonicating, but be sure to use lots of liquid. For example, do not let stoppers exceed the 200mL mark in a 600mL beaker, but fill beaker with liquid up to the 500mL mark.
2. Rinse once in dH_2O and sonicate the parts again in the Branson solution for 30 minutes w/ heat.
3. Rince once in dH_2O and sonicate the parts again in dH_2O for 30 minutes w/heat.
4. Rinse once in dH_2O and dry parts on a sterile drape.
5. Once parts are dry, attach the small rubber stoppers and wrap with a 6 cm long piece of ¼ inch Teflon tape.
6. Attach the large rubber stoppers and wrap with a 9 cm long piece of ½ inch Teflon tape.
7. Place the mandrel assemblies in a clean 500ml beaker and sterilize at 121^{o}C for 10 minutes with 10 minute exhaust.

Prepare ME glass casing

1. Rinse glass tubes in dH_2O then place in a clean beaker and sonicate 30 minues in the Branson solution.
2. Rince once in dH_2O and sonicate the parts again in dH_2O for 30 minutes w/heat.
3. Rinse once in dH_2O and dry parts on a sterile drape.
4. Place in the same beaker as the ME mandrels and autoclave as stated above.

Pluronics F127 Solution

1. Dissolve 5% Pluronic by weight in ddH2O. This may take a couple hours.
2. Run Pluronic solution through a 0.2 μm filter.
   *Note: The pluronic solution may be used three times, with re-filtration between each use.

ME Fabrication

1. Coat glass mandrels and shells in Pluronic for 3 hours.
2. Dry mandrels on a sterile paper towel for 30 minutes.
3. Place mandrels in the shells using sterile gloves.
4. Make Fibrinogen, Thrombin and Cell Solutions (A,B,C), as described below. NOTE: MEs use approximately 6 mL, HM used 200 uL. The recipe below is for

the 3.3 mg/ml fibrin concentration. Make up the thrombin solution as the last step just before casting.

a. Fibrinogen Solution (6 mL total):
    i. 1 mL Fibrinogen (~30 mg/mL)
    ii. 5 mL 20mM HEPES in Saline
b. Cell Solution
    i. 6x concentration of final (final usually $0.5x10^6$ cells/mL => $3x10^6$ cells/mL)
c. Thrombin Solution (~2 mL total):
    i. 2 mL DMEM WITHOUT FBS
    ii. 100 μL Thrombin
    iii. 7.5 μL 2M $CaCl_2$

5. Add the cells to the fibrinogen solution and then add thrombin to catalyze reaction. For 3 MEs we use 10.4 ml fibrinogen solution, 2.6 ml cells, 2.6 ml thrombin solution, i.e 4 parts fibrinogen solution, 1 part cell solution, 1 part thrombin solution.
6. Using the largest syringe needle (18G) draw solution into a 20cc syringe, then slowly inject each ME with solution by inserting the needle between the stopper and the glass casing.
7. Wrap shells in ethanol-sprayed parafilm and place in the incubator for 30 minutes.
8. Expel mandrels out of shells using a teflon rod into a 150 mm cell culture dish containing 120 ml media. Place 6 MEs per dish.
9. Place in incubator (37 degrees, 5% CO2). Change media three times per week using 100 ml per dish after the first feeding.

Table A.1 Standard culture conditions for PAVC, NHDF, nfSMC Constructs

	PAVC	**NHDF**	**nfSMC**
Media	DMEM/F12 C.	DMEM C. (High Fz)	DMEM, 15% FBS, 1% A/A
Supplements	2 mg/ml ACA	No ACA	1 mg/ml ACA
	2 μg/ml Insulin	Same	Same
	1 ng/ml TGF-β	None	Same or add 5 ng/ml EGF
	50 μg/ml Ascorbic Acid	Same	Same

Stock concentrations: 2 g/ml ACA, 2 mg/ml Insulin, 1 μg/ml TGF-β, 5 mg/ml AA, 10 mg/ml EGF. All supplements stored at 1000x, except ACA is at 100x and EGF is at 2000x.

A.2.2 Hemispheres

*Use cell conditions as outlined above.

1. Use the 1 cm circular borer on the permanox slides or in cell culture plates (6 well plates for the NHDFs, 12 well plates for the nfSMCs) to create a circular area for fibrin gel deposition.

2. Make up the fibrin gel solutions, as described above. Mix in 4:1:1 ratio the fibrinogen, cell and thrombin solutions, as above. Note that each HM takes 200 µl.
3. To each etched circle, add 200 µl of solution. Wait 10-15 minutes until HMs begin to get cloudy (gelling), then place in incubator.
4. Add media after 10-20 more minutes. Use the same media noted above.
    A. HM grown on Permanox microscope slides should have an autoclaved Teflon ring affixed around the HM with autoclaved vacuum grease before 2 ml of media is added. 1 ml of media can be used for each subsequent feeding.
    B. HM grown in 6-well plates need 5 ml of media for the first feeding and 3ml thereafter. HM in 12-well plates need 2 ml for the first feeding and 1 ml thereafter.
5. Change media 3 times per week.

A.3 Live Cell Staining

A.3.1 Live/Dead Stain

Calcein AM (live cells), Ethidium homodimer (dead cells)
Molecular Probes Kit L-3224
Storage: -20C, Protected from light.

1. Calcein AM is susceptible to hydrolysis when exposed to moisture; allow the kit to warm to RT prior to opening.
2. Prepare working solutions in PBS just prior to use. Determine optimal dye concentrations for each cell type. Table A.2 shows concentrations that work for NHDFs and rSMCs.

Table A.2 NHDF and rSMC calcein AM and EthD-1 dye concentrations

Dye	Concentration	Dilution	FL Filter	Emission
Calcein AM	4 µM	1:1000	FITC	Green (Live)
EthD-1	4 µM	1:500	TRITC	Red (Dead)

3. Wash constructs or adherent cells in PBS three times for 5 minutes. Longer rinses may be necessary for thick constructs.
4. Add working solution containing Calcein AM and EthD-1 to cover cells or constructs. Incubate 45 minutes at 37C/5% CO_2. *Incubate nrSMCs 30 minutes.
5. Rinse cells or constructs 3 times with PBS.
6. View/Image with microscope. Red=Dead. Green=Good.

A.3.2 CellTracker Live Cell Staining (optimized for human BOECs)

Source: Invitrogen
Catalog #: C34551 (CellTracker Orange CMRA)
20 x 50µg dry powder

Dyes come in various colors. Green CMFDA and Orange CMRA require enzymatic cleavage.
Storage: -20C, dessicated

Label Cells

1. Grow cells in the appropriate culture medium. Cells can be labeled in suspension or as a monolayer.
2. Before opening the dye vial, allow the product to warm to RT. Dissolve the lyophilized product in DMSO to 10 mM (9.1 µl DMSO for CMRA, 10.8 µl DMSO for CMFDA). Dilute the stock solution 1:4000 in warm EBM-2 basal medium (no FBS or supplements) for a final working concentration of 2.5 µM. *Store stock solution in duct tape covered desiccator at -20C.
3. For cells in suspension, harvest cells in the usual method and after centrifugation (220 x g for 5 minutes) add the CellTracker working solution to the cell pellet and resuspend. For adherent cells, remove the medium and add the CellTracker working solution directly to the flask. Incubate the cells in the working solution for 15 minutes in the incubator.
4. Remove the CellTracker solution by centrifuging (cells in suspension; 220 g for 5 min) or aspiration (adherent cells). Add fresh medium and incubate the cells for another 30 minutes on ice (cells in suspension) or in the incubator (adherent cells).
5. After 30 minutes, centrifuge (cells in suspension; 220 g for 5 min) and aspirate off medium (cells in suspension and adherent cells) and add fresh medium.
6. Plate or passage CellTracker Green cells as necessary. Loss of CTG intensity happens within a few days for cells that are dividing often (passaged cells), but will remain obvious for up to a week when cells are seeded as a monolayer. *Fix the cells with 4% formaldehyde in PBS for 10 minutes at room temperature, if desired. The formaldehyde used in standard fixation protocols crosslinks the amines of the protein– or peptide–dye conjugate, maintaining the fluorescence after fixation (and after sectioning of frozen tissue samples).

A.3.3 DiI-ac-LDL Uptake Assay by Endothelial cells

Source: Biomedical Technologies Inc.
Catalog #BT-902
Quantity 200 ug/vial
Concentration: 200 ug/mL
Absorbance Ratio Dil/Protein = 555nm/275nm=1.67
Stable for 3 months when sterile at 4ºC; NEVER FREEZE

General Protocol for DiI-ac-LDL Staining

1. Asceptically dilute Dil-Ac-LDL to 10 ug/mL in standard media (1:20).
2. Add to live cells and incubate for 4 hours at 37°C.
3. Remove media containing Dil-Ac-LDL from your culture.
4. Wash cells several times with probe-free media.
5. Image cells using Fluorescence imaging with the Rhodamine filter.

6. If desired, continue to culture cells in normal medium. *If continuing to culture cells, note that the DiI-ac-LDL may aggregate in the cell over time, producing a punctate effect when imaging. This is normal. However, LDL can also aggregate while being stored. To clarify these aggregates out, simply spin in a microfuge for 2 minutes.
7. OPTIONAL FIXATION: Rinse cells in warm HBSS, then fix cells in 4% PFA for 10 minutes. After fixation, rinse cells 3 times, 5 minutes each in PBS. * Never use methanol or acetone fixation; Dil is soluble in organic solvents.
8. Seal with Kroenings wax or DAKO fluorescent mounting medium. Do not use nail polish. Store at -20°C.

A.4 Immunochemistry

A.4.1 Antibodies

Table A.3 Rat SMCs Antibodies (or contaminating fibroblasts)

Antigen	Source	Host	Dilution	Storage	Fixation	Antigen Retrieval	Stock Soln
α SM actin	Abcam (ab18147)	mouse	1:200	-20C	4% PFA	0.1% Triton-X	0.1 mg/ml
Vimentin	Chemicon (mab3400)	mouse	1:800	4C	4% PFA	0.1% Triton-X	1 mg/ml
SM myosin heavychain-1	Abcam (ab681)	mouse	1:200	4C	4% PFA (alt: acetone for 20 min)	0.1% Triton-X (alt: none)	1-10mg/ml

*alt: alternative method

Table A.4 Rat EC Antibodies

Antigen	Source	Host	Dilution	Storage	Fixation	Antigen Retrieval	Stock Soln
E-Selectin (anti-human)	Santa Cruz (sc-14011)	rabbit	1:100	4C	4% PFA	None	200 ug/ml
ICAM-1 (anti-rat)	Santa Cruz (sc-19584)	mouse	1:100	4C	4% PFA	None	200 ug/ml
VCAM-1 (anti-rat)	Biolegend (200402)	mouse	1:100	4C	4% PFA	None	500 ug/ml
vWF (anti-human)	Abcam (ab6994)	rabbit	1:800 (1:2000 IHC)	-20C	4% PFA	0.1% Triton-X	8.1 mg/ml
Thrombomodulin (anti-rat)	Amer Diagnostica (ad3381)	rabbit	1:100	-20C	4% PFA	None	1 mg/ml
CD31 (anti-rat)	BD Pharmingen	mouse	1:50	4C	4% PFA	None	1 mg/ml

Table A.5 Human EC Antibodies

Antigen	Source	Host	Dilution	Storage	Fixation	Antigen Retrieval	Stock Soln
CD31 (anti-human)	Chemicon (mab2148)	mouse	1:100	4C	4% PFA	None	1 mg/ml
E-Selectin (anti-human)	Santa Cruz (sc-14011)	rabbit	1:100	4C	4% PFA	None	200 ug/ml
ICAM-1 (ant-human)	Chemicon (mab2146)	mouse	1:200	4C		None	1 mg/ml
vWF (anti-human)	Abcam (ab6994)	rabbit	1:800	-20C	4% PFA	0.1% Triton-X	1 mg/ml
Thrombomodulin (anti-human) Xreact: mouse	Amer Diagnostica (ad2375)	mouse	1:100	-20C	4% PFA	None	0.5 mg/ml
Tissue Factor (anti-human)	Amer Diagnostica (ad4501)	goat	1:100	4C	4% PFA	None	1 mg/ml
VCAM-1 (anti-human)	Chemicon (mab2511)	mouse	1:200	-20C	4% PFA	None	1 mg/ml
NOS3 (anti-human)	Santa Cruz (sc-654)	rabbit	1:50, (1:100 IHC)	4C			0.2 mg/ml
VE-Cadherin	Santa Cruz (sc-6458)	goat	1:100	4C	4% PFA	None	1 mg/ml

Table A.6 Ovine EC Antibodies

Antigen	Source	Host	Dilution	Storage	Fixation	Antigen Retrieval	Stock Soln
vWF (anti-human)	Abcam (ab6994)	Rabbit	1:4800 (1:2000 IHC)	-20C	4% PFA	0.1% Triton-X	1 mg/ml

Table A.7 Blood cell Antibodies

Antigen	Source	Host	1º Dilution	Storage	Fixation	Antigen Retrieval	Stock Soln
GP-1b (CD42b; anti-human)	Ab58921	Mouse	1:100	-20C	4% PFA	None	0.1 mg/ml
CD45	Ab10558	Rabbit	1:100	-20C	4% PFA	None	1 mg/ml

Table A.8 Extracellular Matrix Antibodies

Antigen	Source	Host	1º Dilution	Storage	Fixation	Antigen Retrieval	Stock Soln
Collagen I (anti-human) x-react: rat	Novus Bio (NB600-408)	Rabbit	1:500	-20C	3hr 4% PFA	None	1.12 mg/ml
Collagen III (anti-human)	Novus Bio (NBP1-05119)	Mouse	(unstated; tried 1:50-1:500)	4C			1 mg/ml
Collagen IV	Ab6586	Rabbit	1:100; 1:200	-20C	3hr 4% PFA	None	1.2 mg/ml
Fibrin	Amer Diag 3462	Goat	1:500	-20C	3hr 4% PFA	None	1 mg/ml

Fibronectin	Amer Diag 6584	Rabbit	1:1000	-20C	3hr 4% PFA	None	1 mg/ml
Laminin	Ab11575	Rabbit	1:50	-20C	3hr 4% PFA	None	0.5 mg/ml

Table A.9 Donkey Secondary Antibodies (Jackson Immuno)

Secondary	DyLight 488	Dylight 549	Dylight 649	HRP	Storage
Donkey anti-mouse IgG (H+L)	715-485-151	715-505-151	715-495-151	715-035-151	-20C
Donkey anti-rabbit IgG (H+L)	711-485-152	711-505-152	711-495-152	711-035-152	-20C
Donkey anti-goat IgG (H+L)	705-485-147	705-505-147	705-495-147	705-035-147	-20C

** All secondary antibodies stored 1:1 in glycerol in aliquots at -20C.*

A.4.2 Immunocytochemistry

1. Rinse cells or whole tissue in warm HBSS or PBS. *Note: Use HBSS with ECs, as rinsing with PBS may lead to cell detachment.
2. Fix with 4% PFA 10 minutes at room temperature (RT).
3. Rinse 3x 3 minutes with PBS (10 minutes per rinse for whole tissue).
4. OPTIONAL PERMEABLIZATION STEP. Permeabilize with 0.1% Triton-X for 5 minutes. Following this step, rinse 3x with PBS.
5. Block in 5% normal donkey serum (to match secondary antibody host) for 30 minutes at RT.
6. Incubate in 1° antibody (dilutions shown in Antibody tables) 1 hour at RT or overnight at 4°C.
7. Rinse 3x 3 minutes in PBS (10 minute rinses for whole tissue).
8. Incubate in 2° antibody (Cy2 or Cy3 or DyLight antibodies from Jackson Immuno) in PBS 45 minutes at RT. Stock solutions of secondary antibodies are stored at 4C for short durations (recommended <6 weeks) in PBS or this stock solution can be diluted 1:2 in glycerol and stored at -20C.
9. Rinse 1x 3 minutes in PBS (10 minute rinse for whole tissue).
10. Counterstain cell nuclei with Hoechst 33342 at 1 μg/ml for 10 minutes.
11. Rinse 2 x 3 minutes in PBS (10 minute rinses for whole tissue).
12. Coverslip with DAKO fluorescent mounting medium. Use the hardset mounting medium for whole tissue.
13. Store in dark at 4°C.

A.4.3 Infiltration and Embedding of Tissue

Infiltration Solution 1 (IF1)

30% w/v sucrose + 5% w/v DMSO in 1X PBS
e.g. for 100 ml: 30 g sucrose

5 ml DMSO
10 ml 10X PBS
Dilute to 100 ml with ddH_2O

Infiltration Solution 2 (IF2)

50% v/v infiltration solution 1 and 50% v/v OCT
Mix well, avoid bubbles or centrifuge briefly to remove bubbles.

Procedure

1. Rinse the sample 3 x 10 min in PBS at room temperature on orbital shaker.
2. Fix the sample for 3 hours at 4^{o}C in 4% paraformeldahyde (PFA) on orbital shaker.
3. Rinse the sample 3 x 10 min in PBS at RT, orbital shaker if possible.
4. Incubate samples in IF1 overnight at 4^{o}C on a shaker.
5. Place samples in IF2 for 4 hours at room temperature on a shaker.
6. Place samples in dry sample block cup and carefully transfer sample to the block. Top off with OCT. Freeze in pre-chilled isopentane in liquid N_2. Freeze until opaque. Store samples at -80^{o}C.

*Note: All times are dependent on tissue thickness. Times shown are good for 200 μm thick MEs, but should be increase for thicker MEs or native tissue.

A.4.4 Immunostaining of Tissue Sections (non-ECM antibodies)

1. After embedding tissue in OCT, cut 9 μm thick cryostat sections and mount on glass slides. Store slides at -80°C until needed.
3. Before IF staining, warm up slides at room temperature for 30 minutes. Circle each section with a pap pen.
4. Follow protocol for staining cell monolayers starting at step 6 (A.5.2).

A.4.5 Staining for ECM Proteins

1. Use 9 μm thick sections on glass slides for staining. Before staining, warm up slides at room temperature for 30 minutes. Circle each section with a pap pen.
2. Block in 5% normal donkey serum (to match secondary antibody host) for 2 hours at RT.
3. Incubate in 1° antibody (dilutions shown in Antibody tables) overnight at 4°C.
4. Rinse 3x 3 minutes in PBS.
5. Incubate in 2° antibody in PBS 1 hour at RT.
6. Rinse 3x 3 minutes in PBS.
7. Stain cell nuclei with Hoechst 33342 (Invitrogen) at 1 μg/ml for 10 minutes.
8. Coverslip with DAKO fluorescent mounting medium.
9. Store in dark at 4°C.

Appendix B: Implant Studies

B.1 Background

MEs fabricated with porcine valve interstitial cells (PVICs) were cultured for at least 5 weeks and then endothelialized with Fischer rat vascular endothelial cells for 24-48 hours prior to implantation in 8-9 week old male Fischer rats. The intent of this initial implant study was to examine fibrin construct remodeling *in vivo*, verify the seeded endothelium was robust and would prevent thrombosis, and determine if our constructs, with burst pressures of at least 400 mmHg, can withstand rat aortic pressures.

B.2 Results

Seven implants were performed (Table 1). Of these, one animal died due to technical issues and two due implant rupture. In the other four cases, the cause of death was unclear; no mechanical failure occurred and in none of the implants was thrombosis apparent. While the short survival time, from 1-7 hours, makes it impossible to characterize the *in vivo* remodeling of our constructs, these results indicate that our constructs may be strong enough initially to withstand normal rat aortic pressures.

Table B.1 Summary of PVIC ME Implants

Implant #	Culture Time (Weeks)	EC Time (Hours)	Survival Time (Hours)	Burst Pressure (mmHg)	Cause of Death
1	8.5	24	N/A	440	Technique: attempt to cuff implant for surgery
2	8.5	48	2	422	Rupture longitudinally
3	6.5	24	2-2.5	425	Unknown, bleeding from anastomoses
4	6.5	48	6-7	440	Unknown, bleeding from anastomoses
5	5	24	3	421	Unknown, bleeding stopped with surgical glue
6	6.5	24	N/A	435	Nude rat: Did not close after surgery due to inability to stop bleeding
7	6	24	1	407	Rupture

Burst pressure testing, histology, and endothelial cell staining (acLDL, vWF) were used to characterize constructs pre-implant on endothelialized MEs from the same batch. This allowed confirmation of mechanical properties and good endothelial cell coverage prior to implantation. In the first 3 implants, ACA was not contained in the medium used for EC seeding in the final pre-implant step, and a degradation of fibrin and/or other non-collagenous protein was apparent over the 24-48 hours post-endothelialization and prior to implantation (Figure 1).

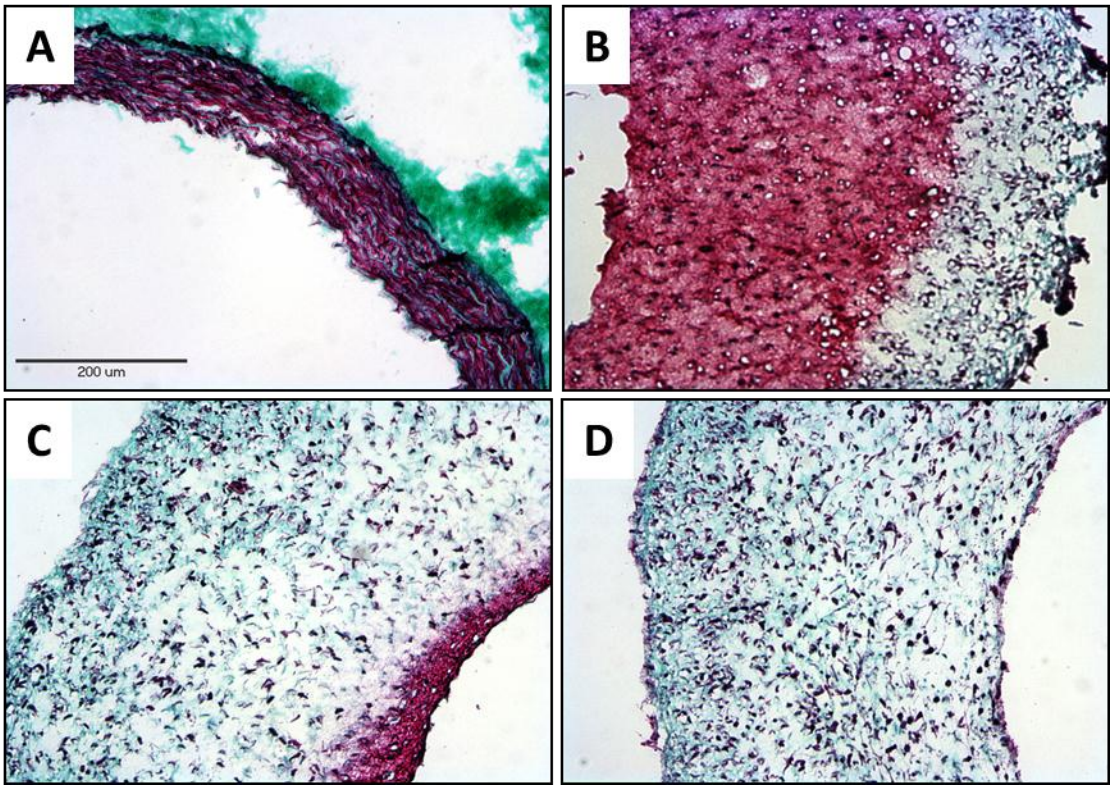

Figure B.1: Lillie's Trichrome Staining of ME pre- and post-implant. A). Native Fischer rat aorta B). 6 week PVIC ME prior to endothelialization C). Endothelialized PVIC ME cultured without ACA in the medium starting at the time of endothelial cell seeding. D). PVIC construct explant (after 2-2.5 hours implantation).

B.3 Summary

A total of 7 implants were performed (6 on fischer rats and 1 on a nude rat). The implants were directly sutured in line with the rat infrarenal abdominal aorta, and in later

implants, surgical glue was used to stop bleeding from the suture site. Without the use of surgical glue, the bleeding could be stopped through application of pressure to the suture site, but bleeding would resume 10-15 minutes later. Of the 7 implantation cases, 1 animal died due to technical issues and 2 due to rupture of the implant. In the other 4 implants, the cause of death was unclear. It was unlikely that bleeding around the sutures was the cause of death, as the amount of blood lost was low and remedying this issue through the use of surgical glue did not increase the survival time. No thrombosis occurred, however questions were raised as to whether this was due to the presence of a confluent endothelium or an effect of hyperacute rejection through dysfunction of the coagulation cascade or, perhaps more likely, a response to the aspirin or heparin dose administered prior to implantation. The complete lack of clotting at the anastomoses is likely the reason for the continued bleeding after implantation. While the short survival time, on the order of hours instead of days or weeks, makes it impossible to characterize the *in vivo* remodeling of our constructs, these results indicate that our MEs are may be strong enough initially to withstand normal rat aortic pressures. The use of Fischer rat cells in the medial layer of our constructs, with continued use of Fischer rat endothelial cells, would remove possible issues with immunological rejection due to cell source.

Appendix C: Cyclic Distention

C.1 Background

This research aimed to address the critical issue of inferior mechanical properties of fibrin-based vascular constructs compared to native vessels, through mechanical strengthening with cyclic distension. Using a custom built bioreactor system, modified to work with 1 mm and 2 mm OD silicone tubing, we were able to cyclically distend tubular fibrin constructs with independent control of frequency, duty cycle, and radial distention {Isenberg, 2003 #42}. A radial distention of up to 20% could be attained with this system. Rat vascular smooth muscle cell (vSMC) constructs, as fabricated in Chapter 2, were subjected to cyclic distension using a 10% radial distension, 0.5 Hz frequency and 12.5% duty cycle (Figure C.1), to mimic the best case conditions demonstrated with porcine valve interstitial cells in larger diameter tubular constructs to date .

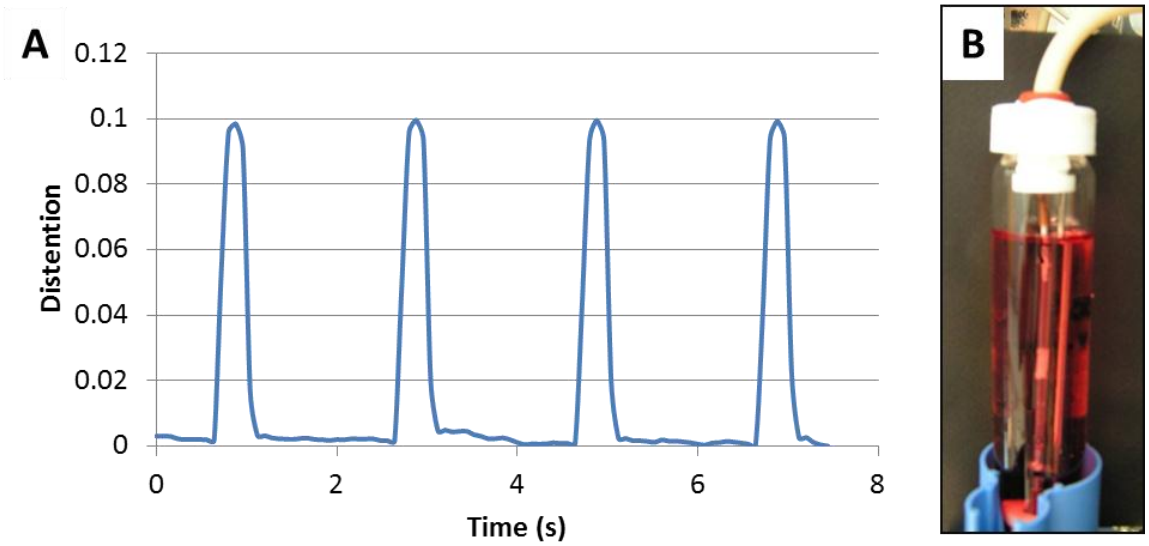

Figure C.1: Cyclic distention of 2 mm MEs. A) Cyclic Distention profile for vSMC MEs distended on silicone tubing. B) Bioreactor for culture and distention of 2 mm MEs.

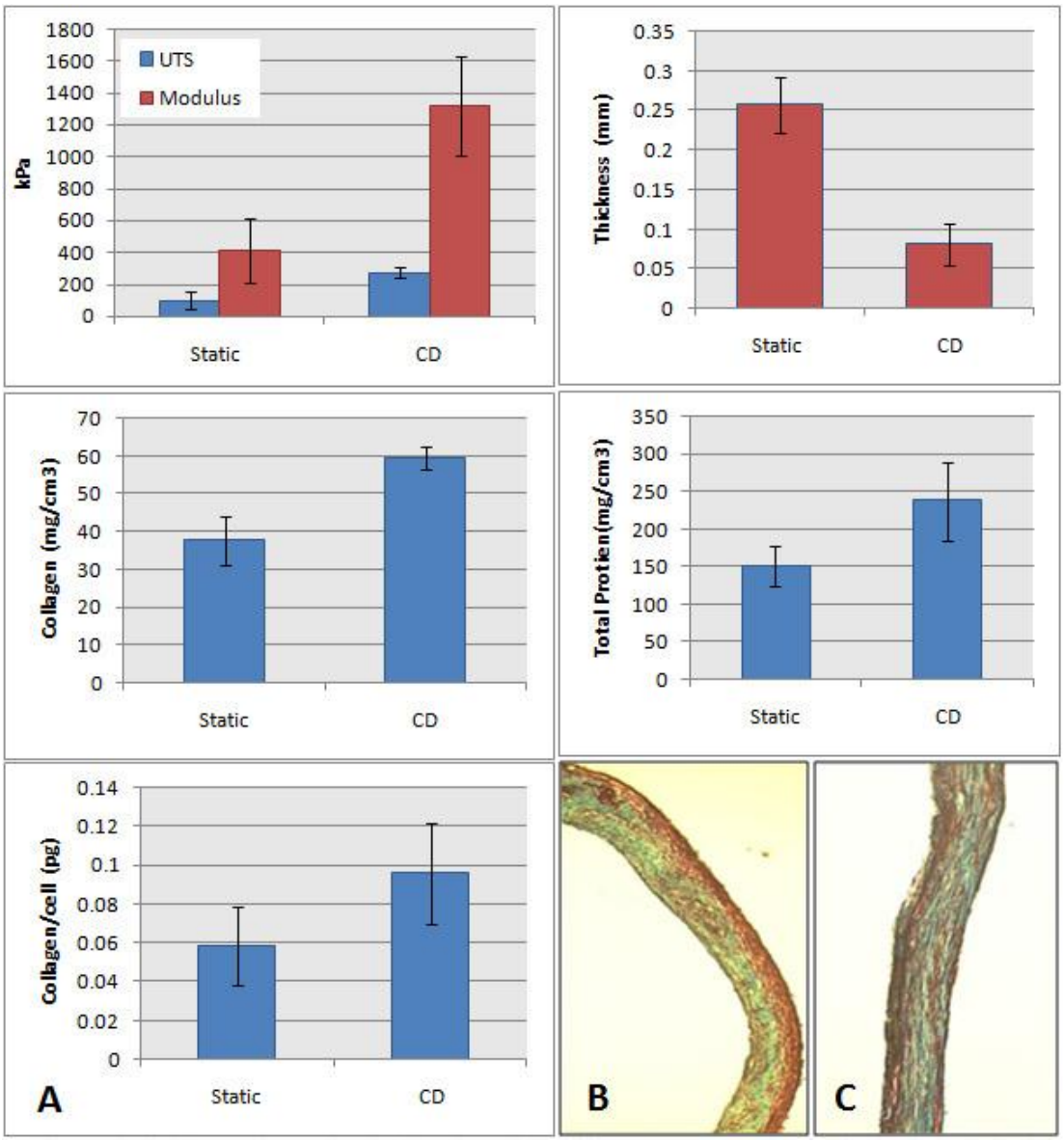

Figure C.1: Effects of CD on vSMC tubular constructs. A) Comparison of statically cultured constructs (Static) versus constructs cyclically distended with 10% strain, 0.5 Hz, and 12.5% duty cycle (CD). Trichrome stain of B) Static and C) CD constructs. Mean ± SD for n=4.

C.2 Results

vSMC MEs were cultured statically for two weeks on a glass mandrel before being transferred to 2 mm OD silicone tubing. Half of these MEs underwent cyclic

distention and the other half were statically cultured for the next 4 weeks. After 4 weeks of cyclic distention, vSMCs had a higher ultimate tensile strength and modulus than the statically cultured MEs and had a higher collagen density (Figure C.2A). Histology showed a more homogenous collagen distribution in the cyclically distended MEs compared to their static counterparts, as well as stronger alignment of the cells in the circumferential direction.

C.3 Summary

Results for the vSMC constructs support the hypothesis that mechanical stimuli can be used to modulate matrix remodeling and improve the mechanical properties of fibrin-based media-equivalents. Significant improvements were seen in the ultimate tensile strength and modulus of cyclically distended versus statically cultured constructs. However, as described in Chapter 3, vSMC MEs had great variability between cell isolations, cell passages, fibrinogen lots, and even between fabrications. Experiments with vSMCs had great variability in mechanical properties, compaction, and collagen and elastin deposition. Thus, while these experiments showed that vSMC were responsive to mechanical stimulation, use of these MEs became impractical when MEs could not be fabricated with consistent results.